
Mg/Ca, B/Ca and U/Ca in shells of benthic foraminifers:

Tracers of temperature and seawater carbonate chemistry

Dissertation zur Erlangung des
akademischen Grades eines Doktors
der Naturwissenschaften

Dr. rer. nat.

im Fachbereich 5 (Geowissenschaften)
der Universität Bremen

Markus Raitzsch

Bremen, 2008

Tag des öffentlichen Kolloquiums

21.11.2008

Gutachter der Dissertation

Prof. Dr. Gerold Wefer

Prof. Dr. Gerhard Bohrmann

Prüfer

PD Dr. Sabine Kasten

Dr. Gert-Jan Reichart

Weitere Mitglieder des Prüfungsausschusses

Dr. Torsten Bickert

Katrin Heindel

ERKLÄRUNG

Name: Markus Raitzsch

Datum: 28.08.2008

Anschrift: Hamburger Straße 29F, 28205 Bremen

Hiermit versichere ich, dass ich

1. die Arbeit ohne unerlaubte fremde Hilfe angefertigt habe,
 2. keine anderen als die von mir angegebenen Quellen und Hilfsmittel benutzt habe und
 3. die den benutzten Werken wörtlich oder inhaltlich entnommenen Stellen als solche kenntlich gemacht habe.
-

_____ Bremen _____, den _____ 28.08.2008 _____

_____ Markus Raitzsch _____

(Unterschrift)

ACKNOWLEDGMENTS

It is almost impossible to thank all these people who accompanied me during the past three years in Bremen and Utrecht. However, I would specifically like to acknowledge the following people and organizations for their assistance and support during this project:

First of all, I like to thank Prof. Dr. Gerold Wefer and Dr. Torsten Bickert who entrusted me with this highly interesting PhD topic. They always gave free rein to me in developing my doctoral thesis, and enabled me to participate in important conferences that benefited the success of this thesis. I want to emphasize Torsten's dedication and expert knowledge which made him an excellent supervisor.

I want to thank my family and my girlfriend Manuela Kreisel who supported me in every situation of life. Without their unfailing encouragement, I would not have probably succeeded on this long journey.

Special thanks are also given to Dr. Henning Kuhnert, Dr. Jeroen Groeneveld and Dr. Ed Hathorne who taught me a lot about foraminifers and laser ablation. I am very happy that we all became good friends during our cooperation. Further, Dr. Mark Trevethan is gratefully acknowledged for proof-reading the introduction, as well as for his critical comments on an earlier draft.

I'm very grateful to Dr. Gert-Jan Reichart for giving me the opportunity to spend five months at the University of Utrecht. He had the great idea of culturing foraminifers specifically to my scientific questions. Gert-Jan and his foraminifer culturing group, including Adriana Dueñas-Bohórquez, Jordahna Haig, Shauna Ní Fhlaithearta, Jos Wit and Sander Ernst, are thanked for the great time in the Netherlands.

I like to thank Dr. Andreas Klügel and Heike Anders for their laboratory assistance, especially at the beginning of my PhD. They and Henning Kuhnert introduced me to the use of the Laser Ablation ICP-MS technique and continuously improved and updated the laboratory equipment available for this project.

Since there are many colleagues from the MARUM and the GEO building with whom I spent a great time in Bremen, I would like to at least mention my office mates Ines Heßler, Catalina Gonzáles and Nick Rackebrandt. The atmosphere in our office was always relaxed, friendly and enjoyable.

Last but not least, the DFG (Deutsche Forschungsgemeinschaft) is gratefully acknowledged for supporting me with a scholarship within the international graduate college EUROPROX.

ABSTRACT

Mg/Ca ratios in benthic foraminiferal shells are frequently used in paleoceanographic studies to estimate past bottom water temperatures. Apart from temperature, other factors may exert additional influences on foraminiferal Mg/Ca. These include the Mg/Ca ratio of seawater, partial dissolution of shell calcite, salinity, physiological effects, and, probably of capital importance, the carbonate chemistry of seawater. In this context, the separate effects of temperature and seawater carbonate chemistry on the magnesium incorporation into benthic foraminiferal calcite are unraveled and quantified in this thesis. Further, B/Ca and U/Ca in benthic foraminifers were investigated as potential carbonate system proxies that may be used to correct for the carbonate ion effect on Mg/Ca.

Mg/Ca in the benthic foraminifer species *Planulina wuellerstorfi* and *Cibicides mundulus* from various South Atlantic core top samples were analyzed to establish temperature calibrations (**Manuscript I**). It was evident that many samples, notably those bathed in North Atlantic Deep Water (NADW), exhibited much higher Mg/Ca ratios than predicted from previous calibrations. The increased Mg/Ca ratios were caused by the high calcite saturation state ($\Delta[\text{CO}_3^{2-}]$) of NADW. Mg/Ca increased by 0.01 and 0.017 mmol/mol per 1 $\mu\text{mol/kg}$ $\Delta[\text{CO}_3^{2-}]$ in *P. wuellerstorfi* and *C. mundulus*, respectively. These gradients are enormous with regard to the generally small change of Mg/Ca at the cold end of the exponential Mg/Ca-temperature relationship. Therefore changes in past seawater carbonate chemistry may skew reconstructions of past temperatures based on benthic Mg/Ca to a considerable degree.

We conducted culturing experiments to verify the effect of calcite saturation state (here reported as Ω) on Mg/Ca in shells of the shallow benthic foraminifers *Heterostegina depressa* and *Ammonia tepida* (**Manuscript II**). In these experiments, Ω was varied by changing $[\text{Ca}^{2+}]$ which had the same effect as changing $[\text{CO}_3^{2-}]$. As a result, Mg/Ca in *H. depressa* increased with increasing Ω at a gradient of 1.67 mmol/mol per unit Ω , whereas Mg/Ca in *A. tepida* decreased at a gradient of -0.21 mmol/mol/unit Ω . While the positive relationship between Ω and Mg/Ca in *H. depressa* is consistent with results from core-top studies of deep-sea benthic foraminifera, the negative correlation of Mg/Ca in *A. tepida* with Ω is rather similar to previous culture studies of planktic foraminifera. This suggests that these species use different biomineralization mechanisms, which in turn are influenced by the calcite saturation state. However, our results demonstrate that the effect of the carbonate chemistry on the Mg incorporation must be quantified separately for each species.

To further develop new independent proxies for the carbonate system, we investigated B/Ca and U/Ca in the benthic foraminifer species *Planulina wuellerstorfi* and *Cibicides mundulus* from South Atlantic core tops (**Manuscript III**). For that purpose, we used a Laser Ablation ICP-MS since this micro-analytical method provides information on intra-test trace element heterogeneity and does not suffer from B blank problems like traditional solution techniques. The results show that B/Ca and U/Ca are closely related to the calcite saturation state of

seawater with the highest correlations between $\Delta[\text{CO}_3^{2-}]$ and B/Ca in *P. wuellerstorfi* (positive linear relationship), and between $\Delta[\text{CO}_3^{2-}]$ and U/Ca in *C. mundulus* (negative exponential relationship). The relationship between B/Ca and $\Delta[\text{CO}_3^{2-}]$ is consistent with a previous study of the same species, but the link between U/Ca and $\Delta[\text{CO}_3^{2-}]$ found in this study is reported for the first time. These carbonate system proxy relationships were used to correct foraminiferal Mg/Ca for the influence of seawater carbonate ion variations. The corrected Mg/Ca-based seawater temperature estimates are more accurate, improving on average from more than $\pm 1.6^\circ\text{C}$ inaccurate to less than $\pm 0.9^\circ\text{C}$ inaccurate.

ZUSAMMENFASSUNG

Mg/Ca-Verhältnisse in Schalen benthischer Foraminiferen werden häufig für paläo-ozeanographische Studien verwendet, um Bodenwassertemperaturen der Vergangenheit abzuschätzen. Abgesehen von der Temperatur können zusätzliche Faktoren das Mg/Ca-Verhältnis in Foraminiferen beeinflussen. Diese umfassen das Mg/Ca-Verhältnis des Meerwassers, partielle Lösung der Kalkschalen, Salinität, physiologische Effekte und, wahrscheinlich von größter Bedeutung, die Karbonatchemie des Meerwassers. In diesem Zusammenhang werden in dieser Arbeit die einzelnen Effekte von Temperatur und Karbonatchemie auf den Einbau von Magnesium in kalzitische Foraminiferenschalen aufgeschlüsselt und quantifiziert. Desweiteren werden B/Ca und U/Ca in benthischen Foraminiferen als mögliche Proxies für das Karbonatsystem des Meerwassers untersucht, die zur Korrektur von Mg/Ca um den Karbonationeneinfluss verwendet werden können.

Wir analysierten Mg/Ca-Verhältnisse in den benthischen Foraminiferenarten *Planulina wuellerstorfi* und *Cibicidoides mundulus* von Oberflächensedimenten aus dem Südatlantik, um Temperaturkalibrierungen durchzuführen (**Manuskript I**). Dabei wiesen viele der Proben, vor allem aus dem Nordatlantischen Tiefenwasser (NADW), weitaus höhere Mg/Ca-Werte auf als man anhand bereits existierender Mg/Ca-Temperatur-Kalibrierungen erwarten würde. Die erhöhten Werte wurden durch die hohe Kalzitsättigung ($\Delta[\text{CO}_3^{2-}]$) des NADW verursacht. Die Mg/Ca-Verhältnisse in *P. wuellerstorfi* stiegen dabei pro 1 $\mu\text{mol/kg}$ $\Delta[\text{CO}_3^{2-}]$ um 0.01 mmol/mol an, und in *C. mundulus* um 0.017 mmol/mol. Diese Gradienten sind im Hinblick auf die allgemein geringe Änderung der Mg/Ca-Werte im kalten Bereich der exponentiellen Mg/Ca-Temperatur-Beziehung enorm. Folglich können erdgeschichtliche Änderungen in der Karbonatchemie des Meerwassers Mg/Ca-basierte Temperaturrekonstruktionen in erheblichem Maße verfälschen.

Wir führten Zuchtversuche durch, um den Effekt der Kalzitsättigung (hier Ω) auf das Mg/Ca-Verhältnis in den benthischen Flachwasserforaminiferen *Heterostegina depressa* und *Ammonia tepida* nachzuweisen (**Manuskript II**). Bei diesen Experimenten wurde Ω durch Änderung der Kalziumkonzentration variiert, das denselben Effekt erzielt wie durch Änderung der Karbonationenkonzentration. Als Folge davon stiegen pro Ω -Einheit die Mg/Ca-Werte in *H. depressa* um 1.67 mmol/mol an, während die Mg/Ca-Verhältnisse in *A. tepida* um -0.21 mmol/mol abfielen. Während die positive Korrelation zwischen der Kalzitsättigung und Mg/Ca in *H. depressa* mit den Ergebnissen aus den Untersuchungen an Tiefseeforaminiferen übereinstimmt, verhält sich das Mg/Ca-Verhältnis in *A. tepida* vielmehr wie in planktischen Foraminiferen aus früheren Zuchtversuchen. Das ist ein Hinweis darauf, dass diese Arten unterschiedliche Mechanismen der Biomineralisation verwenden, die ihrerseits durch die Kalzitsättigung beeinflusst werden. Unsere Ergebnisse verdeutlichen, dass der Einfluss der Karbonatchemie auf den Magnesiumeinbau für jede Foraminiferenart gesondert quantifiziert werden muß.

Um die Entwicklung neuer unabhängiger Proxies für das Karbonatsystem voranzutreiben, untersuchten wir B/Ca- und U/Ca-Verhältnisse in den benthischen Foraminiferenarten *Planulina wuellerstorfi* und *Cibicidoides mundulus* von Oberflächensedimenten aus dem Südatlantik (**Manuskript III**). Dafür verwendeten wir ein an ein ICP-MS gekoppeltes Laserablationssystem, da diese mikroanalytische Methode Aufschluss über die Variabilität der Elemente innerhalb von Schalen gibt und nicht durch ein hohes Bor-Hintergrundsignal wie in der herkömmlichen Flüssigaufschlussmethode behindert wird. Die Ergebnisse zeigen eine enge Beziehung zwischen der Kalzitsättigung und den B/Ca- und U/Ca-Verhältnissen, wobei die höchsten Korrelationen zwischen $\Delta[\text{CO}_3^{2-}]$ und B/Ca in *P. wuellerstorfi* (positive lineare Korrelation) und zwischen $\Delta[\text{CO}_3^{2-}]$ und U/Ca in *C. mundulus* (negative exponentielle Korrelation) bestehen. Der Zusammenhang zwischen B/Ca und $\Delta[\text{CO}_3^{2-}]$ stimmt mit einer früheren Untersuchung an den gleichen Spezies überein, aber über die in dieser Studie gefundene Beziehung zwischen U/Ca und $\Delta[\text{CO}_3^{2-}]$ wird zum ersten Mal berichtet. Diese Karbonationproxies wurden verwendet, um die Mg/Ca-Verhältnisse um den Karbonationeneinfluss zu korrigieren. Die Ungenauigkeit der Temperaturrekonstruktionen wurde dadurch im Durchschnitt von mehr als $\pm 1.6^\circ\text{C}$ auf weniger als $\pm 0.9^\circ\text{C}$ reduziert.

TABLE OF CONTENTS

| | | |
|-------|---|----|
| I. | INTRODUCTION | 1 |
| 1. | Development of Mg/Ca in foraminifers as a temperature proxy | 1 |
| 2. | Additional influences on foraminiferal Mg/Ca..... | 4 |
| 2.1 | Mg/Ca of seawater | 4 |
| 2.2 | Salinity..... | 4 |
| 2.3 | Physiological effects (biomineralization)..... | 4 |
| 2.4 | Dissolution..... | 6 |
| 2.5 | Carbonate system of seawater | 7 |
| 3. | B/Ca and U/Ca as independent carbonate system proxies | 9 |
| 4. | Analytical techniques and samples..... | 12 |
| II. | THESIS OUTLINE | 15 |
| III. | MANUSCRIPTS..... | 19 |
| 5. | Benthic foraminifer Mg/Ca anomalies | 19 |
| 5.1 | Introduction..... | 19 |
| 5.2 | Oceanographic setting..... | 21 |
| 5.3 | Material and methods..... | 24 |
| 5.4 | Results..... | 26 |
| 5.4.1 | Mg/Ca versus water depth..... | 26 |
| 5.4.2 | Mg/Ca versus temperature..... | 27 |
| 5.4.3 | Mg/Ca versus seawater chemistry | 28 |
| 5.5 | Discussion..... | 31 |
| 5.5.1 | Influence of carbonate chemistry on shell Mg/Ca..... | 31 |
| 5.5.2 | Implications for paleothermometry..... | 33 |
| 5.6 | Summary | 34 |
| 6. | Effect of Ω on shell Mg/Ca..... | 35 |
| 6.1 | Introduction..... | 35 |
| 6.2 | Experimental and analytical procedures..... | 36 |
| 6.2.1 | Sample collection and preparation..... | 36 |
| 6.2.2 | Experimental setup..... | 37 |
| 6.2.3 | Element analysis..... | 39 |

| | | |
|-------|---|----|
| 6.3 | Results | 40 |
| 6.3.1 | Survival and growth rates | 40 |
| 6.3.2 | Mg/Ca versus calcite saturation state | 41 |
| 6.4 | Discussion | 44 |
| 6.4.1 | The effect of calcite saturation state on Mg incorporation | 44 |
| 6.4.2 | Biom mineralization mechanisms..... | 44 |
| 6.5 | Conclusions..... | 46 |
| 7. | Carbonate system proxies B/Ca and U/Ca..... | 47 |
| 7.1 | Introduction | 47 |
| 7.2 | Material and methods | 48 |
| 7.3 | Suitability of LA-ICP-MS for determination of B/Ca, Mg/Ca, and U/Ca | 49 |
| 7.4 | B/Ca and U/Ca related to calcite saturation state..... | 51 |
| 7.5 | Correction for the carbonate ion effect on Mg/Ca..... | 53 |
| 7.6 | Appendix 1. Sampling locations..... | 56 |
| 7.7 | Appendix 2. Carbonate standard JCT-1..... | 57 |
| 7.8 | Appendix 3. Intra-test variability | 58 |
| 7.9 | Appendix 4. Correction of Mg/Ca-thermometer..... | 60 |
| IV. | SUMMARY AND OUTLOOK..... | 61 |
| V. | REFERENCES..... | 63 |

I. INTRODUCTION

1. Development of Mg/Ca in foraminifers as a temperature proxy

The ratio of Mg to Ca in calcitic shells of foraminifers as an indicator for water temperature is an excellent example for the development of a proxy in paleoceanography. The first scientists who associated the Mg content of biogenic carbonates with growth temperature were Clarke and Wheeler (1922). In the 1950s and '60s, a relationship found between the distribution of high-Mg shells of neritic foraminifers and latitude confirmed this earlier study, suggesting that the substitution of calcium by magnesium in the calcite lattice is a function of temperature (Chave, 1954; Chilingar, 1962).

The strong linkage between Mg/Ca and water temperature was supported by results from inorganically precipitated calcite (e.g., Katz, 1973; Mucci, 1987; Oomori et al., 1987). However, first attempts to calibrate Mg concentrations in foraminiferal calcite against temperature failed (Krinsley, 1960). Despite single-species calibrations not being successful, Mg/Ca variations between different planktic species demonstrated a strong correlation with water temperature at the estimated calcification depth (e.g., Savin and Douglas, 1973; Bender et al., 1975; Rosenthal and Boyle, 1993). It was not until careful laboratory cultures prepared under controlled conditions were carried out by Nürnberg et al. (1996), that an empirical positive exponential relationship between planktic Mg/Ca and temperature could be established (e.g., Delaney et al., 1985; Anand et al., 2003; and references in Figure 1-1a). Later, studies on benthic foraminifer species also lead to similarly encouraging results, which provided a promising tool for the reconstruction of past bottom water temperatures (e.g., Izuka, 1988; Rathburn and De Deckker, 1997; and references in Figure 1-1b).

The exponential Mg/Ca-temperature relationship is based on the fact that the substitution of magnesium in inorganic calcite is endothermic and therefore favored at higher temperatures. The increase in Mg/Ca is approximately 3% per °C (Lea et al., 1999). This was confirmed by inorganic precipitation experiments (Chilingar, 1962; Katz, 1973; Mucci, 1987; Oomori et al., 1987). However, foraminiferal calcite generally shows a much higher sensitivity of Mg/Ca to temperature (~8-11% per °C), whereas the absolute values are approximately 5-10 times lower than in inorganic calcite. This indicates that the partition coefficient for magnesium ($D_{Mg} = Mg/Ca_{solid} / Mg/Ca_{liquid}$) is largely influenced by the composition of the precipitated calcite. It was shown that D_{Mg} increased with decreasing Mg content of the solid (Mucci and Morse, 1983; Morse and Bender, 1990). This may explain why the sensitivity of Mg/Ca in neritic high-Mg foraminifers to temperature found by Toyofuku et al. (2000) and Toyofuku and Kitazato (2005) is similar to that in inorganic calcite (e.g., Lea, 2003).

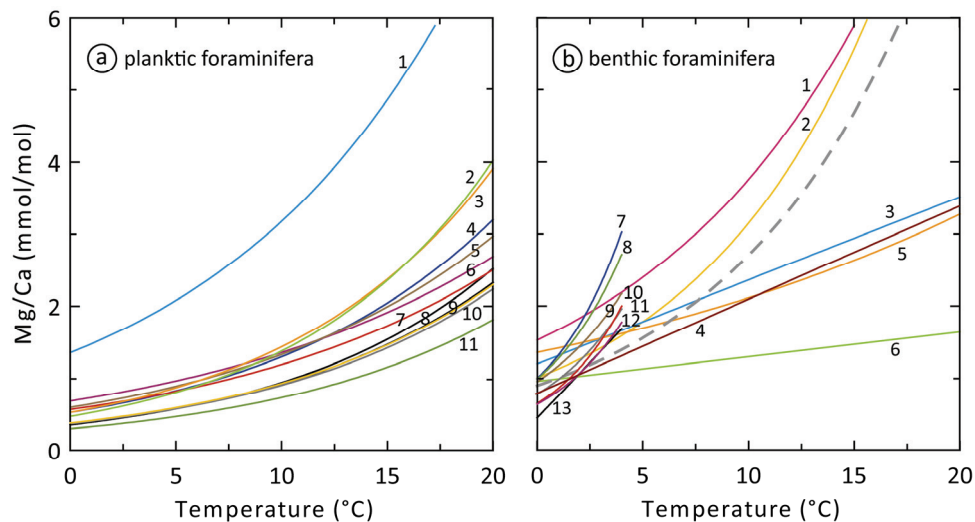


Figure 1-1. Compiled Mg/Ca-temperature single-species calibrations for planktic and benthic foraminifera. **a)** 1 (cyan): *O. universa* (Lea et al., 1999); 2 (light green): *G. bulloides* (Mashiotta et al., 1999); 3 (orange): *G. bulloides* (Lea et al., 1999); 4 (blue): *G. tumida* (Rickaby and Halloran, 2005); 5 (brown): *N. dutertrei* (Dekens et al., 2002); 6 (purple): *G. ruber* (McConnell and Thunell, 2005); 7 (red): *G. ruber* (Whitko et al., 2002); 8 (black): *G. truncatulinoides* (McKenna and Prell, 2004); 9 (yellow): *G. ruber* (Dekens et al., 2002), *G. sacculifer* (Nürnberg et al., 1996); 10 (gray): *G. sacculifer* (Dekens et al., 2002); 11 (dark green): *G. ruber* (Lea et al., 2000). **b)** 1 (magenta): *O. umbonatus* (Rathmann et al., 2004); 2 (yellow): *O. umbonatus* (Lear et al., 2002); 3 (cyan): *C. pachyderma* (Marchitto et al., 2007); 4 (dark red): *C. pachyderma* (Curry and Marchitto, 2008); 5 (orange): *C. pachyderma* (Rosenthal et al., 1997); 6 (light green): *H. elegans* (Rosenthal et al., 2006); 7 (blue): *C. mundulus* (Healey et al., 2008); 8 (dark green): *O. umbonatus* (Healey et al., 2008); 9 (brown): *C. wuellerstorfi* (Russell et al., 1994); 10 (red): *C. wuellerstorfi* (Lear et al., 2002); 11 (gray): *C. wuellerstorfi* (Healey et al., 2008); 12 (purple): *C. wuellerstorfi* (Martin et al., 2002); 13 (black): *C. wuellerstorfi* (Billups and Schrag, 2002). Note that calibrations 7-13 are limited to temperatures below 4°C. The dashed gray line is for global *Cibicidoides* spp. from Elderfield et al. (2006), which includes the Lear et al. (2002) and Martin et al. (2002) data. It is worth noting that calibrations conducted for cold temperatures are steeper than those spanning the whole temperature range (see Chapter 2.5 for further information).

Despite the yet unexplained partition coefficients of most foraminifer species, the Mg/Ca paleothermometer was successfully approved over the past decade in numerous studies using shallow-water planktic foraminifera and deep-water benthic foraminifera (e.g., Elderfield and Ganssen, 2000; Billups and Schrag, 2003; Marchitto and deMenocal, 2003; Rosenthal et al., 2003; Zachos et al., 2003; Saraswat et al., 2005; Groeneveld et al., 2006).

The advantage of this new temperature proxy was that it provided the possibility to eliminate the temperature effect on the stable oxygen isotope fractionation in foraminiferal shells in order to get information on past $\delta^{18}\text{O}$ of seawater (Mashiotta et al., 1999; Elderfield and Ganssen, 2000). The oxygen isotopic composition of seawater is mainly determined by the fractionation during precipitation and evaporation of water at the sea surface. It is, therefore, a recorder of continental ice volume because the lighter isotope ^{16}O is preferentially stored in the ice sheets, whereas the seawater is enriched in the heavier ^{18}O (e.g., Schrag et al., 1996). Additional geographical variations in $\delta^{18}\text{O}$ values of seawater associated with salinity variations exist because of the varying isotopic composition of freshwater (Schmidt et al., 2001). Hence paired measurements of foraminiferal $\delta^{18}\text{O}$ and Mg/Ca allows for the estimation of past global and local seawater salinity variations.

However, early studies of Mg/Ca-temperature calibrations revealed that the calcification temperature is not the sole factor influencing the Mg content of foraminiferal shells (e.g., Bender et al., 1975; Delaney et al., 1985; Nürnberg et al., 1996). Numerous attempts were made to unravel these additional factors by means of downcore, core top and cultured samples. Over the past years, some of the major factors that may affect shell Mg/Ca could largely be separated. These are discussed in the following chapter.

2. Additional influences on foraminiferal Mg/Ca

2.1 Mg/Ca of seawater

The temperature dependence of Mg/Ca in biogenic carbonates was demonstrated in a number of publications, while the influence of seawater Mg/Ca on the Mg incorporation into biogenic calcite was the subject of only a few studies. Delaney et al. (1985) showed that the Mg content in planktic foraminifers increased with increasing Mg/Ca of the solution from which they calcify. Ries (2004) demonstrated that various marine invertebrates (foraminifers not included in this study) recorded the Mg/Ca of ambient seawater, and that the partition coefficients D_{Mg} showed significant changes with ambient seawater Mg/Ca. More recently, culture experiments by Segev and Erez (2006) on shallow benthic foraminifers showed evidence of a considerable positive effect of seawater Mg/Ca on shell Mg/Ca. Changes in Mg/Ca of the past oceans due to tectonic processes and biological evolution (e.g., Stanley and Hardie, 1999; Horita et al., 2002) are therefore one of the main uncertainties which must be considered when applying the Mg/Ca thermometer on longer time scales (e.g., Lear et al., 2000). Nevertheless, past seawater Mg/Ca may present a minor problem on shorter timescales (less than 1.1 Ma) since both Mg and Ca have long residence times in the oceans of 13 and 1.1 Ma, respectively (Broecker and Peng, 1982).

2.2 Salinity

Early culture experiments conducted at different salinities of seawater revealed that salinity has an effect on Mg/Ca in planktic foraminifera, although possibly of minor importance. It was shown that Mg/Ca in *G. sacculifer* increased by approximately 8% per psu (Nürnberg et al., 1996); by 6% per psu in *O. universa* (Lea et al., 1999); and by 5% per psu in *G. ruber* (Kısakürek et al., 2008). The relevance of the salinity effect on Mg/Ca is still a subject of debate. However, increased Mg/Ca ratios observed in planktic foraminifers from the Red Sea and the Mediterranean Sea were attributed to the high salinities of these waters (Ferguson et al., 2008; Groeneveld et al., 2007). Further, the Mg/Ca anomalies observed in Pliocene planktic foraminifers from the Caribbean can possibly be explained with large sea surface salinity fluctuations during the closure of the Panamanian Gateway (Groeneveld et al., 2008). Nonetheless, salinity may also be a factor influencing Mg/Ca in benthic foraminifera, despite supposedly being of minor importance for deep benthic species. This is because of the generally narrow range of salinity in the deep sea, compared to the steep salinity gradients observed in shallow waters.

2.3 Physiological effects (biomineralization)

It was early recognized that the variability of the Mg content between different foraminiferal species is enormous, ranging from less than 0.1 to more than 20 mole% of $MgCO_3$ (Blackmon and Todd, 1959). These differences in Mg/Ca were even observed in different species sharing the same habitat. This suggests that the Mg concentration of shell calcite is related to a biological control on the trace metal uptake. A number of studies demonstrated that Mg/Ca also varied substantially between and within single shells of one species, which can not be

related to environmental changes (Eggins et al., 2003; Hathorne et al., 2003; Reichart et al., 2003; Eggins et al., 2004; Gehlen et al., 2004; Rathmann et al., 2004; Anand and Elderfield, 2005; Sadekov et al., 2005; Toyofuku and Kitazato, 2005; Hintz et al., 2006a, b; Allison and Austin, 2008). This is indicative of physiological factors that strongly govern the incorporation of Mg and other elements into foraminiferal calcite, which are occasionally called “vital effects”.

As already mentioned above, the Mg/Ca ratio in most foraminifer species is considerably lower than in inorganic calcite. The reason for this is that the composition of the solution from which foraminifers precipitate is not equal to that of natural seawater (e.g., Erez, 1978; ter Kuile and Erez, 1988; ter Kuile et al., 1989b; Elderfield et al., 1996). Previous studies showed that foraminifera capture seawater in vacuoles, where the fluid is modified by concentrating essential ions (mainly Ca^{2+}) and increasing pH, in order to achieve supersaturation with respect to calcite (Bentov and Erez, 2005, 2006) (Figure 2-1). It is possible that at the same time the solution is depleted in Mg^{2+} , since it inhibits calcification (e.g., Bender et al., 1975; Mucci and Morse, 1983). After forming a primary wall made of high-Mg calcitic microspherulites embedded within the organic matrix, the vacuoles are then exocytosed (exocytosis = durable process by which a cell directs secretory vesicles out of the cell membrane) into the delimited biomineralization space where the secondary calcite with low Mg is precipitated over the primary calcite (Erez, 2003) (Figure 2-1).

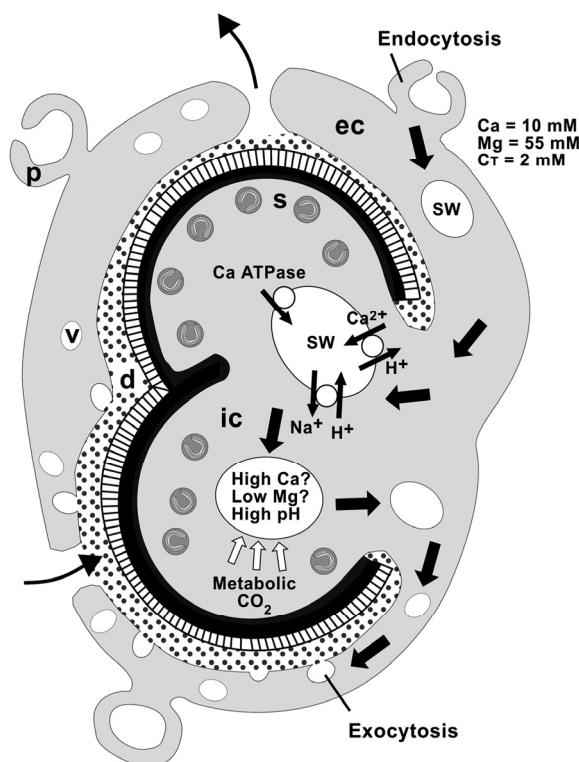


Figure 2-1. Overall scheme describing secondary calcification process in perforate foraminifera. The symbols are: v: vacuole, p: pseudopodia, s: symbiotic algae, d: delimited biomineralization space, ic: intralocellar cytoplasm, ec: extralocellar cytoplasm, sw: seawater. Seawater vacuoles are formed by endocytosis, and during their pathway within the cell various pump and possibly channels operate to increase the pH and possibly Ca^{2+} and the C_T in these vacuoles. These modified seawater vacuoles are exocytosed into the delimited biomineralization space (marked with dense dots) where CaCO_3 is precipitated over the existing shell. It is possible that Mg concentration is lowered in the seawater vacuoles or alternatively an unknown process in the delimited space may sequester it in such a way that low Mg calcite can precipitate (Figure and text from Erez, 2003).

The exact biomineralization mechanisms governing the magnesium uptake are still poorly understood. They comprise physical and chemical processes such as Mg regulation, transport, buffering, and sequestration etc., as well as the temperature effect on ATP hydrolysis and diffusion. The most comprehensive studies on these processes that occur in foraminifers

during calcification are by Erez (2003) and Bentov and Erez (2006). Despite all these complex processes in foraminifers modifying the internal fluid isolated from seawater, shell Mg/Ca appears to record environmental properties of seawater such as temperature. This suggests that there is a distinct inorganic control on Mg/Ca, and possibly a physiological response sensitive to these ambient conditions (Bentov and Erez, 2006).

2.4 Dissolution

The problem of carbonate dissolution affecting the Mg content in foraminiferal shells and other carbonates is one of the best known and most debated issues among “paleothermometrists”. Hecht et al. (1975) and Lorens et al. (1977) recognized that the Mg content in planktic foraminifera was susceptible to dissolution in waters undersaturated with respect to calcite (at $\Delta[\text{CO}_3^{2-}]$ below ~ 0 $\mu\text{mol}/\text{kg}$, Figure 2-2). In the 1990s, several studies revealed that planktic Mg/Ca decreased with increasing water depth at the sites samples were collected from. This suggested that these differences are related to dissolution when shells sink to the seafloor after the death of the foraminifer (Rosenthal and Boyle, 1993; Russell et al., 1994; Brown and Elderfield, 1996; Hastings et al., 1998). Furthermore, Yu et al. (2007a) demonstrated that the use of citrate (a weak acid) for cleaning foraminiferal shells lowered Mg/Ca, in contrast to samples where no citrate was added.

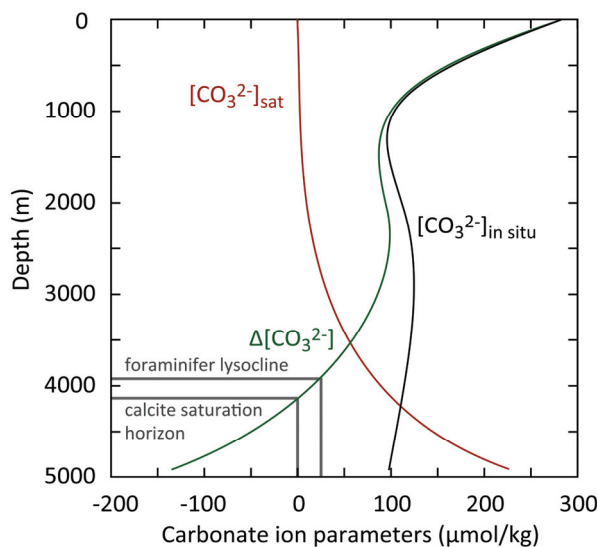


Figure 2-2. Typical carbonate ion profiles in the South Atlantic (GEOSECS station 102). The calcite saturation state $\Delta[\text{CO}_3^{2-}]$ is the difference between the *in-situ* $[\text{CO}_3^{2-}]$ and the calcite saturation concentration $[\text{CO}_3^{2-}]_{\text{sat}}$. The calcite saturation horizon is defined as the depth where $\Delta[\text{CO}_3^{2-}]$ has 0 $\mu\text{mol}/\text{kg}$. Above this level, seawater is oversaturated with respect to calcite. The foraminifer lysocline is the level below which foraminiferal shells start to dissolve. This level is species-specific and lies roughly between 18 and 26 $\mu\text{mol}/\text{kg}$ for planktic foraminifers (Regenberg et al., 2006).

Brown and Elderfield (1996) and Rosenthal et al. (2000) assumed that Mg-rich shell parts are preferentially dissolved, rather than those low in Mg. This idea was previously suggested by Berger (1970) and Savin and Douglas (1973). Such a finding may also explain why the Mg/Ca ratio in foraminiferal shells is distinct between different species. It is therefore plausible that low-Mg species evolved and predominated in geological times with high atmospheric CO_2 and low CaCO_3 saturation, for example during the Eocene (e.g., Demicco et al., 2003), in order to make their shells less susceptible to dissolution, whereas high-Mg species appeared when low $p\text{CO}_2$ and high CaCO_3 saturation conditions prevailed (Martin, 1995).

Since the loss in Mg of planktic foraminifera due to postdepositional dissolution may skew the reconstruction of past water temperatures, several efforts were made to correct for this dissolution effect on Mg/Ca. Rosenthal et al. (2000) suggested using a correction factor based on size-normalized shell mass that is a function of the calcite saturation state. This approach yields consistent glacial-interglacial changes in sea surface temperatures both above and below the lysocline (Rosenthal and Lohmann, 2002). Other studies used a depth-correction to eliminate the dissolution effect on Mg/Ca by assuming that the Mg loss is linear with increasing water depth below certain calcite saturation levels (Lea et al., 2000; Dekens et al., 2002; Regenberg et al., 2006). Basically, the calcite saturation state ($\Delta[\text{CO}_3^{2-}]$) is the difference between the *in-situ* carbonate ion concentration ($[\text{CO}_3^{2-}]$) and the calcite saturation concentration ($[\text{CO}_3^{2-}]_{\text{sat}}$) (Figure 2-2). Dissolution of calcite actually takes place when seawater is undersaturated with respect to calcite ($\Delta[\text{CO}_3^{2-}] < 0 \mu\text{mol/kg}$). It is worth noting that planktic foraminiferal shells start to dissolve at $\Delta[\text{CO}_3^{2-}]$ values of approximately 25 $\mu\text{mol/kg}$, which is well above the modern lysocline (e.g., Dittert and Henrich, 2000; Regenberg et al., 2006).

The effect of dissolution on Mg/Ca in benthic foraminifers is less well defined, since both $\Delta[\text{CO}_3^{2-}]$ and temperature decrease with increasing water depth. Therefore it is difficult to distinguish between the effects of these two factors (Lea, 2003). Nevertheless, benthic foraminiferal shells are generally thought to have higher preservation potential than planktics (e.g., Lear et al., 2000). The study of Lear et al. (2000) on deep-water temperatures over the entire Cenozoic revealed that the benthic Mg/Ca record used was unlikely to be affected by dissolution and/or diagenesis, even when influenced by waters undersaturated with respect to calcite. On the other hand, the core top data of Martin et al. (2002) showed that Mg/Ca in benthic *Cibicidoides* species from the deepest sites fall along a steeper line than predicted from the temperature calibration (Figure 2-3). Depth-related decreases were also found for Cd/Ca, Sr/Ca, and Ba/Ca in the epibenthic species *Planulina (=Cibicidoides) wuellerstorfi* (McCorkle et al., 1995). This suggests that the trace metal content in benthic foraminifera is affected by the carbonate chemistry of seawater (McCorkle et al., 1995; Rosenthal et al., 1997; Martin et al., 2002).

2.5 Carbonate system of seawater

A recent study by Elderfield et al. (2006) observed in the same species collected from global core tops that the residual Mg/Ca ($\Delta\text{Mg/Ca} = \text{Mg/Ca}_{\text{measured}} - \text{Mg/Ca}_{\text{calculated}}$), which represents the portion of Mg/Ca not influenced by temperature, showed a clear positive linear relationship with $\Delta[\text{CO}_3^{2-}]$. This positive trend appeared in both samples stained with Rose Bengal (recently living) and unstained samples. They concluded that the observed anomalies are not related to selective dissolution, but most likely to a primary control of the calcite saturation state on the Mg uptake into shells of benthic foraminifers (Elderfield et al., 2006). A similar relationship between Mg/Ca and $\Delta[\text{CO}_3^{2-}]$ was also reported by Rosenthal et al. (2006) for the aragonitic foraminifer species *Hoeglundina elegans*. Very recently, Raitzsch et al. (2008) (Chapter 5) and Healey et al. (2008) verified this so-called "carbonate ion effect" on benthic Mg/Ca, which is particularly strong at temperatures of less than 4°C.

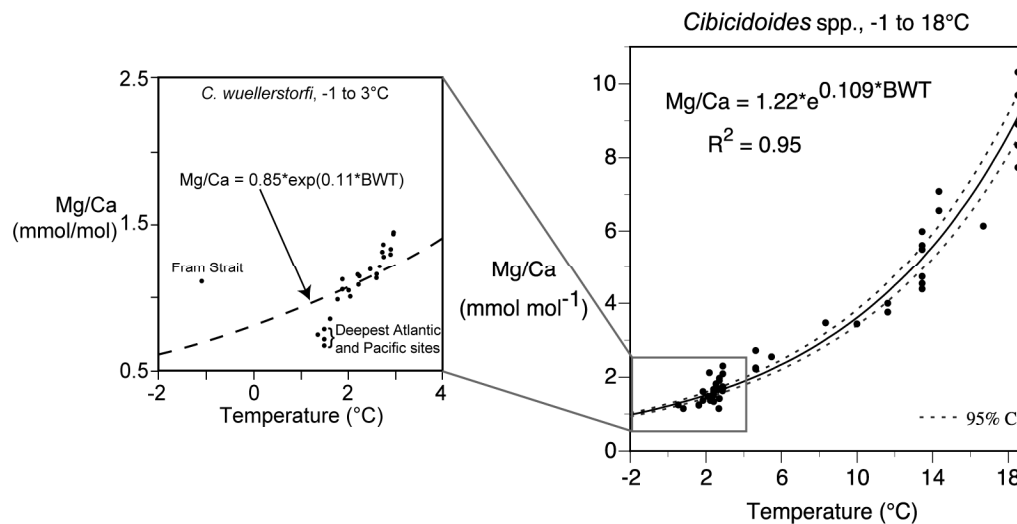


Figure 2-3. Calibration of Mg/Ca in *Cibicidoides* spp. as a function of temperature (modified after Martin et al., 2002). The single-species calibration for *P. wuellerstorfi* within the temperature range from -1 to 3°C yielded a steeper slope (left panel) than predicted from the calibration curve spanning the -1 to 18°C temperature range (right panel). This is very likely related to the carbonate ion effect on benthic Mg/Ca, which is particularly strong at low temperatures where the response of Mg/Ca to temperature is also low.

These new studies showed that the carbonate ion effect is an important factor at low temperatures where the exponential response of Mg/Ca to temperature is low (Figure 2-3). The observed gradients of $\Delta\text{Mg/Ca}$ in benthic foraminifers are between 0.008 and 0.017 mmol/mol per $\mu\text{mol/kg } \Delta[\text{CO}_3^{2-}]$ (Elderfield et al., 2006; Rosenthal et al., 2006; Raitzsch et al., 2008; Healey et al., 2008). This is at odds with results from culture experiments on planktic foraminifera, which revealed that at low pH Mg/Ca decreased with increasing pH or $[\text{CO}_3^{2-}]$ (Lea et al., 1999; Russell et al., 2004; Kısakörek et al., 2008). This indicated that the relationship between Mg/Ca and carbonate ions is opposite between planktic and benthic species. It is even possible that the Mg incorporation into shell calcite in response to changing seawater carbonate chemistry is opposed between different benthic species (see Chapter 6). This suggests that the Mg uptake into shells with regard to varying carbonate ions is mainly biologically controlled. However, it appears that the carbonate ion effect must be quantified for each species, by means of further culture and core top samples.

The strong influence of seawater carbonate chemistry on the Mg uptake into benthic foraminifers is critical, since it may bias Mg/Ca based temperature reconstructions to a considerable degree. Further, it was reported that carbonate ions also have an effect on the stable isotopic composition of foraminifera (Spero et al., 1997; Bijma et al., 1999). Hence the use of an independent carbonate ion proxy obtained from the same biotic carrier provides the opportunity to correct for the carbonate ion effect on both Mg/Ca and stable isotopes in foraminiferal shells. In Chapter 3, the boron and uranium composition of shell calcite are discussed as new and very promising tools for estimating carbonate system variations of seawater.

3. B/Ca and U/Ca as independent carbonate system proxies

Since the mid 1990s, the boron isotopic composition $\delta^{11}\text{B}$ ($^{11}\text{B}/^{10}\text{B}$) in foraminifers has been used to reconstruct past ocean pH, for both surface waters from planktic foraminifers (e.g., Spivack et al., 1993; Wara et al., 2003; Foster, 2008) and deep waters from benthic foraminifers (e.g., Sanyal et al., 1995; Sanyal et al., 1997; Hönisch et al., 2008). The boron composition of marine carbonates is a suitable tracer for the carbonate system, since the fractionation between the two aqueous boron species $\text{B}(\text{OH})_4^-$ and $\text{B}(\text{OH})_3$ in seawater is controlled by pH (Figure 3-1a). Since only $\text{B}(\text{OH})_4^-$ is incorporated into carbonate minerals with insignificant fractionation during uptake, the relative amount of this species in calcite is supposed to represent the pH condition during precipitation (Hemming and Hanson, 1992; Hemming et al., 1995). A strong correlation in the boron composition of calcite with pH was verified by inorganic calcification experiments (Hemming et al., 1995; Sanyal et al., 2000). Based on this pH-boron speciation relationship, the boron content in foraminiferal shells, measured as the ratio of B to Ca (B/Ca), is also expected to vary as a function of pH.

The equilibrium between both species is defined as follows:



The equilibrium constant, K_B^* , is defined as:

$$K_B^* = \frac{[\text{H}^+][\text{B}(\text{OH})_4^-]}{[\text{B}(\text{OH})_3]} \quad (3-2)$$

Hemming and Hanson (1992) proposed the following mechanism for boron substitution into carbonate:



The exchange distribution coefficient, K_D , for B can be expressed by:

$$K_D = \frac{[\text{B}/\text{Ca}]_{\text{solid}}}{[\text{B}(\text{OH})_4^-/\text{HCO}_3^-]_{\text{seawater}}} \quad (3-4)$$

Equation 3-4 predicts that B/Ca in calcite is a function of $[\text{B}(\text{OH})_4^-/\text{HCO}_3^-]$ in seawater, which in turn is controlled by pH (Yu and Elderfield, 2007). However, this is not entirely correct for benthic foraminifera. The empirical study of Yu and Elderfield (2007) on benthic species from a wide range of core top samples revealed that shell B/Ca is not simply a function of pH. Rather, it is dependent on the calcite saturation state, which suggests that the boron enrichment factor in the internal calcification pool is proportional to $\Delta[\text{CO}_3^{2-}]$. The internal [B] in turn controls the internal $[\text{B}(\text{OH})_4^-/\text{HCO}_3^-]$. Consequently, a strong relationship between B/Ca in benthic foraminifera and $\Delta[\text{CO}_3^{2-}]$ exists (Yu and Elderfield, 2007).

The B/Ca ratio in benthic foraminifera seems a robust tool for estimating past deep water $\Delta[\text{CO}_3^{2-}]$, despite large differences in K_D found between different species. However, secondary effects such as temperature or dissolution appear to be minimal (Yu and Elderfield, 2007; Yu et al., 2007a). Yu and Elderfield (2007) demonstrated that the deep water $\Delta[\text{CO}_3^{2-}]$ during the Last Glacial Maximum, calculated with benthic B/Ca, were in good agreement with other geochemical proxies.

Compared with boron, little attention has been paid to the uranium content in foraminiferal shells. Similarly to boron, uranium exists as different species in seawater, whose relative amounts are also dependent on pH (Figure 3-1b). Russell et al. (1994) showed through culture experiments that U/Ca in planktic foraminifera is proportional to U/Ca of seawater from which shells calcified. U/Ca in the core top samples of Russell et al. (2004) decreased with water depth (more significant in planktic than in benthic species). Since U is conservative in seawater, Russell et al. (1994) assumed that shell U/Ca is affected by partial dissolution leading to lower U concentrations. However, downcore records over the Last Glacial Maximum revealed that U/Ca in planktic foraminifera correlated well with Mg/Ca. This indicated that U/Ca is possibly controlled by temperature and/or carbonate ion concentration. Russell et al. (1996) ruled out that observed U/Ca variations were caused by dissolution because of the same trend in different cores with different dissolution histories. Also potential changes in seawater U/Ca were unlikely since the magnitude was too large to be caused by variation of riverine input.

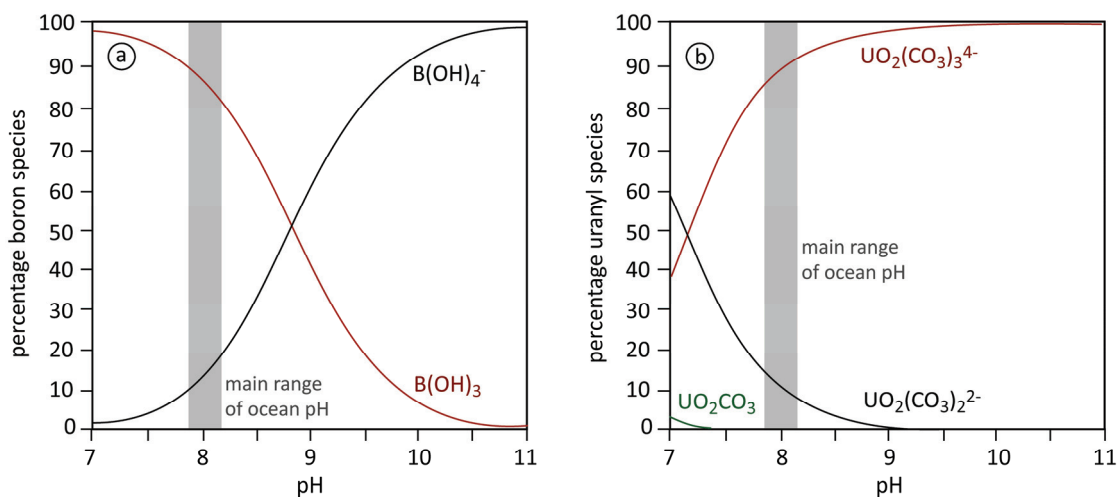


Figure 3-1. Boron and uranyl speciation in seawater as a function of pH. Gray bars indicate the pH range in the modern oceans. **a)** Boron exists as two species in seawater where $B(OH)_4^-$, incorporated into calcite, is more abundant at high pH (figure modified after Hemming and Hanson, 1992). **b)** Uranium exists in seawater mainly as three uranyl carbonate complexes of which UO_2CO_3 and $UO_2(CO_3)_2^{2-}$ are preferentially incorporated into calcite. Hence U/Ca in foraminifer tests tends to decrease with increasing pH (speciation calculated with the program of Puigdomenech (2004)).

Culture experiments on planktic foraminifer species provided evidence that shell U/Ca was strongly influenced by pH in a way that U/Ca decreased exponentially with increasing pH or $[CO_3^{2-}]$ (Russell et al., 2004). No variations with changing temperature were found between 15 and 25°C, which suggested that planktic U/Ca is a suitable tool for the reconstruction of past sea surface $[CO_3^{2-}]$. Based on U/Ca, Caribbean and tropical Atlantic sea surface $[CO_3^{2-}]$ were estimated to be about 110 and 80 $\mu\text{mol/kg}$, respectively, higher in the last glacial period. When compared to Holocene values, these estimations are consistent with other pH proxies such as boron isotopes (Russell et al., 2004).

Uranium exists in seawater as a group of carbonate complexes (Djogic et al., 1986), mainly consisting of three species, the relative abundances of which are dependent on pH. The chemical reactions are defined as follows:



Russell et al. (2004) assumed that owing to the coordination changes required to incorporate $\text{UO}_2(\text{CO}_3)_3^{4-}$ into calcite, UO_2CO_3 and/or $\text{UO}_2(\text{CO}_3)_2^{2-}$ were incorporated instead. As the abundance of these species decreased with increasing $[\text{CO}_3^{2-}]$ (Figure 3-1b), the uptake of either or both into the calcite lattice in preference to UO_2CO_3 is consistent with the inverse correlation of U/Ca with $[\text{CO}_3^{2-}]$ (Russell et al., 2004). However, a similar relationship for benthic foraminifera has not yet been published. As part of this dissertation, I will show that there is evidence for a close link between U/Ca in benthic foraminifers and the calcite saturation state, providing a promising tool for the estimation of past deep water $\Delta[\text{CO}_3^{2-}]$ (see Chapter 7).

4. Analytical techniques and samples

Laser Ablation Inductively Coupled Plasma Mass Spectrometry (LA-ICP-MS) was used as a main analytical tool for this thesis. It is a micro-analytical technique for the determination of element concentrations in solid samples. Laser ablation in combination with the speed, sensitivity and multi-element capability of ICP-MS rivals with other micro-analytical techniques (e.g., electron microprobe or ion probe). This enables the measurement of a large number of elements at low levels, in contrast to electron microprobe or ion probe which are limited to a narrower range of elements.

For an analysis, the sample is placed in a sample chamber mounted on a stage that can be moved in three directions related to the laser beam (z direction for focusing the laser beam). The manual positioning of the sample is facilitated by a camera attached on top of the laser ablation system. This allows the observation of the ablation process on a monitor (Figure 4-1). Laser ablation is a physical process for mechanical break-up of a solid sample induced by a pulsed UV laser beam that produces micro-particles. The instrument settings used in this study are a repetition rate of 5-10 Hz, a laser wavelength of 193 nm, and a beam diameter of 35-80 μm . The aerosol is transported out of the sample chamber by a helium carrier gas and admixed with argon before entering the torch of the introduction system ICP-MS (Figure 4-1).

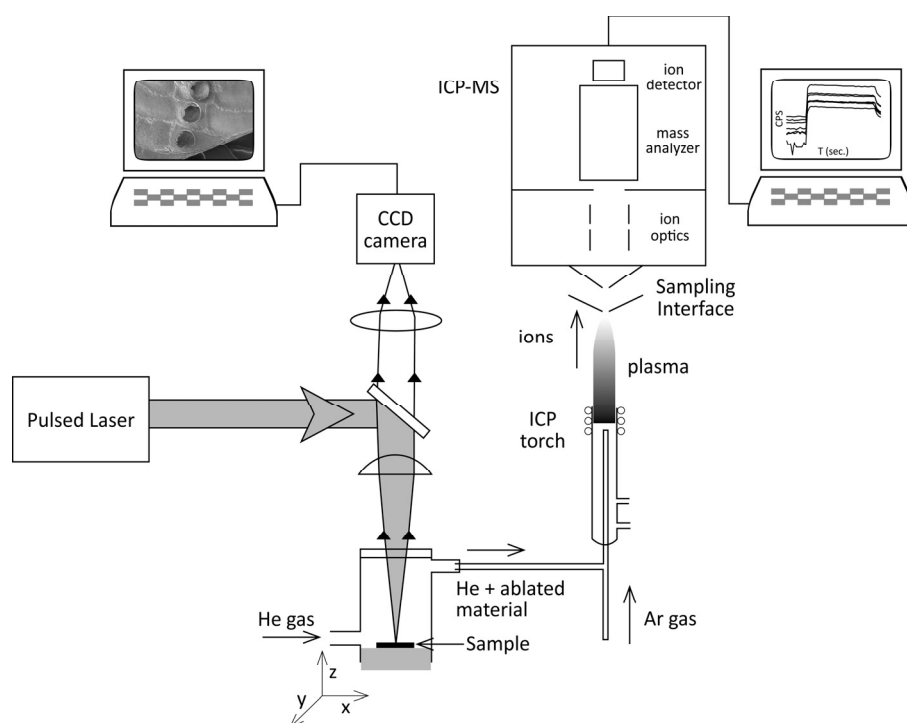


Figure 4-1. Scheme of a laser ablation system connected to an inductively coupled plasma mass spectrometer (ICP-MS). The ablated material is transported out of the sample chamber by a helium carrier gas and admixed with argon before entering the plasma torch of the introduction system. Both the ablation process and the time resolved signal recording can be observed on separate monitors (Scheme modified after Applied Spectra – A Laser Solutions Company, <http://www.appliedspectra.com/index.php>, date accessed: 03 July 2008).

Within the torch an Ar plasma of approximately 6000°C the sample particles are ionized and then sucked by a high-powered vacuum through the interface into the mass spectrometer. Electromagnetic lenses focus the ion beam into the mass analyzer, where the ions are detected according to their atomic masses (Figure 4-1). The output data (in counts per second (CPS)) have to be converted to concentrations (ppm). This is achieved using an external standard with well-known concentrations (usually silicate standards of the NIST series) and calcium as an internal standard for foraminiferal calcite that is known to have ~40%wt (for further information, see Chapters 5.3., 6.2.3 and 7.2).

For this thesis, the LA-ICP-MS method was used to analyze element to calcium ratios in the deep-sea benthic foraminifer species *Planulina wuellerstorfi* and *Cibicidoides mundulus* from core top sediments, as well as in cultured specimens of the shallow-water benthic species *Heterostegina depressa* and *Ammonia tepida* (Figure 4-2).

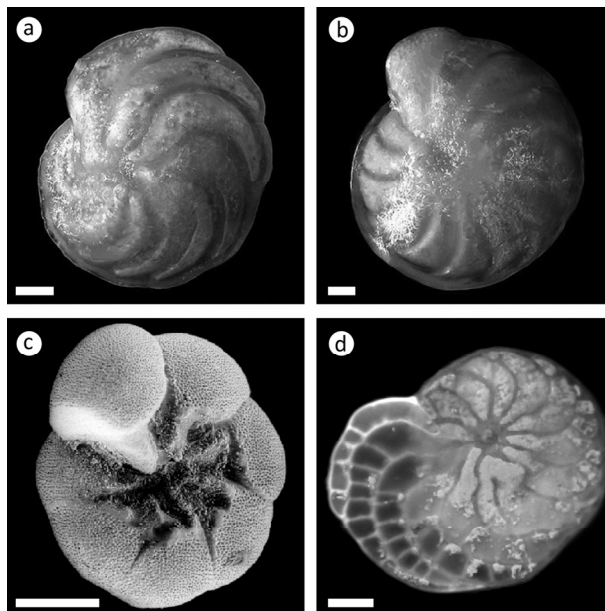


Figure 4-2. Photographs of foraminifer species used for this thesis. Scale bars are 100 μm . Deep-sea foraminifers: **a)** *Planulina* (=Cibicidoides) *wuellerstorfi*, epibenthic (from Holbourn and Henderson, 2002); **b)** *Cibicidoides mundulus* (=kullenbergi), epi- to shallow endobenthic (from Holbourn and Henderson, 2002). Shallow-water foraminifers: **c)** *Ammonia tepida*, temperate, epi- to infaunal, opportunistic (SEM picture from University of California Museum of Paleontology, <http://www.ucmp.berkeley.edu>); **d)** *Heterostegina depressa*, tropical, epibenthic, with endosymbiotic algae (microscope photograph taken at Utrecht University).

Apart from other biogenic carbonate samples, LA-ICP-MS has been successfully employed to measure the trace elemental composition in foraminiferal shells by Eggins et al. (2003), Hathorne et al. (2003), Reichart et al. (2003), Eggins et al. (2004), Rathmann et al. (2004) and de Nooijer et al. (2007). This technique has several advantages over the traditional solution method:

- (1) It enables the determination of intra-shell and inter-shell element variability.
- (2) It is micro-destructive and therefore enables remeasurements and/or subsequent stable isotope measurements on the same biotic carrier.
- (3) It is a powerful and precise method, particularly in case of limited sample material. Basically, single shells or even shell fragments can be analyzed.
- (4) Since there is no need or a minimum of sample preparation, uncertainties related to effects of cleaning procedures on trace element concentrations can be minimized.

(5) The absence of acids and water, used in the solution method, greatly reduces the interferences by oxide ions.

Conversely, LA-ICP-MS is less accurate than the solution method because the element concentrations of one sample are averaged over a number of spatially limited analyses (Figure 4-3). On the other hand, the solution method provides information on the average concentrations of numerous individuals pooled together. Based on five measurements of the relatively homogeneous JCT-1 carbonate standard with LA-ICP-MS, the reproducibility for Mg/Ca is better than 3%, whereas it is approximately 18% for foraminiferal calcite (Chapter 7.7). Therefore the accuracy of laser ablation analyses of foraminiferal element concentrations is limited by intra-shell heterogeneities, rather than by analytical precision.

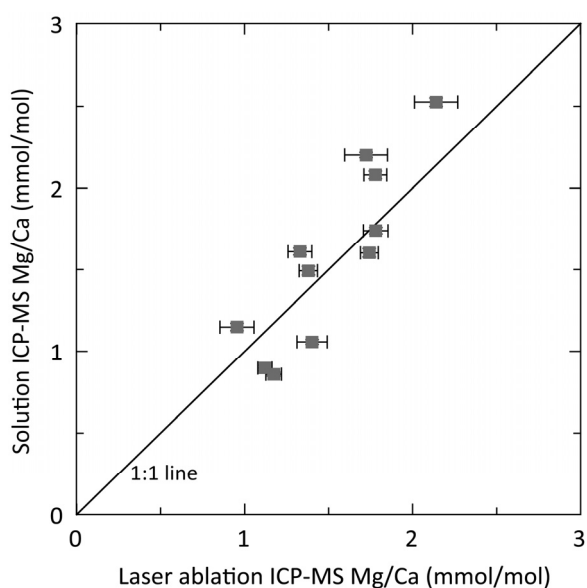


Figure 4-3. Comparison of solution ICP-MS with laser ablation-derived Mg/Ca data. Error bars are standard errors of the mean. Due to the intra-test heterogeneity of Mg/Ca, LA-ICP-MS analyses are more inaccurate than the solution method. Note that shells are from one sample, but different shells were used for each method.

Further, there is a need for more homogeneous external carbonate standards for matrix-matched calibration when measuring foraminiferal calcite. However, non matrix-matched calibration using the silicate standards NIST610 or NIST612 was proven accurate for many elements such as for magnesium, boron and uranium reported in this thesis (see Chapter 7.7).

II. THESIS OUTLINE

The focus of this thesis was to unravel and to quantify the separate effects of temperature and seawater carbonate chemistry on Mg/Ca in benthic foraminiferal shells, which are supposed to exert the main influences on the Mg incorporation. Further, B/Ca and U/Ca were examined as new carbonate ion proxies that may be used to correct for the carbonate ion effect on Mg/Ca. The results arising from these studies are presented in the following three manuscripts:

Chapter 5: Benthic foraminifer Mg/Ca anomalies in South Atlantic core top sediments and their implications for paleothermometry

Markus Raitzsch, Henning Kuhnert, Jeroen Groeneveld, Torsten Bickert (2008)

Geochemistry Geophysics Geosystems, 9(5), Q0510, doi:10.1029/2007GC001788

This manuscript addresses Mg/Ca in the benthic foraminifer species *P. wuellerstorfi* (Figure 4-2a) and *C. mundulus* (Figure 4-2b), which are the most frequently used species in paleoceanography for estimations of past bottom water conditions. In this context, we quantified the effects of both temperature and seawater carbonate chemistry on Mg/Ca from core top samples taken in the South Atlantic. We could confirm recent studies of Elderfield et al. (2006) and Rosenthal et al. (2006) that $\Delta[\text{CO}_3^{2-}]$ plays an important role in the Mg uptake into shell calcite.

Chapter 6: The effect of calcite saturation state on Mg/Ca in cultured benthic foraminifera: *Heterostegina depressa* and *Ammonia tepida*

Markus Raitzsch, Adriana Dueñas-Bohórquez, Gert-Jan Reichart, Torsten Bickert

In preparation for *Geochimica et Cosmochimica Acta*

In this manuscript, results from growth experiments in collaboration with the University of Utrecht are presented. These experiments on *A. tepida* (Figure 4-2c) and *H. depressa* (Figure 4-2d) show that the effect of calcite saturation state on Mg/Ca in benthic foraminifers is a fundamental phenomenon. The calcite saturation state (Ω) can also be changed by varying the calcium concentration, instead of carbonate ion concentration. Therefore we conducted experiments with different $[\text{Ca}^{2+}]$ but constant Mg/Ca, in order to rule out an influence of seawater Mg/Ca. To our knowledge, such an experiment was not yet carried out before. We can show that not only the magnitude but also the direction Ω influences benthic Mg/Ca is completely species-specific.

Chapter 7: B/Ca and U/Ca in benthic foraminifers: New proxies for the seawater carbonate system

Markus Raitzsch, Ed C. Hathorne, Henning Kuhnert, Jeroen Groeneveld, Torsten Bickert

Under review in *Geology*

This article deals with B/Ca and U/Ca in benthic foraminifers from core top samples as promising independent proxies for $\Delta[\text{CO}_3^{2-}]$. Benthic B/Ca was shown by Yu and Elderfield (2007) to faithfully record $\Delta[\text{CO}_3^{2-}]$, but the link between U/Ca and $\Delta[\text{CO}_3^{2-}]$ is a novelty. Besides important information on the past seawater carbonate system, these proxies provide the possibility to correct shell Mg/Ca for the carbonate ion effect examined in Chapters 5 and 6. Our study shows that inaccuracy of temperature estimations improved significantly in this manner.

Apart from my own PhD topic, I am also involved in three projects to which I will contribute as a coauthor in future publications. The results of these studies were preliminarily presented at following conferences:

Salinity influence on planktonic foraminiferal Mg/Ca: A case study from the Red Sea

Jeroen Groeneveld, Markus Raitzsch, Michael Siccha, Gabriele Trommer, Christoph Hemleben, Michal Kučera

9th International Conference on Paleoceanography, Shanghai (2007), Program and Abstracts: p. 54

Planktic foraminiferal Mg/Ca ratios in core top and plankton tow samples from the Red Sea, determined with the solution method, were considerably higher than predicted from the Mg/Ca-temperature relationship. The increased Mg/Ca ratios are possibly related to the high salinity of the Red Sea. I analyzed the trace element distribution in selected shells with Laser Ablation ICP-MS in order to detect potential sedimentary contaminants and inorganic precipitates attached to the shells.

Mg/Ca ratios of *Globigerina bulloides* and *Globorotalia inflata* from Coretops and Plankton Tows in the Western Mediterranean Sea

Ulrike van Raden, Jeroen Groeneveld, Markus Raitzsch, Christoph Hemleben, Michal Kučera

SwissSed (16th Meeting of Swiss Sedimentologists), Fribourg (2008): Poster

Similarly to the study mentioned before, increased Mg/Ca ratios found in planktic foraminifers collected from surface sediments and plankton tows in the Mediterranean Sea are presumably related to the increased salinity of this water. Also here, I analyzed selected shells using LA-ICP-MS to detect possible contaminants.

Non matrix-matched calibration of 193nm laser ablation ICP-MS analysis of calcium carbonate samples using NIST 612 and 610 glasses: Inaccurate Mg calibration and variable laser parameters

Ed C. Hathorne, Markus Raitzsch, Henning Kuhnert

9th European Workshop on Laser Ablation in Elemental and Isotopic Analysis, Prague (2008), Workshop programme and abstracts: p. 54

This study focuses on the use of silicate standards (NIST) for laser ablation analyses of biogenic carbonates. Due to its hardness, the silicate standard is usually ablated with a higher energy density than the carbonate sample in order to enhance signal stability. This procedure may lead to different element fractionation factors between the silicate and the carbonate. We therefore conducted a number of measurements using different carbonate reference materials (J Cp-1, J Ct-1, OKA calcite, in-house CaCO₃ powder pellet) in order to survey the non matrix-matched calibration against the NIST. We can show for many elements that non matrix-matched calibration produces accurate element concentrations, even when instrumental parameters such as energy density and beam diameter were changed between standard and sample. I carried out parts of the measurements and data analysis.

III. MANUSCRIPTS

5. Benthic foraminifer Mg/Ca anomalies

Benthic foraminifer Mg/Ca anomalies in South Atlantic core top sediments and their implications for paleothermometry

Markus Raitzsch, Henning Kuhnert, Jeroen Groeneveld, Torsten Bickert

MARUM – Center for Marine Environmental Sciences, University of Bremen, Leobener Straße, 28359 Bremen, Germany

Published in *Geochemistry Geophysics Geosystems*, 9(5), Q0510, doi:10.1029/2007GC001788

We used modern epibenthic foraminifer tests of *Cibicidoides mundulus* and *Planulina wuellerstorfi* from South Atlantic core top sediments in order to establish Mg/Ca-temperature relationships for the temperature range from 0 to 15°C. We obtained the following calibrations: Mg/Ca (mmol/mol) = $0.830 \cdot \exp(0.145 \cdot \text{BWT } (^{\circ}\text{C}))$ for *P. wuellerstorfi*, and Mg/Ca (mmol/mol) = $0.627 \cdot \exp(0.143 \cdot \text{BWT } (^{\circ}\text{C}))$ for *C. mundulus*. However, a number of tests, especially those bathed in North Atlantic Deep Water, revealed higher Mg/Ca ratios than predicted from the calibration. Our data suggest that $\Delta[\text{CO}_3^{2-}]$ of bottom water exerts a significant control on $\Delta\text{Mg/Ca}$ (temperature-corrected) of *C. mundulus* ($\Delta\text{Mg/Ca} = 0.017 \cdot \Delta[\text{CO}_3^{2-}] - 0.14$), while $\Delta\text{Mg/Ca}$ of *P. wuellerstorfi* is more likely to be governed by TCO_2 ($\Delta\text{Mg/Ca} = -0.007 \cdot \text{TCO}_2 + 15$). Since both $\Delta[\text{CO}_3^{2-}]$ and TCO_2 are closely linked to $[\text{CO}_3^{2-}]$, it is inferred that carbonate ion acts as secondary control, after temperature, on benthic shell Mg/Ca below ~4°C. A drop in $[\text{CO}_3^{2-}]$ by 25 $\mu\text{mol/kg}$ at 4 km water depth, as suggested for the Last Glacial Maximum, would decrease Mg/Ca by up to 0.4 mmol/mol, which leads to an underestimation of bottom water temperature by ~3.5°C. Therefore our results indicate that the Mg/Ca thermometer should be used cautiously for benthic foraminifers where changes in the carbonate chemistry are present in the paleoceanographic record.

5.1 Introduction

A close relationship between the ratio of Mg to Ca in foraminiferal shells and calcification temperature was first recognized in the early 1970s by Savin and Douglas (1973) and Bender et al. (1975). Over the past decade, the Mg/Ca thermometer has developed into a widely used tool in paleoceanography (e.g., Elderfield and Ganssen, 2000; Lea et al., 1999; Lea et al., 2000; Mashiotta et al., 1999; Nürnberg et al.,

1996; Nürnberg and Groeneveld, 2006). Mg/Ca-temperature calibrations have also been established for the benthic genus *Cibicidoides*, most of which revealed empirical exponential relationships (Billups and Schrag, 2002; Elderfield et al., 2006; Lear et al., 2002; Marchitto et al., 2007; Martin et al., 2002; Rathburn and De Deckker, 1997; Rosenthal et al., 1997). Since many calibrations on *Cibicidoides spp.* are

based on multiple species, some uncertainties due to tense interspecific differences remain. Therefore it is recommended to use single-species calibrations (Elderfield et al., 2006; Rosenthal et al., 1997).

Although Mg/Ca is primarily a temperature proxy, secondary factors that affect Mg incorporation into foraminiferal tests need to be considered, including salinity (Groeneveld et al., 2008; Nürnberg et al., 1996), pH (Lea et al., 1999; Russell et al., 2004), seawater Mg/Ca (Segev and Erez, 2006), carbonate ion concentration (Russell et al., 2004) and carbonate ion saturation state (Elderfield et al., 2006). Furthermore, a physiological control on shell Mg/Ca is indicated by significant variations between and within single shells (e.g., Anand and Elderfield, 2005; Bentov and Erez, 2006; Eggins et al., 2004; Hathorne et al., 2003; Hintz et al., 2006a, b; Rathmann et al., 2004; Reichart et al., 2003; Toyofuku and Kitazato, 2005). Apart from factors governing the primary shell composition, Mg/Ca is also influenced by post-depositional processes including selective dissolution of Mg-rich shell parts and layers (e.g., Brown and Elderfield, 1996; Dekens et al., 2002; Regenberg et al., 2006; Rosenthal and Lohmann, 2002; Rosenthal et al., 2000).

As indicated above, the carbonate chemistry of the ambient water exerts an important control on the incorporation of Mg during shell growth. Rosenthal et al. (2006) ascertained lowered Mg/Ca in the aragonitic benthic species *Hoeglundina elegans* in response to decreasing $\Delta[\text{CO}_3^{2-}]$ with a sensitivity of 0.017 mmol/mol per $\mu\text{mol/kg}$ below a threshold value of 15 $\mu\text{mol/kg}$, while above this level no influence of

$\Delta[\text{CO}_3^{2-}]$ was observable. They attributed this effect to biological manipulation of the calcifying solution in undersaturated waters in order to reach internal oversaturation with respect to aragonite. Such a threshold value has not been observed by Elderfield et al. (2006) for the calcitic benthic species *Planulina wuellerstorfi*, although it is not clear whether there is one above ~ 70 $\mu\text{mol/kg}$, the highest $\Delta[\text{CO}_3^{2-}]$ value in their data set. The sensitivity for *P. wuellerstorfi* is 0.0086 mmol/mol per $\mu\text{mol/kg}$. This value is lower than that for *H. elegans*, but the direction $\Delta[\text{CO}_3^{2-}]$ influences benthic shell Mg/Ca seems to be the same for calcitic and aragonitic genera. In general, the potential impact of the carbonate system on shell Mg/Ca is particularly important for deep-sea foraminifera: at low temperatures the sensitivity of the Mg/Ca thermometer is also low (most empirical relationships are exponential). At the same time, the carbonate saturation state is low, which potentially increases its influence on Mg/Ca.

In this study we aim at (I) establishing temperature calibrations and (II) quantifying the impact of the carbonate chemistry (total inorganic carbon, carbonate ion concentration, and carbonate ion saturation state) of the ambient seawater on shell Mg/Ca for the common benthic species *Planulina wuellerstorfi* and, for the first time, *Cibicidoides mundulus*. Other potential factors have also been considered but seem to be insignificant compared to seawater temperature and carbonate chemistry. A relevant influence of seawater Mg/Ca is unlikely since its variability in the open ocean is too small to explain large differences in shell Mg/Ca

(Broecker and Peng, 1982). Carbonate dissolution effects can also be excluded as tests used for the calibration were recently living, indicated by Rose Bengal staining. We used South Atlantic core tops in ~200 to ~4700 m depth, which cover the temperature range from ~0 to ~15°C and represent all major intermediate and deep-water masses.

5.2 Oceanographic setting

North Atlantic Deep Water (NADW) is a major component of the sub-surface South Atlantic. This water mass is slightly supersaturated with respect to calcite (Broecker and Peng, 1982, 1989) and occupies the depth interval between around 1500 and 4000 m. It thins toward the south, where it subdivides the northward flowing Circum-

polar Deep Water into a lower (LCDW) and an upper (UCDW) branch (Figure 5-1).

The LCDW can be distinguished from NADW by a drop in the saturation state with respect to calcium carbonate. The LCDW and the underlying Weddell Sea Deep Water (WSDW) are frequently referred to as Antarctic Bottom Water (AABW). Because the Walvis Ridge and the Mid-Atlantic Ridge (MAR) act as submarine barriers, only small quantities of AABW can enter the eastern South Atlantic via the Walvis Passage (Shannon and Chapman, 1991) and the Romanche Fracture Zone (Mercier et al., 1994). Therefore the Guinea and Angola Basins are predominantly filled with NADW (Figure 5-1).

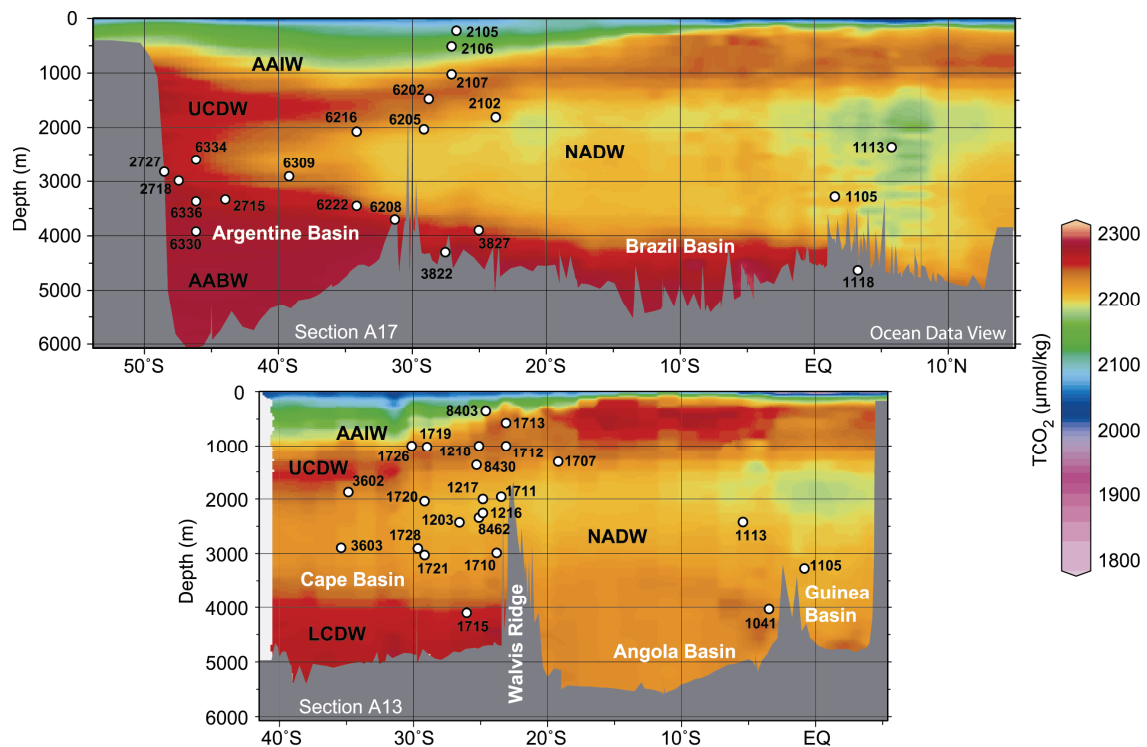


Figure 5-1. WOCE (World Ocean Circulation Experiment) sections A13 and A17 (generated with Ocean Data View (Schlitzer, 2005)) showing total inorganic carbon distribution in the South Atlantic (Schlitzer, 2000). See Figure 5-2 for tracks of sections. Nearby GeoB stations (Table 1, Figure 5-2) are shown as well. Water mass bodies are abbreviated as follows: AAIW, Antarctic Intermediate Water; UCDW, Upper Circumpolar Water; NADW, North Atlantic Deep Water; LCDW, Lower Circumpolar Water; AABW, Antarctic Bottom Water.

Table 1. Sample Stations^a

| Station | Latitude | Longitude | Water Depth, m | BWT, °C | Mg/Ca, mmol/mol | | Geochemical Sampling Stations | | | Units in $\mu\text{mol/kg}$ | | | Salinity, psu |
|-----------------|----------|-----------|-------------------|------------|-------------------------|--------------------|----------------------------------|----------|-----------|-----------------------------|----------------------------------|----------------------------|------------------|
| | | | | | <i>P. wuellerstorfi</i> | <i>C. mundulus</i> | Station | Latitude | Longitude | TCO ₂ | [CO ₃ ²⁻] | $\Delta[\text{CO}_3^{2-}]$ | |
| Brazil Basin | | | | | | | | | | | | | |
| GeoB 1118 | -3.34 | -16.26 | 4675 | 0.86 | 0.99 | - | SAVE 27 | -2.41 | -20.15 | 2252.99 | 100.82 | -3.43 | 34.72 |
| GeoB 2102 | -23.983 | -41.2 | 1805 | 3.88 | 1.98 | - | SAVE 110 | -23.99 | -40.17 | 2176.87 | 107.41 | 46.81 | 34.9 |
| GeoB 2105 | -26.738 | -46.738 | 202 | 14.85 | - | 5.47 | | | | | | | |
| GeoB 3809 | -31.053 | -16.33 | 3470 | 2.11 | 1.73 | 1.52 | | | | | | | |
| GeoB 3810 | -31.133 | -16.838 | 3810 | 1.77 | 1.76 | - | | | | | | | |
| GeoB 3812 | -31.615 | -19.76 | 4204 | 1.68 | 1.40 | 0.95 | | | | | | | |
| GeoB 3822 | -27.627 | -37.95 | 4273 | 0.43 | 0.84 | 0.52 | GEOSECS 58 | -27.00 | -37.02 | 2261.54 | 98.54 | 1.91 | 34.67 |
| GeoB 3827 | -25.032 | -38.548 | 3842 | 1.53 | 1.37 | 0.71 | GEOSECS 58 | -27.00 | -37.02 | 2235.90 | 109.77 | 20.70 | 34.77 |
| Argentine Basin | | | | | | | | | | | | | |
| GeoB 1707 | -19.695 | 10.655 | 1234 | 3.59 | 1.51 | - | | | | | | | |
| GeoB 2106 | -27.098 | -46.497 | 502 | 9 | 1.88 | - | | | | | | | |
| GeoB 2107 | -27.18 | -46.457 | 1052 | 3.55 | 1.48 | 1.10 | | | | | | | |
| GeoB 2715 | -43.903 | -57.662 | 3277 | 0.94 | 1.02 | - | | | | | | | |
| GeoB 2718 | -47.307 | -58.173 | 2991 | 1.2 | 0.94 | 0.91 | SAVE 177 | -47.02 | -57.78 | 2264.18 | 96.72 | 20.89 | 34.72 |
| GeoB 2727 | -48.013 | -56.538 | 2819 | 1.39 | 1.04 | - | SAVE 177 | -47.02 | -57.78 | 2261.94 | 97.45 | 24.04 | 34.72 |
| GeoB 6202 | -29.087 | -47.17 | 1493 | 3.35 | 1.55 | 1.60 | | | | | | | |
| GeoB 6205 | -29.5 | -46.918 | 2004 | 3.81 | 1.43 | 1.70 | | | | | | | |
| GeoB 6208 | -31.808 | -45.665 | 3693 | 0.39 | 0.84 | - | GEOSECS 60 | -32.97 | -42.51 | 2246.79 | 104.77 | 18.17 | 34.73 |
| GeoB 6216 | -34.617 | -51.234 | 2032 | 3.69 | 1.55 | - | SAVE 312 | -35.16 | -51.45 | 2179.10 | 118.70 | 55.43 | 34.86 |
| GeoB 6222 | -34.081 | -48.615 | 3450 | 1.27 | 1.23 | - | SAVE 307 | -36.32 | -49.50 | 2234.33 | 101.41 | 18.70 | 34.75 |
| GeoB 6309 | -39.167 | -54.145 | 2869 | 0.93 | 1.15 | 0.95 | | | | | | | |
| GeoB 6330 | -46.145 | -57.557 | 3874 | 0.43 | 0.95 | - | SAVE 177 | -47.02 | -57.78 | 2277.61 | 96.30 | 6.69 | 34.7 |
| GeoB 6334 | -46.087 | -58.518 | 2597 | 1.57 | 1.27 | 1.12 | SAVE 177 | -47.02 | -57.78 | 2259.70 | 97.37 | 26.98 | 34.72 |
| GeoB 6336 | -46.142 | -57.845 | 3398 | 0.92 | 1.17 | - | SAVE 177 | -47.02 | -57.78 | 2268.66 | 96.98 | 15.08 | 34.69 |
| Guinea Basin | | | | | | | | | | | | | |
| GeoB 1041 | -3.48 | -7.59 | 4035 | 2.51 | 1.57 | - | GEOSECS 109 | -2.00 | -4.50 | 2207.69 | 119.49 | 27.11 | 34.87 |
| Angola Basin | | | | | | | | | | | | | |
| GeoB 1729 | -28.892 | 1.002 | 4401 | 2.36 | 1.49 | 1.16 | SAVE 217 | -30.00 | -1.25 | 2221.64 | 118.54 | 19.55 | 34.86 |
| GeoB 3803 | -30.348 | -8.572 | 4173 | 2.43 | 1.30 | 1.21 | SAVE 136 | -30.02 | -5.04 | 2202.56 | 120.42 | 25.60 | 34.87 |
| GeoB 3804 | -30.743 | -8.77 | 3882 | 2.43 | 1.54 | 1.65 | SAVE 136 | -30.02 | -5.04 | 2205.13 | 121.68 | 31.93 | 34.87 |
| Cape Basin | | | | | | | | | | | | | |
| GeoB 1710 | -23.43 | 11.7 | 2987 | 2.57 | 1.50 | 1.25 | GEOSECS 103 | -23.99 | 9.44 | 2221.15 | 114.52 | 38.74 | 34.86 |
| GeoB 1711 | -23.32 | 12.38 | 1964 | 3.16 | 1.20 | 1.06 | | | | | | | |
| GeoB 1712 | -23.26 | 12.8 | 1007 | 3.66 | 1.50 | 1.12 | | | | | | | |
| GeoB 1713 | -23.22 | 13.02 | 597 | 5.81 | 1.21 | - | | | | | | | |
| GeoB 1715 | -26.468 | 11.635 | 4095 | 1.43 | 1.08 | - | GEOSECS 103 | -23.99 | 9.44 | 2256.41 | 103.93 | 10.50 | 34.76 |
| GeoB 1719 | -28.95 | 14.18 | 1021 | 3.46 | 1.34 | - | SAVE 233 | -29.97 | 14.10 | 2228.36 | 92.10 | 39.84 | 35.46 |
| GeoB 1720 | -29 | 13.83 | 2011 | 2.95 | 1.42 | - | SAVE 232 | -29.99 | 13.83 | 2201.49 | 116.31 | 53.29 | 34.85 |
| GeoB 1721 | -29.17 | 13.09 | 3045 | 2.43 | 1.79 | - | GEOSECS 102 | -31.52 | 8.50 | 2207.69 | 116.17 | 39.55 | 34.85 |

Table 1. (continued)

| Station | Latitude | Longitude | Water Depth, m | BWT, °C | Mg/Ca, mmol/mol | | Geochemical Sampling Stations | | | Units in $\mu\text{mol/kg}$ | | Salinity, psu | | |
|--------------------|----------|-----------|-------------------|------------|-------------------------|--------------------|----------------------------------|----------|-----------|-----------------------------|----------------------------------|------------------|----------------------------|-------|
| | | | | | <i>P. wuellerstorfi</i> | <i>C. mundulus</i> | Station | Latitude | Longitude | TCO ₂ | [CO ₃ ²⁻] | | $\Delta[\text{CO}_3^{2-}]$ | |
| GeoB 3602 | -34.798 | 17.755 | 1885 | 2.36 | 1.16 | - | | | | | | | | |
| GeoB 3603 | -35.125 | 17.543 | 2840 | 2.18 | 1.28 | 1.55 | | | | | | | | |
| GeoB 8403 | -24.25 | 13.61 | 320 | 10.41 | - | 3.12 | | | | | | | | |
| GeoB 8430 | -25.61 | 13.28 | 1330 | 3.33 | 2.02 | - | | | | | | | | |
| GeoB 8462 | -25.53 | 12.94 | 2293 | 2.91 | 1.07 | - | | | | | | | | |
| Walvis Ridge | | | | | | | | | | | | | | |
| GeoB 1203 | -26.548 | 5.017 | 2395 | 2.67 | 1.44 | - | | | | | | | | |
| GeoB 1216 | -24.925 | 6.788 | 2263 | 2.85 | 1.38 | 1.70 | | | | | | | | |
| GeoB 1217 | -24.945 | 6.725 | 2007 | 3.05 | 1.33 | 1.42 | | | | | | | | |
| GeoB 1218 | -25.168 | 5.918 | 1023 | 3.58 | 1.72 | 1.78 | | | | | | | | |
| GeoB 1726 | -30.27 | 3.262 | 1006 | 3.59 | 1.87 | 1.75 | | SAVE 221 | -30.01 | 3.70 | 2223.88 | 95.04 | 42.93 | 34.42 |
| GeoB 1728 | -29.838 | 2.407 | 2887 | 2.35 | 1.74 | 1.70 | | SAVE 219 | -30.00 | 1.01 | 2210.45 | 120.96 | 46.60 | 34.85 |
| Mid-Atlantic Ridge | | | | | | | | | | | | | | |
| GeoB 1105 | -1.67 | -12.43 | 3231 | 2.36 | 1.73 | - | | SAVE 32 | -0.003 | -17.69 | 2186.57 | 127.69 | 48.33 | 34.9 |
| GeoB 1113 | -5.745 | -11.035 | 2373 | 3.08 | - | 1.74 | | | | | | | | |
| GeoB 3807 | -30.75 | -13.198 | 2515 | 2.51 | 2.01 | - | | SAVE 130 | -28.39 | -13.70 | 2190.30 | 117.76 | 48.45 | 34.86 |
| GeoB 3808 | -30.812 | -14.71 | 3213 | 2.41 | 1.58 | 1.62 | | SAVE 130 | -28.39 | -13.70 | 2188.06 | 120.60 | 41.52 | 34.85 |

^a BWT, in situ bottom water temperature. Also shown are laser ablation-derived shell Mg/Ca ratios from the benthic foraminifera *P. wuellerstorfi* and *C. mundulus*. TCO₂, [CO₃²⁻], $\Delta[\text{CO}_3^{2-}]$, and salinity values were interpolated from GEOSECS and SAVE data.

The upper branch of the Circumpolar Deep Water, the UCDW, separates the NADW from the Antarctic Intermediate Water (AAIW). The AAIW can be distinguished from the underlying UCDW due to a minimum salinity core (Siedler et al., 1996), occurring between ~500 and ~1000 m water depth. AAIW and UCDW are jointly characterized by low $[\text{CO}_3^{2-}]$ and by undersaturation with respect to aragonite (Gerhardt and Henrich, 2001), in comparison with the surrounding water mass bodies.

5.3 Material and methods

A total of 50 samples used for this study was taken from multicorer and box corer surface sediments in the South Atlantic between 1°S and 48°S, and between 58°W and 17°E (Table 1 and Figure 5-1). From washed and sieved samples, approximately five Rose Bengal stained individuals of *Cibicoides mundulus* (= *C. kullenbergi*) and *Planulina wuellerstorfi* (= *Cibicoides wuellerstorfi*) (Holbourn and Henderson, 2002) of the fraction >250 μm were picked for laser ablation analyses.

Measurements of trace and minor elemental compositions were performed with a NewWave UP193 Solid State Laser Ablation System ($\lambda=193\text{ nm}$) connected to a Thermo-Finnigan Element 2 sector field ICP-MS (inductively coupled plasma mass spectrometer) at the department of Geosciences at Bremen University. This technique enables simultaneous analyses of a number of elements in foraminifer tests without the need for the rigorous cleaning procedures which are essential for the liquid analysis method. A camera attached to the laser ablation system facilitates the avoidance of

contaminated sections. In any case ferro-manganese coatings and high-magnesium calcite overgrowths adhered to the shell surface, or clay fills inside test chambers or within pores can be easily detected during analysis (see Rathmann et al., 2004). Any contaminated sections were rejected for the subsequent data evaluation.

The foraminiferal tests were fixed with double-sided adhesive tape mounted on a piece of acetate sheet. Shells were ablated by a laser beam (irradiance: ~0.14 GW/cm^2) with a pulse rate of 5 Hz and a spot size of 35-50 μm . A helium flow of 0.39 l/min transported the ablated material out of the sample chamber and was admixed with argon before entering the plasma. Each test was ablated five times in different places. The data reported for each sediment sample are based on the mean of 25 single measurements (five tests per sample, five measurements per test). Data were calibrated against the NIST610 glass standard reference material (SRM) that contains a number of trace elements with certified concentrations (Pearce et al., 1997). The SRM was measured before and after each shell.

Elemental concentrations were determined on the isotopes ^{43}Ca and ^{25}Mg . Calcium was used as internal standard, assuming a concentration of 40.04%wt. The error in this assumption affects the absolute element concentrations but not the element-to-calcium ratios that are routinely used in paleoceanographic studies, and only the latter are reported here. In order to avoid contamination by ablating the sample holder, clay fills or ferro-manganese coatings of the foraminifer tests, we used

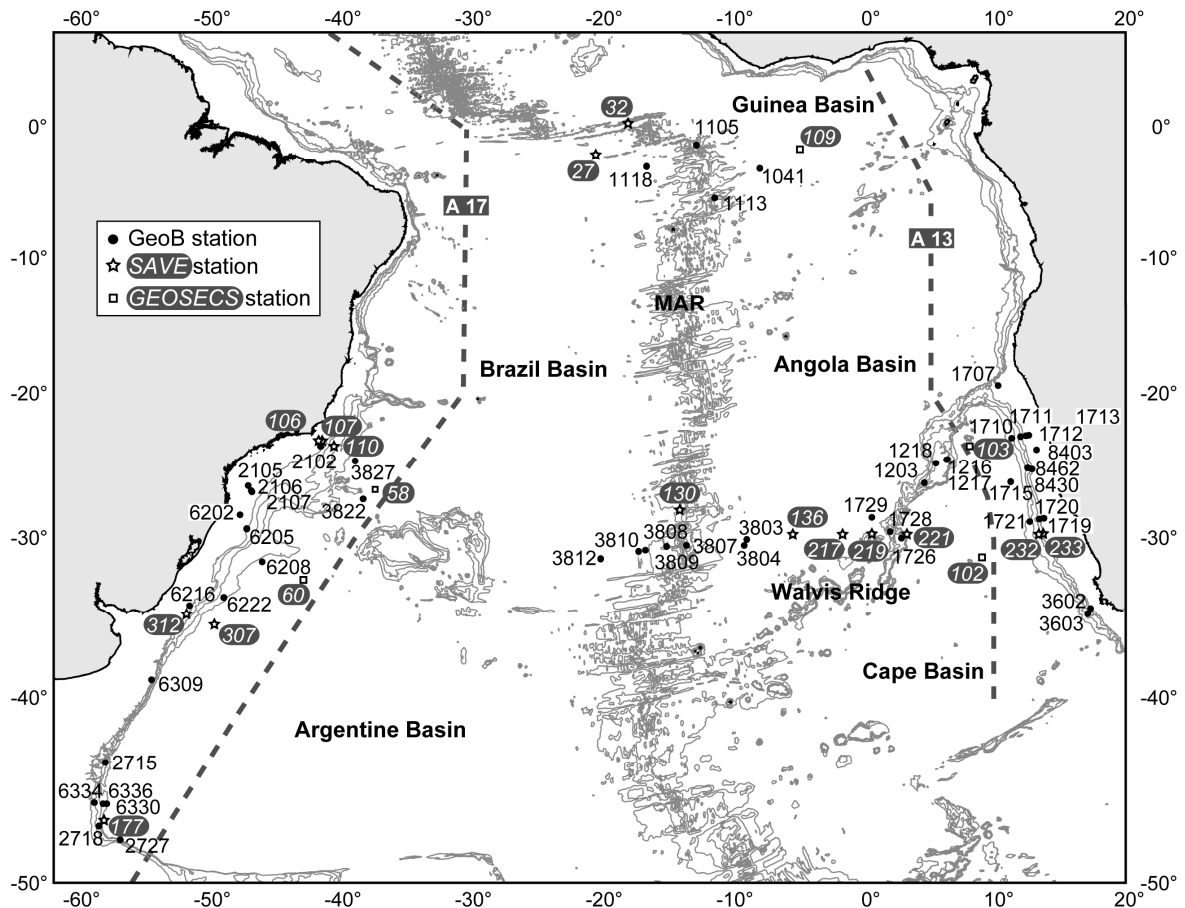


Figure 5-2. Bathymetric map of the South Atlantic (generated with PanMap (Diepenbroek et al., 2000)) including GeoB stations where samples used for this study originate. Nearby GEOSECS (Bainbridge, 1981) and SAVE (Takahashi et al., 1995) sampling stations were consulted for comparison of shell Mg/Ca to local hydrochemical data. WOCE sections A13 and A17 from Figure 5-1 are charted as well.

the isotopes ^{64}Zn , ^{27}Al , and ^{55}Mn as indicators. The raw data were evaluated with the *GeoPro*TM (CETAC) software package that facilitates the blank subtraction and the subsequent conversion of intensities (counts per second) to concentrations (ppm).

For most stations, CTD (conductivity-temperature-depth probe) measurements provided in-situ bottom water temperatures. Where CTD data were not available, temperatures were derived from the World Ocean Atlas (WOA) 2001 (Stephens et al., 2002). For comparison of shell Mg/Ca to seawater carbonate chemistry and salinity, we used local data

derived from SAVE (South Atlantic Ventilation Experiment) (Takahashi et al., 1995) and from GEOSECS (Geochemical Ocean Sections Study) (Bainbridge, 1981). Since spatial variations in the carbonate chemistry of seawater are potentially high, particularly in upwelling areas, we only used stations at a distance of not more than 250 km from our sampling positions (Figure 5-2). For the SAVE data, carbonate ion concentrations were calculated from total alkalinity and total inorganic carbon with the *co2sys* program (Lewis and Wallace, 1998; Pierrot et al., 2006) using the GEOSECS option where carbonate system constants are from Mehrbach et al. (1973). The carbonate ion saturation state was

determined by subtracting the critical carbonate ion concentration, which was calculated with the revised equation of Jansen et al. (2002), from the carbonate ion concentration of seawater.

5.4 Results

5.4.1 Mg/Ca versus water depth

In shells of both *C. mundulus* and *P. wuellerstorfi*, Mg/Ca follows, more or less, the temperature profile suggesting a positive relationship between benthic foraminiferal Mg/Ca and calcification temperature (Figure 5-3). We employed the exponential equation of Elderfield et al. (2006) to assess whether Mg/Ca indicates water temperature (Figure 5-3). Above ~1000 m depth, measured Mg/Ca ratios in *C. mundulus* are close to the predicted values. Below this depth, Mg/Ca in numerous samples exceed

the values predicted from temperature by up to 80%, which corresponds to a temperature difference of up to 4°C.

The depth range of these anomalous values differs from basin to basin (Figure 5-3). In the Brazil Basin Mg/Ca ratios in *P. wuellerstorfi* are anomalously high between 1700 and 3800 m water depth but decrease in the 3800 to 4700 m depth range, and reach normal values below 4000 m. Although *C. mundulus* data in the Brazil Basin are restricted to water depths below 3500 m, there is also a trend of decreasing Mg/Ca down to 4300 m, where two values are even lower than expected. The deviation of Mg/Ca in Argentine Basin samples is not as pronounced as in the Brazil Basin. There it is only slightly increased between approximately 1000 and 2000 m before decreasing with depth below 2000 m.

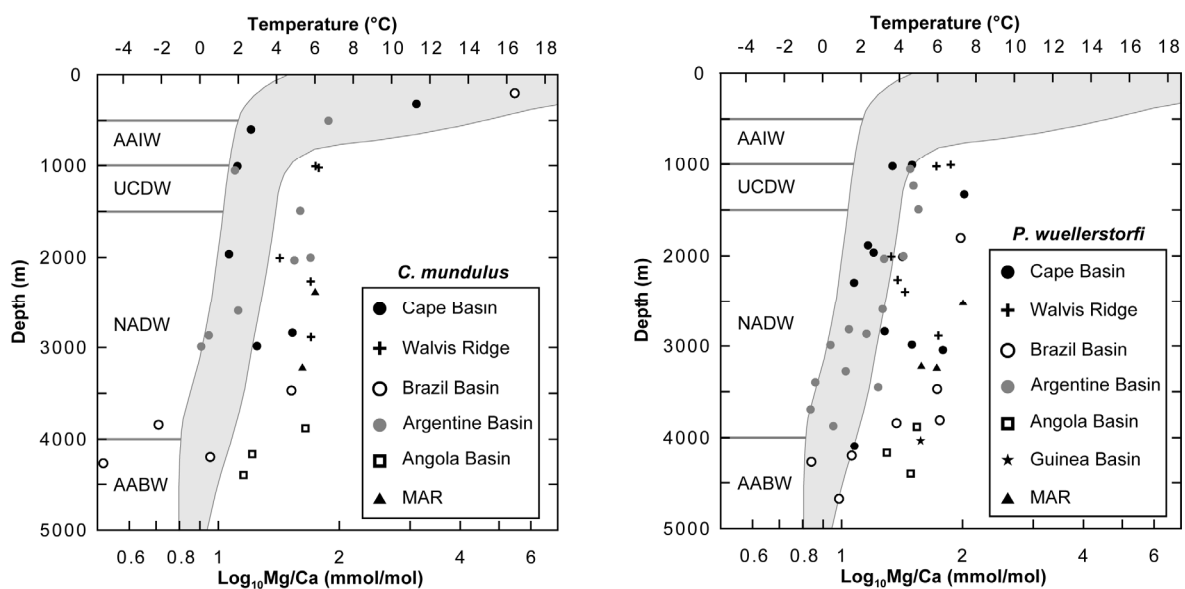


Figure 5-3. Shell Mg/Ca plotted against water depth. The shaded area represents the temperature range in the South Atlantic. Also shown are the approximate limits of the different water masses at 30°S (cp. Figure 5-1). The Mg/Ca axis is adjusted to the temperature axis using an exponential relationship (adopted from Elderfield et al., 2006). Mg/Ca ratios are predominantly increased between ~1000 and ~4500 m. Differences in the depth range of anomalous values between different basins can be distinguished.

This difference between the Brazil and Argentine Basin indicates that the depth range of anomalously high Mg/Ca coincides with the distribution of NADW (Figure 5-1). The NADW roughly occupies the depth interval between 1500 and 4000 m in the Brazil Basin. It thins further south and is only present between 2000 and 3000 m in the southernmost Argentine Basin (Figure 5-1). The assumption of a link between high Mg/Ca and NADW is supported by samples from deep sites in the Angola Basin, even though very limited in number. They all exhibit higher Mg/Ca ratios than predicted from temperature (Figure 5-3), presumably due to the lack of AABW in this basin which is predominantly filled with NADW.

5.4.2 Mg/Ca versus temperature

Since significantly increased Mg/Ca ratios are confined to the distribution of NADW, we excluded all samples bathed in NADW from the determination of the temperature calibration (Figure 5-4). In this case, both

benthic species show a close positive exponential relationship of Mg/Ca to bottom water temperature as also documented in previous studies on *Cibicidoides* species (Elderfield et al., 2006; Lear et al., 2002; Martin et al., 2002; Rosenthal et al., 1997). We obtain the following equations:

$$\text{Mg/Ca (mmol/mol)} = 0.830 * \exp(0.145 * \text{BWT } (^{\circ}\text{C})),$$

$$(R^2 = 0.89) \text{ for } P. \text{ wuellerstorfi} \quad (5-1)$$

$$\text{Mg/Ca (mmol/mol)} = 0.627 * \exp(0.143 * \text{BWT } (^{\circ}\text{C})),$$

$$(R^2 = 0.95) \text{ for } C. \text{ mundulus} \quad (5-2)$$

Our calibrations have slightly steeper slopes than those in other studies (Figure 5-4) but reinforce the exponential relationships determined by Elderfield et al. (2006), Lear et al. (2002), and Martin et al., (2002) for the same genera. Interspecific differences are inferable from the pre-exponential constants. At the cold end, Mg/Ca ratios in *C. mundulus* are ~0.2 mmol/mol lower than those in *P. wuellerstorfi*.

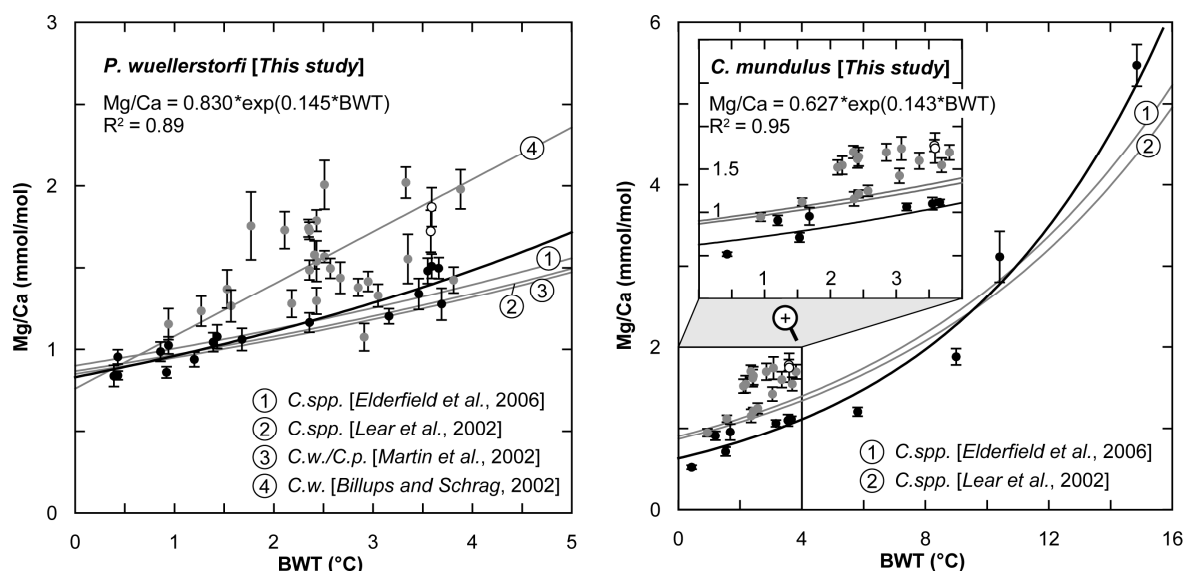


Figure 5-4. Shell Mg/Ca plotted against bottom water temperature. Error bars represent standard errors. Values from samples bathed in NADW (gray symbols) as well as outliers from the Walvis Ridge (open symbols) were rejected for the determination of the calibration curves (black lines). Published temperature calibrations (gray lines) on *Cibicidoides* spp. (containing *wuellerstorfi* and *kullenbergi*) are shown as well. Note that there is no previous published single-species calibration on *C. mundulus*.

Table 2. Summary of Linear Regressions From Figure 5^a

| | <i>P. wuellerstorfi</i> (n = 25) | | | <i>C. mundulus</i> (n = 12) | | | | |
|----------------------------------|--|----------------|-------------|-----------------------------|--|----------------|---------|------------------|
| | Equation: $\Delta\text{Mg}/\text{Ca} =$ | R ² | p Value | Significance | Equation: $\Delta\text{Mg}/\text{Ca} =$ | R ² | p Value | Significance |
| TCO ₂ | -0.007 (± 0.001) * TCO ₂ + 15.05 (± 2.32) | 0.64 | $\ll 0.001$ | highly significant | -0.007 (± 0.003) * TCO ₂ + 16.79 (± 6.18) | 0.41 | <0.05 | significant |
| [CO ₃ ²⁻] | 0.016 (± 0.003) * [CO ₃ ²⁻] - 1.45 (± 0.37) | 0.48 | <0.001 | highly significant | 0.012 (± 0.008) * [CO ₃ ²⁻] - 0.98 (± 0.94) | 0.18 | >0.05 | not significant |
| $\Delta[\text{CO}_3^{2-}]$ | 0.010 (± 0.002) * $\Delta[\text{CO}_3^{2-}] - 0.03$ (± 0.08) | 0.45 | <0.001 | highly significant | 0.017 (± 0.004) * $\Delta[\text{CO}_3^{2-}] - 0.14$ (± 0.14) | 0.63 | <0.01 | very significant |

^a R², coefficient of determination. P values obtained from F tests give information about the statistical significance for each empirical relationship of $\Delta\text{Mg}/\text{Ca}$ to the parameters tested with respect to a significance level of 5% (see text for further details).

5.4.3 Mg/Ca versus seawater chemistry

In order to detect probable causes for the anomalies described above, we compared Mg/Ca to salinity and carbonate chemistry data provided by GEOSECS (Bainbridge, 1981) and SAVE (Takahashi et al., 1995) (Figure 5-1 and Table 1). Since the data sets are restricted to temperatures below 4°C, shallow Mg/Ca data from the Cape and Brazil margins, for instance, are not used in the compilation.

The compiled carbonate system parameters comprise total dissolved inorganic carbon TCO₂, carbonate ion concentration [CO₃²⁻], and carbonate ion saturation state $\Delta[\text{CO}_3^{2-}]$. TCO₂ is the sum of [CO₃²⁻], [HCO₃⁻] and [CO₂]_{aq}, the relative proportions of these three species control the pH. $\Delta[\text{CO}_3^{2-}]$ is the difference between in-situ [CO₃²⁻] and the critical carbonate ion concentration [CO₃²⁻]_{crit}. As [CO₃²⁻]_{crit} increases with increasing water depth and decreasing temperature, $\Delta[\text{CO}_3^{2-}]$ decreases concomitantly.

Since the influence of temperature potentially obscures the effect of seawater chemistry on shell Mg/Ca, we subtracted the temperature component using the species-specific calibrations established in section 5.4.2 (equations (5-1) and (5-2)):

$$\Delta\text{Mg}/\text{Ca} = \text{Mg}/\text{Ca}_{\text{measured}} - \text{Mg}/\text{Ca}_{\text{calc.}} \quad (5-3)$$

Linear regression analyses were carried out to examine the relation of $\Delta\text{Mg}/\text{Ca}$ (response variable) to the carbonate system parameters (explanatory variables). The resulting regression equations are summarized in Table 2. The goodness of fit of each regression model is described by the coefficient of determination R² (e.g., R² = 0.7 means 70% of the variation may be

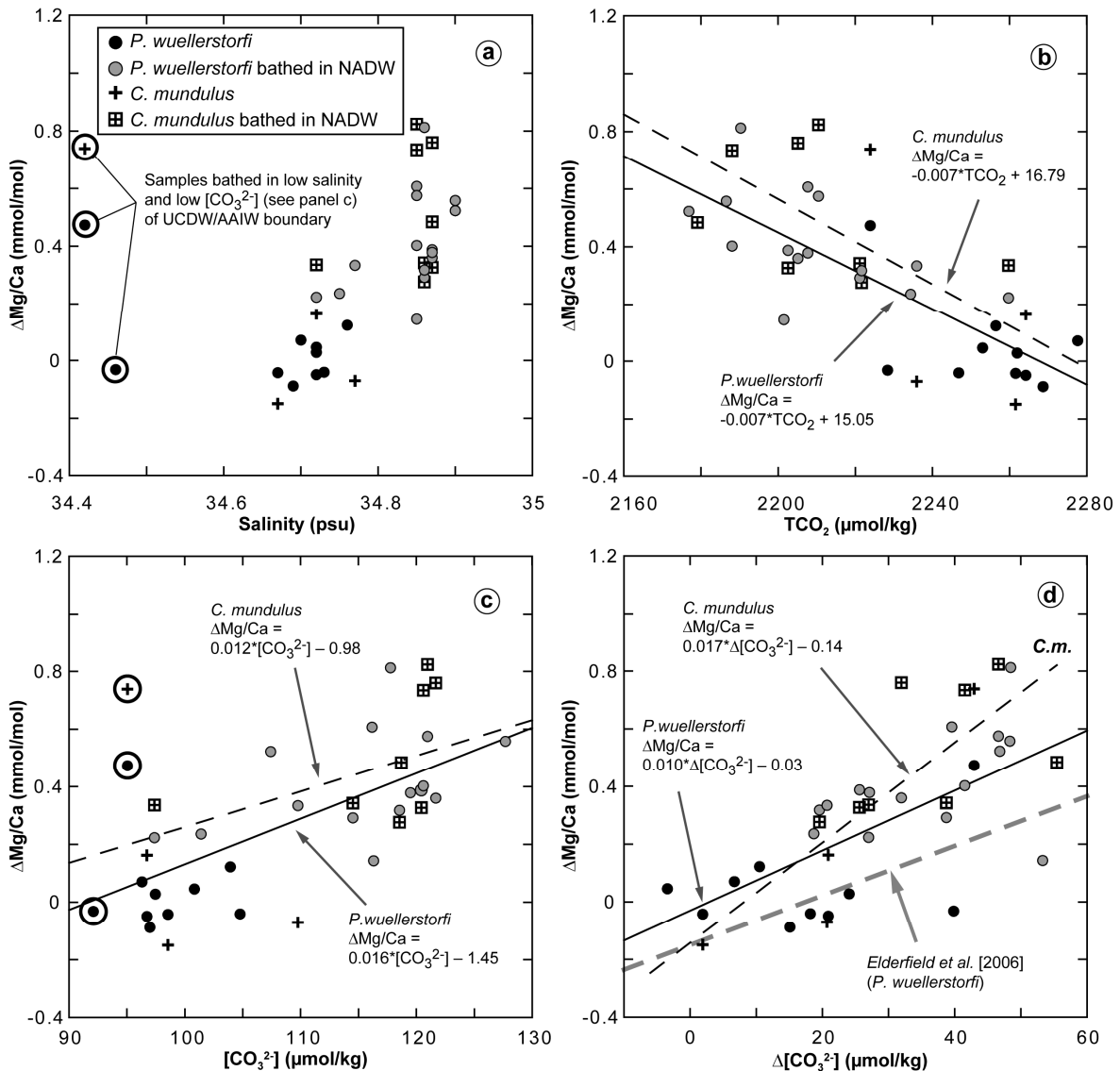


Figure 5-5. $\Delta\text{Mg}/\text{Ca}$ ($= \text{Mg}/\text{Ca}_{\text{measured}} - \text{Mg}/\text{Ca}_{\text{calculated}}$) plotted against **a)** salinity, **b)** TCO_2 , **c)** $[\text{CO}_3^{2-}]$, and **d)** $\Delta[\text{CO}_3^{2-}]$, derived from GEOSECS and SAVE data sets. The results of regression analyses are summarized in Table 2. The solid lines are for *P. wuellerstorfi* and the dashed lines for *C. mundulus*. The dashed gray line in d) represents the regression curve determined by Elderfield et al. (2006) from global *P. wuellerstorfi* data. The values framed by black circles in a) and c) belong to samples from the UCDW-AAIW boundary that is characterized by low salinity and low $[\text{CO}_3^{2-}]$ (cp. Figure 5-6).

explained by the model). Statistical significance is checked by an F test of the overall fit, based on the null hypothesis that the coefficients are zero. The p value of the F test is the probability that the results observed (or results more extreme) could have occurred by chance. In other words, the smaller the p value, the greater the inconsistency of the null hypothesis. The null hypothesis is rejected when the p value is smaller than or equal to the significance

level, often represented by α (typically 0.05). The statistical significance of a regression model is usually categorized in the following way: not significant (p value > 0.05), significant (0.01 < p value < 0.05), very significant (0.001 < p value < 0.01), and highly significant (p value < 0.001).

In the scatter graph of $\Delta\text{Mg}/\text{Ca}$ against salinity, three apparent outliers are evident (Figure 5-5a). The corresponding samples

are from the Walvis Ridge (*C. mundulus*) and from the Namibian continental slope (*P. wuellerstorfi*). At least one of these outliers is also clearly identifiable in the plot against $[\text{CO}_3^{2-}]$ (Figure 5-5c). The water depths of ~ 1000 m indicate that these samples were bathed in low salinity and low $[\text{CO}_3^{2-}]$ of the UCDW-AAIW boundary (Figure 5-3). On the other hand, $\Delta\text{Mg}/\text{Ca}$ from these samples do not show such deviations from the general trend versus TCO_2 (Figure 5-5b) and $\Delta[\text{CO}_3^{2-}]$ (Figure 5-5d). These parameters exhibit moderate values at this water depth, compared to salinity and $[\text{CO}_3^{2-}]$ (Figure 5-6). Based on this observation along with F test statistics that yield non-significant correlations with $\Delta\text{Mg}/\text{Ca}$, we presume that salinity within the narrow range of 0.5 psu is not the driving factor responsible for large Mg/Ca offsets inferred from our data. Moreover, the study of Nürnberg et al. (1996) on cultured planktonic foraminifera showed that salinity changes <3 psu have no systematic impact on shell Mg/Ca.

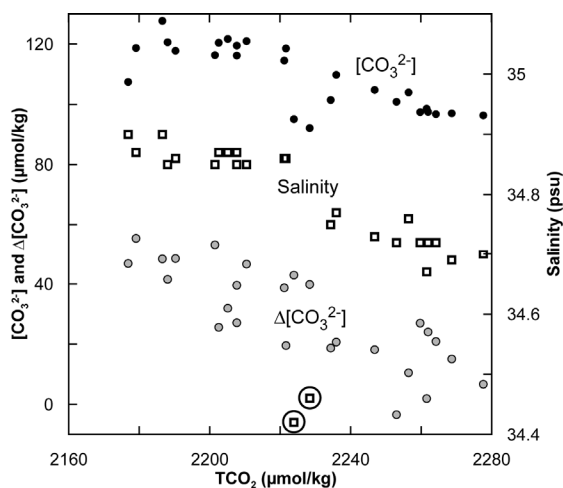


Figure 5-6. TCO_2 plotted against $[\text{CO}_3^{2-}]$, $\Delta[\text{CO}_3^{2-}]$ and salinity from datasets used for correlations with $\Delta\text{Mg}/\text{Ca}$ in Figure 5-5. The low salinity values (framed by black circles) are due to low salinity and low $[\text{CO}_3^{2-}]$ but moderate TCO_2 and high $\Delta[\text{CO}_3^{2-}]$ of the UCDW-AAIW boundary.

$\Delta\text{Mg}/\text{Ca}$ from *C. mundulus* yields the best regression versus $\Delta[\text{CO}_3^{2-}]$ (Figure 5-5d) with the highest statistical significance (Table 2). In contrast, correlations with TCO_2 (Figure 5-5b) and $[\text{CO}_3^{2-}]$ (Figure 5-5c) are less significant and not significant, respectively. $\Delta\text{Mg}/\text{Ca}$ from *P. wuellerstorfi* correlates well with TCO_2 (Figure 5-5b), and the accordant regression model reveals the highest statistical significance (Table 2). F tests yield also very low p values for $\Delta\text{Mg}/\text{Ca}$ against $\Delta[\text{CO}_3^{2-}]$ and $[\text{CO}_3^{2-}]$, but regression fits have lower R^2 s in comparison with TCO_2 . Both $[\text{CO}_3^{2-}]$ and $\Delta[\text{CO}_3^{2-}]$ themselves are linked to TCO_2 (Figure 5-6) in that $[\text{CO}_3^{2-}]$ is governed by pH within the 3-phase TCO_2 system, which in turn is controlled by alkalinity and the carbon dioxide flux.

Regression analyses of $\Delta\text{Mg}/\text{Ca}$ from *C. mundulus* against the parameters tested generally exhibit lower R^2 s and higher p values than from *P. wuellerstorfi* (Table 2), possibly owing to the smaller sample size ($n=11$ vs. $n=23$). But slopes of the regression equations are similar for both species, indicating a similar sensitivity to all parameters tested.

The relationship between $\Delta\text{Mg}/\text{Ca}$ and carbonate chemistry is not confined to samples from any particular water mass, nor does it merely reflect differences between water masses. It is present for all samples from temperatures below 3.9°C , the highest temperature in our data set for which GEOSECS and SAVE data were available.

5.5 Discussion

5.5.1 Influence of carbonate chemistry on shell Mg/Ca

Our results suggest that benthic foraminiferal Mg/Ca is not solely dependent on temperature but is significantly influenced by the carbonate chemistry of seawater. This is in line with the observation that anomalously high Mg/Ca ratios are linked to the presence of NADW. One characteristic property is its higher carbonate ion saturation state compared with the surrounding water masses. The high correlation of $\Delta\text{Mg/Ca}$ from *C. mundulus* with $\Delta[\text{CO}_3^{2-}]$ (Figure 5-5d) suggests that the carbonate ion saturation state plays an important role in Mg/Ca, wherever temperature drops below $\sim 4^\circ\text{C}$. From 0 to 4°C , Mg/Ca in *C. mundulus* increases by 0.48 mmol/mol (Figure 5-4). Such increase in $\Delta\text{Mg/Ca}$ is equivalent to a range of $\Delta[\text{CO}_3^{2-}]$ from 0 to 28 $\mu\text{mol/kg}$, which in turn is equivalent to an increase in Mg/Ca by 0.34 mmol/mol (Figure 5-5d). Therefore the influence of $\Delta[\text{CO}_3^{2-}]$ on Mg/Ca is slightly less than that of temperature below 4°C .

The slope of 0.017 mmol/mol per 1 $\mu\text{mol/kg}$ $\Delta[\text{CO}_3^{2-}]$ for *C. mundulus* (Figure 5-5d), indicated by our data, is identical to that determined by Rosenthal et al. (2006) for the aragonitic species *Hoeglundina elegans*. For *P. wuellerstorfi*, the slope of 0.01 mmol/mol $\Delta\text{Mg/Ca}$ per 1 $\mu\text{mol/kg}$ $\Delta[\text{CO}_3^{2-}]$ is close to 0.0086 mmol/mol found by Elderfield et al. (2006) for the same species (Figure 5-7). Hence our finding confirms previous studies that, apart from temperature, the dependence of foraminiferal Mg/Ca on the carbonate ion saturation state is a fundamental phenomenon.

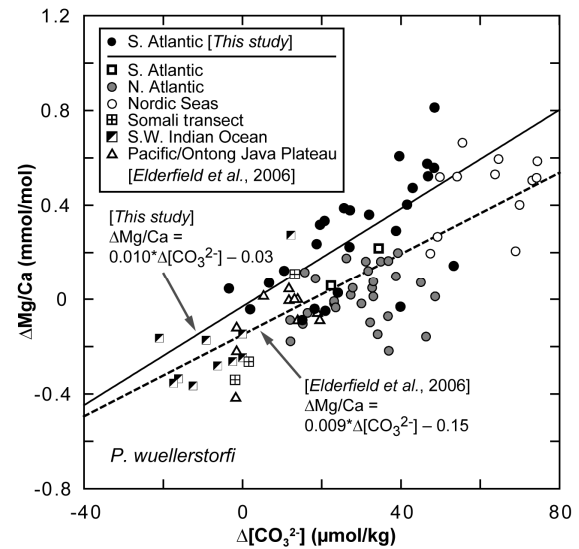


Figure 5-7. $\Delta\text{Mg/Ca}$ for *P. wuellerstorfi* plotted together with global data of Elderfield et al. (2006) against $\Delta[\text{CO}_3^{2-}]$. The solid line shows the regression for our samples with a similar equation to that determined by Elderfield et al. (2006), represented by the dashed line.

Interestingly, our data indicate that $\Delta\text{Mg/Ca}$ from *P. wuellerstorfi* is more dependent on TCO_2 , rather than on $\Delta[\text{CO}_3^{2-}]$ (Figure 5-5 and Table 2). We hypothesize that the Mg precipitation in shells of *P. wuellerstorfi* is driven by a combination of carbonate and bicarbonate ion concentrations (the main contributors to TCO_2). Decreasing TCO_2 , which is induced by decreasing $[\text{HCO}_3^-]$ and increasing $[\text{CO}_3^{2-}]$ (Figure 5-6), enhances shell Mg/Ca (Figure 5-5b). An accordant trend is also observed for Mg/Ca in *C. mundulus*, but the additional effect of bicarbonate ions seems to be more pronounced for *P. wuellerstorfi*. This may be attributed to species-specific differences in the calcification process since both CO_3^{2-} and HCO_3^- are possible carbon sources for marine calcifiers (e.g., Gao et al., 1993; Wolf-Gladrow et al., 1999).

Another factor that may explain the interspecies differences are the microhabitats of both species. *Planulina wuellerstorfi* prefers

a somewhat elevated position above the sediment-water interface (Lutze and Thiel, 1989), completely surrounded by bottom water. In contrast, *C. mundulus* lives predominantly at different depths within the sediment-water interface, depending on its ontogenetic stage (Rathburn and Corliss, 1994), and may thus be partially influenced by pore water chemistry. It has been shown that pore water chemistry changes rapidly within the uppermost millimeters of sediment, both in South Atlantic deep and intermediate waters (e.g., Hensen and Zabel, 2003). Typically, the pH decreases from 8 at the sediment surface to 7.8 at 5 mm below the sediment surface. When using this drop in pH and an alkalinity decrease by 20 $\mu\text{mol/kg}$, while leaving temperature and salinity unchanged, a decrease in $[\text{CO}_3^{2-}]$ by $\sim 40 \mu\text{mol/kg}$ results, which in turn would decrease shell Mg/Ca by $\sim 0.4 \text{ mmol/mol}$ (Figure 5-5c). This value is higher than the average difference of 0.2 mmol/mol between *P. wuellerstorfi* and *C. mundulus* but still of comparable magnitude.

As pore waters tend to equilibrate rapidly with CaCO_3 (Martin and Sayles, 1996, 2006), infaunal foraminifera calcifying only from pore waters live at $\Delta[\text{CO}_3^{2-}]$ close to 0 $\mu\text{mol/kg}$ and would be expected to show no or less of a $\Delta[\text{CO}_3^{2-}]$ effect compared with epifaunal foraminifera. However, contrary to the infaunal *Oridorsalis umbonatus* (Rathmann and Kuhnert, 2008) and *Uvigerina spp.* data (Elderfield et al., 2006), $\Delta\text{Mg/Ca}$ of *C. mundulus* from our data shows a strong correlation with bottom water $\Delta[\text{CO}_3^{2-}]$ (Figure 5-5d). The infaunal habitat of *Uvigerina* species, presumably unaffected by bottom water $\Delta[\text{CO}_3^{2-}]$, suggests that Mg/Ca of this genus is potentially more

reliable for estimating past water temperatures. However, further calibrations are required since there may still be uncertainty as to differences in the exponential constant between the calibrations from Martin et al. (2002), Lear et al. (2002), and Elderfield et al. (2006).

The choice of our own calibrations for the temperature correction of Mg/Ca seems to be appropriate since a significant difference in the pre-exponential constant between both species is apparent (Figure 5-4). Furthermore, it is possible that previous Mg/Ca-temperature calibrations also include a carbonate ion effect. However, using the calibration of Elderfield et al. (2006) for correcting Mg/Ca of *P. wuellerstorfi*, the resulting relationship of $\Delta\text{Mg/Ca}$ with TCO_2 ($\Delta\text{Mg/Ca} = -0.008 \cdot \text{TCO}_2 + 17.19$) gives $\Delta\text{Mg/Ca}$ values that are close to those derived from our equation (Table 2). In contrast, the correlation of $\Delta\text{Mg/Ca}$ of *C. mundulus* with $\Delta[\text{CO}_3^{2-}]$ ($\Delta\text{Mg/Ca} = 0.019 \cdot \Delta[\text{CO}_3^{2-}] - 0.44$) yields $\Delta\text{Mg/Ca}$ values by $\sim 0.2 \text{ mmol/mol}$ higher than those calculated with our equation (Table 2). This reflects the species-specific difference in the pre-exponential constant between the Mg/Ca temperature equations (Figure 5-4).

Although $\Delta\text{Mg/Ca}$ in *P. wuellerstorfi* and *C. mundulus* exhibit highest correlations with different parameters of the carbonate system, the results are consistent since $\Delta[\text{CO}_3^{2-}]$ and TCO_2 are both linked to $[\text{CO}_3^{2-}]$. $\Delta[\text{CO}_3^{2-}]$ increases with rising $[\text{CO}_3^{2-}]$, which in turn decreases with an increase of TCO_2 (Figure 5-6), associated with oxidation of organic carbon resulting in a lowering of pH. In principle, this is also in accordance with the systematic Mg/Ca change associated with

changes in pH, determined by Lea et al. (1999) and Russell et al. (2004) on cultured planktonic foraminifera, since an increase of pH shifts the TCO_2 partitioning toward a higher carbonate ion concentration. However, there is a general difference in the direction the seawater carbonate system influences shell Mg/Ca in planktonic and benthic foraminifera. The planktonic species (*Globigerina bulloides*, *Orbulina universa*) investigated by Russell et al. (2004) show a decrease in Mg/Ca by ~ 0.02 to ~ 0.03 mmol/mol per $1 \mu\text{mol/kg}$ $[\text{CO}_3^{2-}]$ increase. This is at odds with our results where Mg/Ca in *P. wuellerstorfi* increases by ~ 0.016 mmol/mol per $1 \mu\text{mol/kg}$ $[\text{CO}_3^{2-}]$ increase (Figure 5-5c).

If we only consider the sign of the slope, the available data lead to a contradictory picture. There is no obvious influence of the mineralogy (no difference between calcitic benthics and the aragonitic *H. elegans*; (Rosenthal et al., 2006)), nor of the presence of endosymbionts (no difference between the endosymbiotic *O. universa* and the symbiont-barren *G. bulloides*; (Russell et al., 2004)). The only systematic difference is between planktonic and benthic foraminifera. This suggests different metabolic controls on mineralization processes between planktonic and benthic foraminifers, but studies on more species are required to obtain a comprehensive picture.

5.5.2 Implications for paleothermometry

Since at low temperatures the influence of temperature on Mg/Ca in *P. wuellerstorfi* and *C. mundulus* is potentially masked by

variations in the carbonate system, reconstructed past bottom water temperatures can be afflicted with sizable errors. Significant differences in the carbonate chemistry of Atlantic seawater between glacial and interglacial times have been suggested. Broecker and Clark (2001) showed that the $[\text{CO}_3^{2-}]$ gradient within the transition zone between AABW and NADW was much steeper during the Last Glacial Maximum than it is today, with $[\text{CO}_3^{2-}]$ concentrations increased by $\sim 28 \mu\text{mol/kg}$ at 2.8 km and decreased by $\sim 23 \mu\text{mol/kg}$ at 4 km depth. Similarly, glacial $[\text{CO}_3^{2-}]$ in the North Atlantic was elevated by 25-30 $\mu\text{mol/kg}$ at 1-2 km and lowered by 20-25 $\mu\text{mol/kg}$ at 3.5-4 km water depth (Yu and Elderfield, 2007).

Our data suggest that a 25 $\mu\text{mol/kg}$ drop in $[\text{CO}_3^{2-}]$ would decrease $\Delta\text{Mg/Ca}$ by up to 0.4 mmol/mol. This in turn would lead to an underestimation of bottom water temperature by $\sim 3.5^\circ\text{C}$ at an actual temperature of 3°C . Therefore potential changes in the carbonate chemistry of the ambient seawater have to be considered in reconstructions of deep water temperatures. Furthermore, we strongly recommend to scrutinize the species-specific response of Mg/Ca to both temperature and carbonate chemistry since it seems to be crucial for unraveling the different factors that have control on the Mg incorporation into benthic foraminiferal shells. The use of an independent carbonate ion proxy, e.g., B/Ca (Yu and Elderfield, 2007), would allow to account for the carbonate ion effect on Mg/Ca in future studies.

5.6 Summary

From our core top data we conclude that Mg/Ca in *P. wuellerstorfi* and *C. mundulus* is not a simple function of temperature in the South Atlantic below $\sim 4^{\circ}\text{C}$. Comparison to hydrochemical parameters from nearby GEOSECS and SAVE stations reveals that shell Mg/Ca is also controlled by the carbonate chemistry of the ambient seawater. The most important parameters are $\Delta[\text{CO}_3^{2-}]$ for *C. mundulus* (positive correlation) and TCO_2 for *P. wuellerstorfi* (negative correlation). Both $\Delta[\text{CO}_3^{2-}]$ and TCO_2 are closely linked to $[\text{CO}_3^{2-}]$, therefore the carbonate ion effect on foraminiferal Mg/Ca can be confirmed. For this reason, shells of benthic foraminifera exhibit anomalously high Mg/Ca ratios when they are bathed by NADW that is slightly supersaturated in carbonate ion. The carbonate ion effect on Mg/Ca is slightly less important than the influence of temperature below $\sim 4^{\circ}\text{C}$. The potential impact of changes in the seawater carbonate chemistry should be considered for paleotemperature reconstructions that are based on benthic Mg/Ca, particularly on the glacial-to-interglacial timescale.

Acknowledgments

Sincere thanks are given to Ed C. Hathorne for comments and improvements of the laser ablation technique and to Andreas Klügel and Heike Anders for their continuous improvement of the laboratory equipment. Many thanks go also to Heather Johnstone for proofreading and to Gert-Jan Reichart for his helpful suggestions. Laurent Labeyrie as well as an anonymous reviewer is gratefully acknowledged for constructive reviews of this manuscript. This study was carried out within the international graduate college EUROPROX (Project II-2), funded by the Deutsche Forschungsgemeinschaft (DFG).

6. Effect of Ω on shell Mg/Ca

The effect of calcite saturation state on Mg/Ca in cultured benthic foraminifera: *Heterostegina depressa* and *Ammonia tepida*

Markus Raitzsch¹, Adriana Dueñas-Bohórquez², Gert-Jan Reichart², Torsten Bickert¹

¹MARUM – Center for Marine Environmental Sciences, University of Bremen, Leobener Straße, 28359 Bremen, Germany

²University of Utrecht, Department of Earth Sciences – Geochemistry, Budapestlaan 4, 3584 CD Utrecht, The Netherlands

In preparation for *Geochimica et Cosmochimica Acta*

Laboratory culture experiments were investigated in order to verify the effect of the calcite saturation state (Ω) on Mg/Ca in benthic foraminiferal shells. We maintained the shallow-water species *Heterostegina depressa* and *Ammonia tepida* for a period of two months for each experiment. We varied Ω by changing $[\text{Ca}^{2+}]$, which had the advantage over changing $[\text{CO}_3^{2-}]$ that the experiments were not sealed for keeping the seawater in disequilibrium with atmospheric CO_2 . As a result, Mg/Ca in *H. depressa* increased with increasing Ω , which basically accords with results from previous core-top studies on deep-sea benthic foraminifera. The observed gradient is 1.67 mmol/mol per unit Ω , which is relatively low compared to the high Mg/Ca ratios of >130 mmol/mol in this species. In contrast, Mg/Ca in *A. tepida* decreased with increasing Ω at a gradient of -0.21 mmol/mol per unit Ω , in good agreement with results from previous culturing studies on planktic foraminifera. However, the different magnitudes and directions calcite saturation state influenced the Mg uptake into shell calcite suggested that these species use different biomineralization mechanisms. We hypothesize that the high-Mg foraminifer *H. depressa* calcified its shell via a transient amorphous CaCO_3 precursor that was stabilized by Mg as an inhibitor for spontaneous precipitation at higher Ω values. Conversely, the low-Mg species *A. tepida* removed Mg from the calcification site through Mg^{2+} buffering by ATP in order to favor the precipitation of calcite. If the Mg^{2+} buffer capacity was reduced at higher Ω values, this resulted in lower shell Mg/Ca ratios.

6.1 Introduction

The ratio of magnesium to calcium (Mg/Ca) in benthic foraminiferal shells is a widely used tool to estimate past bottom water temperatures (e.g., Lear et al., 2000; Martin et al., 2002; Billups and Schrag, 2003; Lear et al., 2003; Skinner et al., 2003; Kristjánssdóttir et al., 2007; Katz et al., 2008; Shevenell et al., 2008). In combination with $\delta^{18}\text{O}$ measured in the same samples, it has

been used to reconstruct past salinity of seawater. However, recent studies showed that in addition to temperature the calcite saturation state $\Delta[\text{CO}_3^{2-}]$ plays an important role in the Mg uptake into benthic foraminiferal shells (Elderfield et al., 2006; Rosenthal et al., 2006; Raitzsch et al., 2008; Healey et al., 2008). Calibrations using foraminifers of surface sediments yielded a

species-specific increase in Mg/Ca between 0.008 and 0.017 mmol/mol per $\mu\text{mol/kg}$ $\Delta[\text{CO}_3^{2-}]$. This is contrary to results from culture experiments on planktic foraminifers, which demonstrated that Mg/Ca decreased with increasing pH or $[\text{CO}_3^{2-}]$ (Lea et al., 1999; Russell et al., 2004; Kısakürek et al., 2008). $\Delta[\text{CO}_3^{2-}]$ varies with water depth and the carbonate ion concentration $[\text{CO}_3^{2-}]$ of seawater, which is intrinsically linked to the other carbonate system parameters of DIC, alkalinity and pH (Zeebe and Wolf-Gladrow, 2001). Hence the direction $[\text{CO}_3^{2-}]$ influences shell Mg/Ca is apparently opposite between planktic and benthic foraminifera.

Given the empirical exponential relationship, Mg/Ca changes only slightly within the generally narrow temperature range in the deep ocean of roughly 5°C . Therefore potential changes in deep-sea $\Delta[\text{CO}_3^{2-}]$, for example in the North Atlantic during the Last Glacial Maximum by $\sim 25\text{-}30 \mu\text{mol/kg}$ inferred from benthic foraminiferal B/Ca (Yu and Elderfield, 2007), would bias Mg/Ca based temperature estimations to a significant degree. Hence for the ongoing development of this paleo-thermometer, it is essential to quantify the separate effects of both temperature and calcite saturation state on benthic Mg/Ca.

In this context, we aimed at verifying the so-called carbonate ion effect on Mg/Ca in benthic foraminifers by means of culturing experiments under controlled laboratory conditions at the University of Utrecht. For this study, we employed the neritic to intertidal benthic species *Heterostegina depressa* (tropical, symbiont-bearing) and *Ammonia tepida* (temperate, symbiont-barren).

Compared to deep-sea foraminifers, these species are relatively easy to culture and therefore promising for the success of experimental studies. We varied the calcite saturation state (here reported as Ω) by changing the calcium concentration $[\text{Ca}^{2+}]$, which has the same effect as changing $[\text{CO}_3^{2-}]$. We expect either increasing Mg/Ca with increasing Ω as observed in core top samples from the deep sea or decreasing Mg/Ca as previously shown for cultured planktic foraminifera.

6.2 Experimental and analytical procedures

6.2.1 Sample collection and preparation

Foraminifer individuals of the benthic species *Ammonia tepida*, originating in the Bay of Biscay, were picked from sediment stocks stored in a dark cooling room at 10°C . Specimens of the symbiont-bearing *Heterostegina depressa*, provided by the Burger's Zoo (Arnhem, The Netherlands), were picked from an aquarium that was exposed to artificial light (15 W tropical reef lamp) for 14 hrs/day in an incubator at 24°C .

Only living individuals bearing visible cytoplasm were selected and put into vials with natural seawater admixed with calcein (fluorexon, fluorescein complex) at a concentration of 7 mg/l. Calcein is a fluorescent dye that is incorporated into shell calcite when chambers are newly formed, whereas preexisting calcite is not affected (Bernhard et al., 2004). Since calcein is fluorescent, these labeled chambers are then clearly distinguishable from other chambers (Figure 6-1).

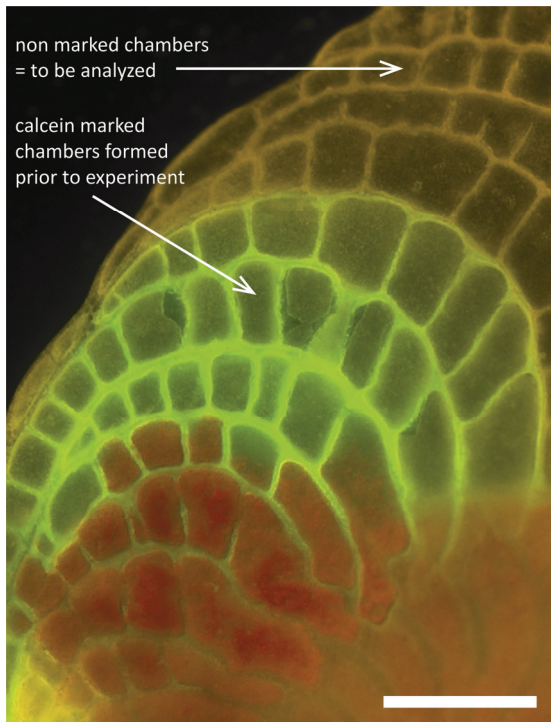


Figure 6-1. Micrograph of *Heterostegina depressa* under a fluorescence microscope. Shell calcite marked with calcein was built prior to the experiment. The non marked chambers were formed during the experiment and were aimed to be analyzed with LA-ICP-MS. Scale bar is 100 μm .

After being maintained in an incubator for 2-4 weeks, foraminifers were checked for new chambers under a fluorescence microscope. Only specimens with fully calcein-marked chambers were selected for the culture experiments. Experimental seawater was not admixed with calcein, therefore chambers formed during the experiment were easily distinguishable from calcein-marked chambers being previously built (Figure 6-1).

Upon finishing the experiments, only foraminiferal individuals with new, non calcein-labeled chambers were selected for element analysis with laser ablation ICP-MS. Specimens were shortly plunged (a few seconds) in a 5% NaOCl solution in order to remove the cytoplasm and organic material attached to the shells. The shells were then

immediately washed thoroughly in MilliQ water. Subsequently, foraminifer tests were mounted on a sample holder and photographed under the fluorescence microscope.

6.2.2 Experimental setup

The experiment was designed to attain four groups with different calcite saturation state values. For that, we varied parameters of the following relationship:

$$\Omega = \frac{[\text{CO}_3^{2-}] \cdot [\text{Ca}^{2+}]}{K_{\text{sp}(\text{Cc})}^*} \quad (6-1)$$

where Ω is the calcite saturation state and $K_{\text{sp}(\text{Cc})}^*$ is the solubility product of calcite. Instead of changing $[\text{CO}_3^{2-}]$, we varied Ω by changing $[\text{Ca}^{2+}]$. This approach had the advantage over varying $[\text{CO}_3^{2-}]$ that the experiment had not to be sealed for keeping the solutions in disequilibrium with atmospheric $p\text{CO}_2$.

Since the chemical composition of seawater had to be modified, experiment solutions were composed of 50% natural seawater (NSW) from the eastern Mediterranean Sea and 50% artificial seawater (ASW). Basically, the ASW was prepared according to the methods of Kester et al. (1967) and Berges et al. (2001). The addition of the volumetric salts 1M CaCl_2 and 1M MgCl_2 was equally modified in order to maintain the same Mg/Ca ratio between the different solutions (~ 5 mol/mol). Since Cl^- is the major constituent of sea salt anions, the different amounts of CaCl_2 and MgCl_2 were compensated by accordant addition of 2M NaCl. In this manner, salinity was kept constant between the different solutions (Table 1).

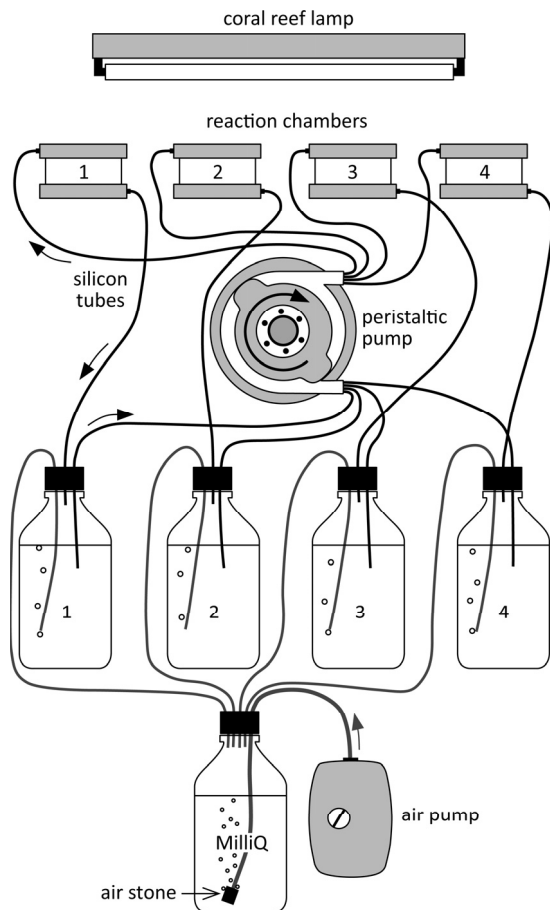


Figure 6-2. Scheme of the instrumental setup. A peristaltic pump circulates the seawater through the reaction chambers containing the foraminifers. The different solutions are continuously bubbled with air purified in MilliQ water before. The experiment is conducted in an incubator at a constant temperature. Artificial light was required for photosynthesis of *H. depressa*'s endosymbionts.

After preparing 500 ml of ASW for each group, ASW was mixed with 500 ml NSW, filtered and bubbled for 24 hrs in order to equilibrate the seawater with the atmosphere. Finally, the individual solutions had roughly the following calcium concentrations: (1) $\frac{1}{2}$ of natural $[\text{Ca}^{2+}]$, (2) natural $[\text{Ca}^{2+}]$, (3) 1.5x natural $[\text{Ca}^{2+}]$, (4) 2x natural $[\text{Ca}^{2+}]$ (Table 1).

15 individuals of *H. depressa* and 25-30 individuals of *A. tepida*, respectively, were transferred into each reaction chamber, whose bottoms were thinly covered with

silty quartz sediment. A tiny amount (with the tip of a thin brush) of freeze-dried algae/diatoms was added as food. The reaction chamber consists of a plastic bottom and lid, separated by a diaphanous Plexiglas ring. Bottom and lid have apertures that allowed the seawater to flow through the chamber (Figure 6-2). The chambers were connected with silicon tubes to 1l glass bottles that contained the modified seawater. A peristaltic pump circulated the seawater through the system at a speed of ~ 1 ml/h. The seawater was bubbled continuously with air purified before in a separate MilliQ water bottle (Figure 6-2). Shortly before setting up the experiment, all material was thoroughly cleaned several times with 1N HCl and MilliQ water, and then rinsed with the accordant seawater.

The whole instrumental system was stored in an incubator at a constant temperature. The *Ammonia* experiment was kept at 18°C, while the *Heterostegina* experiment was conducted at 24°C and exposed to artificial light for 14 hrs/day, to account for the photosynthesis of endosymbionts. Each experiment was operated for two months. At the beginning and at the end of each experiment, seawater was subsampled for determination of elemental concentrations with ICP-OES, and for alkalinity using a titration machine (702 SM Titrino). Salinity was monthly checked and adjusted when required. As seawater was in equilibrium with the atmosphere, a $p\text{CO}_2$ value of 365 μatm (Striegl et al., 2001) was chosen to calculate the other carbonate system parameters using the *co2sys* program of Pierrot et al. (2006).

TABLE 1. EXPERIMENTAL CULTURING CONDITIONS

| Experiment I | | Group 1 | Group 2 | Group 3 | Group 4 |
|--|--|---------|---------|---------|---------|
| <i>H. depressa</i> | | | | | |
| Temperature (°C) | | 24 | 24 | 24 | 24 |
| Salinity (psu) | | 36.2 | 35.8 | 35.6 | 35.6 |
| Alkalinity ($\mu\text{mol/kg}$) | | 2440 | 2436 | 2400 | 2384 |
| DIC ($\mu\text{mol/kg}$)* | | 2087 | 2085 | 2059 | 2046 |
| [Ca ²⁺] ($\mu\text{mol/kg}$) | | 4847 | 9534 | 13760 | 18439 |
| [CO ₃ ²⁻] ($\mu\text{mol/kg}$)* | | 246 | 243 | 237 | 234 |
| Ω † | | 2.76 | 5.39 | 7.58 | 10.04 |
| $\Delta[\text{CO}_3^{2-}]$ ($\mu\text{mol/kg}$) [§] | | 79.7 | 198.3 | 297.0 | 408.3 |
| Experiment II | | Group 1 | Group 2 | Group 3 | Group 4 |
| <i>A. tepida</i> | | | | | |
| Temperature (°C) | | 18 | 18 | 18 | 18 |
| Salinity (psu) | | 35.2 | 35.3 | 35.2 | 35.3 |
| Alkalinity ($\mu\text{mol/kg}$) | | 2385 | 2378 | 2363 | 2385 |
| DIC ($\mu\text{mol/kg}$)* | | 2111 | 2105 | 2093 | 2111 |
| [Ca ²⁺] ($\mu\text{mol/kg}$) | | 5427 | 9786 | 14146 | 18138 |
| [CO ₃ ²⁻] ($\mu\text{mol/kg}$)* | | 201 | 200 | 198 | 200 |
| Ω † | | 2.51 | 4.51 | 6.46 | 8.37 |
| $\Delta[\text{CO}_3^{2-}]$ ($\mu\text{mol/kg}$) [§] | | 67.0 | 155.8 | 242.0 | 326.9 |

* DIC and [CO₃²⁻] were calculated from $p\text{CO}_2$ and alkalinity using the *co2sys* program (Pierrot et al., 2006).

† Ω is the product of [CO₃²⁻] and [Ca²⁺], divided by the solubility product of calcite (see equation 6-1).

§ $\Delta[\text{CO}_3^{2-}]$ was calculated using equation 6-4.

6.2.3 Element analysis

Element concentrations of cultured samples were measured at the University of Utrecht using a GeoLas 200Q 193nm Excimer laser (Lambda Physik) connected to a quadrupole ICP-MS (Micromass Platform). Only newly formed chambers of the foraminifers were ablated, identifiable from non calcein-marked chambers on photographs taken before under the fluorescence microscope. Beam diameter was 60-80 μm (depending on size of area available for analysis), repetition rate was 6 Hz, and energy density was set at 1 J/cm². Element concentrations were determined on the isotopes ²⁴Mg, ²⁶Mg, ²⁷Al, ⁴²Ca, ⁴³Ca, ⁴⁴Ca, ⁵⁵Mn, and ⁸⁸Sr.

Calcium was handled as internal standard assuming 40%wt, which enables to correctly calculate element to calcium ratios routinely reported in paleoceanography. Before and after ~10 sample analyses, a NIST 610 silicate standard with well-known concentrations (Pearce et al., 1997) was measured three times each as an external standard. Since the NIST was ablated with a higher energy density (4 J/cm²) in order to enhance signal quality, an in-house spar calcite ablated with low energy was employed as second, matrix-matched standard. However, calibration of many elements such as Mg, Ca, B, U, and Sr in carbonates against the NIST 610 were proven accurate when using a 193nm laser,

even though instrumental settings were changed between the glass standard and carbonate samples (Hathorne et al., 2008b).

Al and Mn were monitored in order to detect contaminant clay fills and Mn-rich overgrowths, respectively. Since foraminifer individuals lived during the experiment on artificial fine-grained quartz sediment, measurements did not suffer from such contaminants. Al/Ca and Mn/Ca were usually well below 0.1 and 0.01 mmol/mol, respectively.

Time resolved raw data in counts per second (CPS) were converted to element concentrations (ppm) using the GLITTER software (New Wave Research, Inc.). This data reduction software facilitates graphically the manual selection of intervals for the background and sample signal.

6.3 Results

6.3.1 Survival and growth rates

Surprisingly, the survival rate of foraminifer individuals was exceedingly high with almost 100% in both experiments. Three specimens (out of 30) of *A. tepida* merely died in the seawater with the highest calcite saturation state. In contrast, six juvenile foraminifers were found in the same group. The number of individuals which added new chambers is more or less constant between the different groups. On average, 29% of *A. tepida* formed new chambers, while 47% of the *H. depressa* specimens precipitated new calcite. These results indicate that the foraminifers were not extremely stressed by the environmental conditions during the experiments.

When counting the newly formed chambers of each foraminifer test, we observed in both species a trend of increasing chamber addition with increasing calcite saturation state (Figure 6-3). In the Groups 1 and 2 with the lowest Ω values, no considerable difference in chamber addition was apparent. *Ammonia tepida* calcified by up to twice the number of chambers in Groups 3 and 4, compared with the other groups. *Heterostegina depressa* added significantly more chambers only in the seawater with the highest Ω . Therefore we reasoned that the growth rate (amount of added calcite during the 2 months experiment) increased with increasing calcite saturation state above certain levels (Figure 6-3). Although growth rate is not necessarily equal to calcification rate, our results coincide with laboratory experiments on corals where an increase in $[Ca^{2+}]$ had the same effect on the precipitation rate as an increase in $[CO_3^{2-}]$ (Gattuso et al., 1998; Langdon et al., 2000).

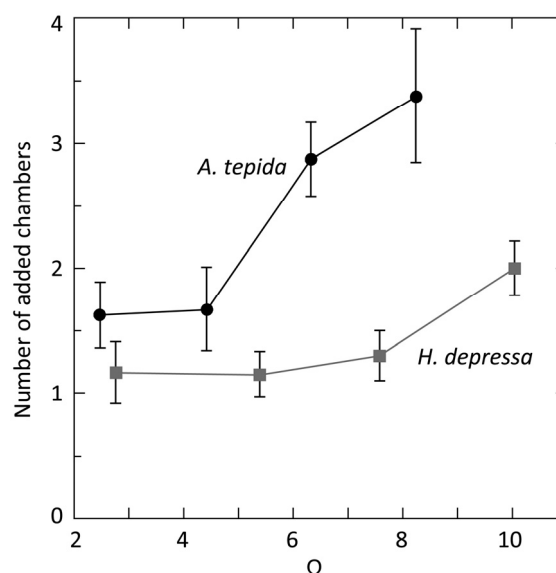


Figure 6-3. Number of new chambers added over two months versus Ω . Error bars are standard errors of the mean. For both foraminifer species, number of new chambers tends to increase with increasing Ω . This is suggestive of an influence of the calcite saturation state on the growth rate at higher Ω values.

TABLE 2. Mg/Ca RATIOS AND EMPIRICAL RELATIONSHIPS WITH Ω

| Experiment I | Group 1 | Group 2 | Group 3 | Group 4 |
|-------------------------|--|---------|---------|---------|
| <i>H. depressa</i> | | | | |
| Number of individuals* | 6 | 7 | 5 | 7 |
| Mg/Ca (mmol/mol) | 143.34 | 145.56 | 151.57 | 155.00 |
| Standard deviation (%)† | 8.30 | 5.92 | 5.51 | 7.22 |
| Equation | Mg/Ca = 1.67 (\pm 0.27)* Ω + 137.90 (\pm 1.85) ($R^2=0.96$) | | | |
| Experiment II | Group 1 | Group 2 | Group 3 | Group 4 |
| <i>A. tepida</i> | | | | |
| Number of individuals* | 6 | 4 | 8 | 7 |
| Mg/Ca (mmol/mol) | 2.41 | 1.78 | 1.60 | 3.65 |
| Standard deviation (%)† | 21.24 | 26.04 | 18.35 | 53.43 |
| Equation | Mg/Ca = -0.21 (\pm 0.03)* Ω + 2.87 (\pm 0.15) ($R^2=0.92$) | | | |

* Refers to analyzed individuals. Not all grown foraminifers were analyzed because of limited space available for LA.

† Standard deviation calculated from single measurements over all tests of one sample.

6.3.2 Mg/Ca versus calcite saturation state

The experiment on *H. depressa* revealed that shell Mg/Ca increased linearly with increasing Ω (Figure 6-4a). The gradient is approximately 1.7 mmol/mol per one unit Ω . Although this appears to be a steep gradient, it is only a slight increase when considering the generally high Mg concentration in shells of this species (>130 mmol/mol). However, the p value of <0.05 from F tests suggests that this relationship is statistically significant. Conversely, Mg/Ca in *A. tepida* showed a decrease with increasing Ω (Figure 6-4c). The exceedingly high Mg/Ca ratios measured in Group 4 indicated that the accordant shells were probably overgrown with inorganic high-Mg calcite. It is possible that the solution with Ω of 8.4 was sufficiently supersaturated with respect to calcite to induce the precipitation of inorganic calcite. It was shown that such carbonates might be precipitated in textural gaps within biogenic carbonate (Macintyre and Reid, 1995, 1998; Hover et al., 2001). This suggestion is also

supported by the extremely high standard deviation for this group, compared with the other groups (Table 2). In general, the intra-sample Mg/Ca variability for *A. tepida* is considerably higher than for *H. depressa* (Table 2), but of comparable magnitude to variability found in deep-sea benthic foraminifera (Raitzsch et al., unpubl. data).

Since in paleoceanography the calcite saturation state is usually reported as $\Delta[\text{CO}_3^{2-}]$, following relationships can be used to calculate it:

$$\Delta[\text{CO}_3^{2-}] = [\text{CO}_3^{2-}]_{in\ situ} - [\text{CO}_3^{2-}]_{sat} \quad (6-2)$$

$$[\text{CO}_3^{2-}]_{sat} = \frac{[\text{CO}_3^{2-}]_{in\ situ}}{\Omega} \quad (6-3)$$

where $[\text{CO}_3^{2-}]_{sat}$ is the calcite saturation concentration. However, the calculations of $\Delta[\text{CO}_3^{2-}]$ using these equations are more appropriate for natural seawater, where $[\text{Ca}^{2+}]$ is relatively constant and changes in the calcite saturation state are mainly determined by changes in $[\text{CO}_3^{2-}]$.

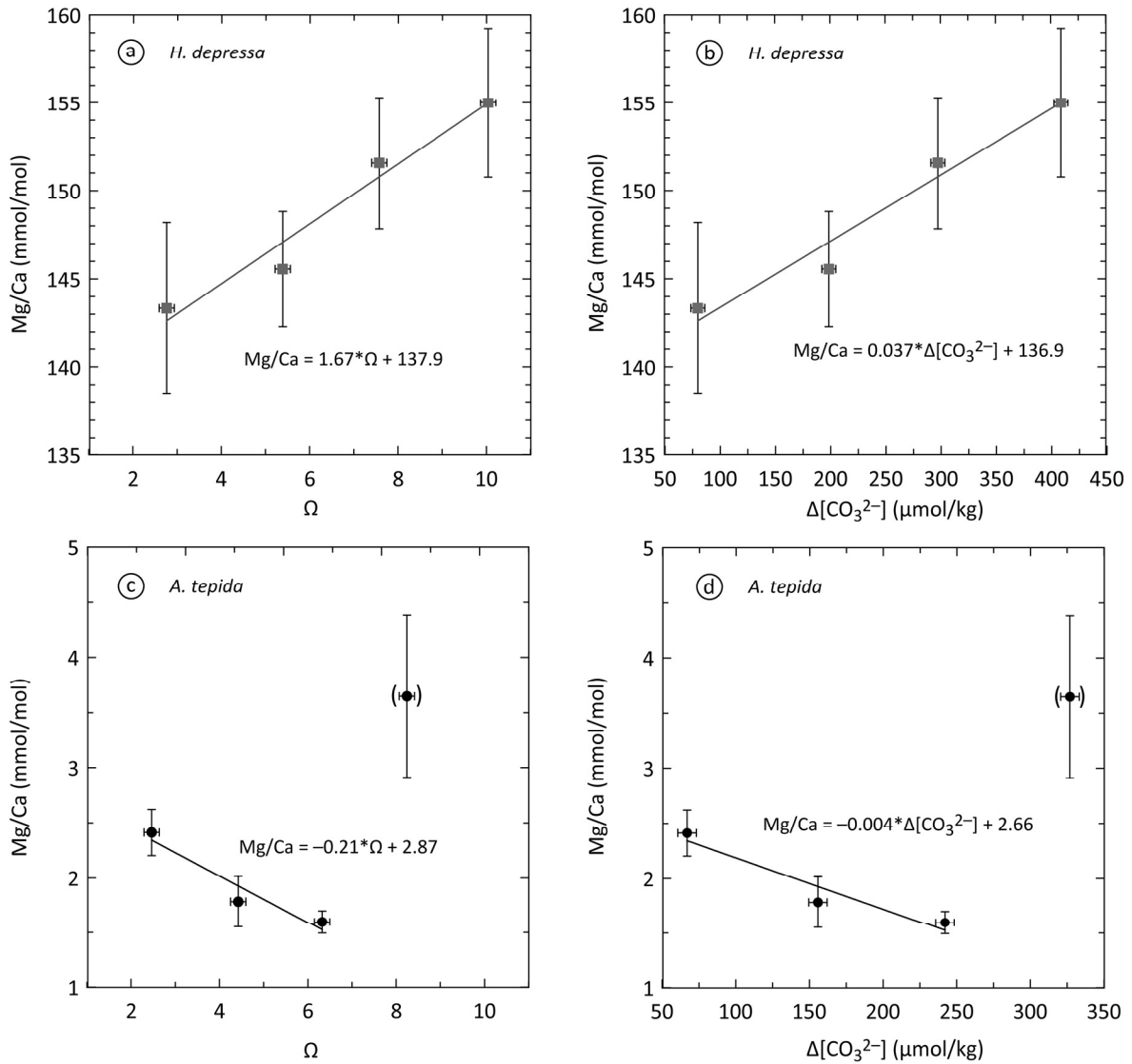


Figure 6-4. Mg/Ca in cultured foraminifers as a function of calcite saturation state. Error bars represent standard errors. **a)** Mg/Ca in *Heterostegina depressa* increases linearly with increasing Ω . **b)** The change in Mg/Ca with $\Delta[\text{CO}_3^{2-}]$ shows that the gradient is relatively small, compared to the generally high Mg concentration in this species. **c)** In contrast to *H. depressa*, Mg/Ca in *Ammonia tepida* tends to decrease with increasing Ω . The framed data point is considered to be affected by overgrowth with inorganically precipitated high-Mg calcite, and was therefore excluded from line fitting. Because of the remaining three data points it is not clear whether the best fit is linear. **d)** The sensitivity of Mg/Ca to $\Delta[\text{CO}_3^{2-}]$ is relatively weak, but comparable to results from planktonic culture studies (see Figure 6-6).

Therefore the $\Delta[\text{CO}_3^{2-}]$ values obtained by varying $[\text{Ca}^{2+}]$ are not comparable with those achieved by varying $[\text{CO}_3^{2-}]$, even if Ω is the same in both calculations (Figure 6-5). To compare our data with previous core-top and culture studies, we postulated that Ω from our experiments is proportional to $\Delta[\text{CO}_3^{2-}]$ like in natural systems (Figure 6-5). For that, we kept $[\text{Ca}^{2+}]$ constant at a

concentration derived from Group 2 (close to natural seawater, Table 1) and considered the change in Ω as a result of changing $[\text{CO}_3^{2-}]$. In this manner, we simulated $\Delta[\text{CO}_3^{2-}]$ values by combining equations 6-1, 6-2 and 6-3, simplified to:

$$\Delta[\text{CO}_3^{2-}] = \frac{K_{\text{sp}}^*(\Omega-1)}{[\text{Ca}^{2+}]} \quad (6-4)$$

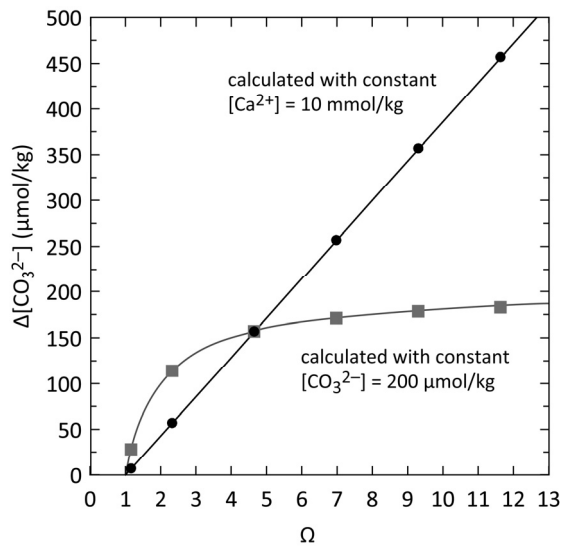


Figure 6-5. Ω versus $\Delta[\text{CO}_3^{2-}]$. Using equations 6-1, 6-2 and 6-3, calculations yield different relationships between Ω and $\Delta[\text{CO}_3^{2-}]$, when assuming either a constant $[\text{Ca}^{2+}]$ or a constant $[\text{CO}_3^{2-}]$, even if Ω is the same in both calculations (representative values used here are typical for sea surface waters).

The resulting $\Delta[\text{CO}_3^{2-}]$ values allow to establish relationships with foraminiferal Mg/Ca that are comparable to existing calibrations. For *H. depressa*, the Mg/Ca ratios show a linear increase with increasing $\Delta[\text{CO}_3^{2-}]$, with a gradient of 0.037 mmol/mol per $\mu\text{mol/kg}$ (Figure 6-4b). This sensitivity is higher than those found for deep-sea species, but very low compared to the high Mg content of *H. depressa*.

In contrast, Mg/Ca in *A. tepida* decreased in a presumably linear way with increasing $\Delta[\text{CO}_3^{2-}]$ (Figure 6-4c). The gradient of -0.004 mmol/mol per $\mu\text{mol/kg}$ agrees well with results from the culture experiments on planktic foraminifers by Russell et al. (2004). In their study, the dependence of Mg/Ca on pH and $[\text{CO}_3^{2-}]$ was examined. For direct comparison with our data, we therefore calculated $\Delta[\text{CO}_3^{2-}]$ from $[\text{CO}_3^{2-}]$ and Ω , provided in the Russell et al. (2004) dataset, using the equations 6-2 and 6-3. The resulting plots are given in Figure 6-6.

The response of Mg/Ca to $\Delta[\text{CO}_3^{2-}]$ seems to be similar in the same range of calcite saturation state for both species, although Mg/Ca ratios in *O. universa* are by a factor of 3 higher than in *A. tepida* (Figure 6-6). Since Russell et al. (2004) obtained a much wider range of $\Delta[\text{CO}_3^{2-}]$ than we did, the similarity between both species could not be verified over the entire spectrum. However, Mg/Ca in *O. universa* decreased in a logarithm-like manner with increasing $\Delta[\text{CO}_3^{2-}]$ (Figure 6-6). Regardless of this general trend, we chose a linear fit through the data between ~ 60 and $\sim 250 \mu\text{mol/kg}$, which coincides with the $\Delta[\text{CO}_3^{2-}]$ range available for our data. The observed gradient of -0.006 mmol/mol per $\mu\text{mol/kg}$ is very close to that determined for *A. tepida* in this study (Figure 6-6).

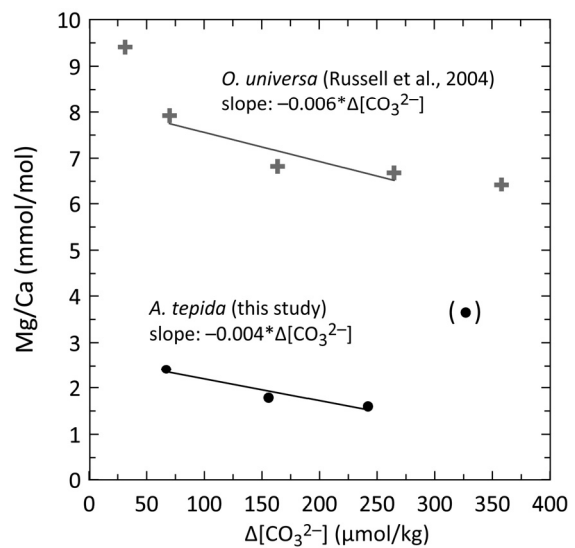


Figure 6-6. Mg/Ca in *Ammonia tepida* from Figure 6-4 plotted together with the Russell et al. (2004) data for the planktonic species *Orbulina universa*. The response of Mg/Ca in *O. universa* to $\Delta[\text{CO}_3^{2-}]$ appears to be negatively logarithmic. However, when postulating a linear decrease within the $\Delta[\text{CO}_3^{2-}]$ range available for the *A. tepida* data, the gradients for both species are nearly identical. The framed data point was not considered due to possible overgrowth by inorganic high-Mg calcite.

6.4 Discussion

6.4.1 The effect of calcite saturation state on Mg incorporation

Our results from culturing experiments demonstrate that the effect of calcite saturation state on the Mg/Ca ratio in benthic foraminifer shells is poorly understood. The two species of the benthic foraminifera group we employed showed an opposite response of Mg incorporation to changes in Ω . The decreasing Mg/Ca in *Ammonia tepida* with increasing calcite saturation state (Figures 6-4c, d) is generally in good agreement with results from culture experiments on various planktonic foraminiferal species (Lea et al., 1999; Russell et al., 2004; Kısakörek et al., 2008). In these laboratory experiments, Mg/Ca was negatively correlated with $[\text{CO}_3^{2-}]$ at lower pH values between 7.6 and 8.4, whereas above this pH range no significant changes in Mg/Ca were found. Although these authors obtained the Mg dependence on $[\text{CO}_3^{2-}]$, we could show with the Russell et al. (2004) dataset that Mg/Ca in *O. universa* versus $\Delta[\text{CO}_3^{2-}]$ followed a similar trend as *A. tepida* in this study (Figure 6-6).

Contrary to *A. tepida*, Mg/Ca in *H. depressa* increased linearly with increasing calcite saturation state (Figures 6-4a, b). In consideration of the generally high Mg concentration in shells of this species, the observed gradients of 1.67 mmol/mol per unit Ω and 0.037 mmol/mol per $\mu\text{mol/kg}$ $\Delta[\text{CO}_3^{2-}]$, respectively, are very low. For example, when $\Delta[\text{CO}_3^{2-}]$ increases by 50 $\mu\text{mol/kg}$, this would cause Mg/Ca to increase by only 1%. This is a small change within this large $\Delta[\text{CO}_3^{2-}]$ range, compared to roughly 30% observed for the deep-sea

benthic species *P. wuellerstorfi* (Elderfield et al., 2006; Raitzsch et al., 2008; Healey et al., 2008). Since *A. tepida* of Group 4 was potentially affected by high-Mg calcite overgrowth (Figure 6-4), the question arose whether Mg/Ca in *H. depressa* also suffered from such carbonates at higher calcite saturation state values. We rule out this possibility, because first, we did not observe a considerable change in the intra-shell variability, and second, we would even expect a lowering in Mg/Ca due to the lower Mg concentration of inorganic calcite than in *H. depressa* (e.g., Katz, 1973; Mucci, 1987; Oomori et al., 1987).

However, we could not find any coherent relationship between Mg/Ca of different foraminifer species and calcite saturation state. Therefore we presume that the sensitivities and the direction seawater carbonate chemistry influences Mg/Ca are distinct between benthic and planktic foraminifer species. This study now supplies evidence for different behaviors even within the benthic foraminifera group. An explanation for this may be found in different biomineralization mechanisms, which in turn may be influenced by the calcite saturation state (see below).

6.4.2 Biomineralization mechanisms

In their comprehensive studies on biomineralization processes, Erez (2003) and Bentov and Erez (2006) presented numerous processes that occur in foraminifers, which control the Mg content in shell calcite. Some of them may explain why Mg/Ca increased in *H. depressa*, and decreased in *A. tepida* with increasing Ω .

It was shown that echinoderms and mollusks form their calcite from transient amorphous calcium carbonate, which is a metastable phase that transforms into a stable crystalline calcite phase within minutes (Beniash et al., 1997; Addadi et al., 2003). Laboratory experiments showed that the formation of inorganic high-Mg calcite was enabled through initial amorphous calcium carbonate (Raz et al., 2000). Therefore it was suggested that high-Mg foraminifera use this mechanism for calcification (e.g., Bentov and Erez, 2006). Further, it may explain why Mg/Ca in *H. depressa* increased with increasing Ω , since in such biomineralization systems Mg is likely used for inhibiting spontaneous precipitation of inorganic calcite (e.g., Raz et al., 2000). Therefore it is plausible that in our experiments with high calcite saturation state values, Mg was enriched at the calcification site in order to inhibit inorganic carbonate crystallization. This Mg enrichment is now reflected in the higher Mg/Ca ratios in the shells (Figures 6-4a, b).

In contrast to high-Mg foraminifera, magnesium plays a negative role in the calcification process of low-Mg foraminifera. Since Mg inhibits the precipitation of carbonates, foraminifers possess various mechanisms to decrease the internal Mg/Ca ratio by Mg removal and/or Ca enrichment from/in the parent solution (Erez, 2003). These include several Mg transport systems (e.g., the most abundant $\text{Na}^+/\text{Mg}^{2+}$ exchange), Mg sequestration within cellular organelles, and Mg buffering by organic compounds. One constituent of the Mg^{2+} buffering system is ATP (a multifunctional nucleotide), which is one of the major binding molecules for cellular Mg^{2+} because

of its high affinity for Mg^{2+} (Bentov and Erez, 2006). It was shown that a decrease in intracellular pH reduced the Mg^{2+} buffer capacity of ATP (Mulquiney and Kuchel, 1997). Therefore any process that increases ATP hydrolysis may reduce the buffer capacity and may, in turn, result in higher shell Mg/Ca ratios (Bentov and Erez, 2006). It is possible that increasing calcite saturation state is one of these factors that decrease ATP hydrolysis, which may cause lower Mg/Ca in shell calcite as seen in *A. tepida* (Figures 6-4c, d).

Our assumption that *H. depressa* and *A. tepida* use different biomineralization mechanisms, which are in turn affected by changes in Ω , is only a hypothesis. But it may explain why the response of Mg uptake into shell calcite to changes in the calcite saturation state is distinct between different foraminifer species. Another issue not discussed so far is the role of the photosynthesizing symbionts in *H. depressa* for calcification. Since CO_2 is removed by photosynthesis that increases pH, and calcification releases CO_2 , which in turn serves for photosynthesis, both processes can enhance each other. In most symbiotic associations, the processes of photosynthesis and calcification in foraminifers are decoupled, as examined in experiments in which the inhibition of either process did not affect the other (ter Kuile et al., 1989a, b). It was further shown that *H. depressa* has a large internal carbon pool that serves for calcification, but not for photosynthesis (ter Kuile and Erez, 1987). However, photosynthetic activity of symbiotic algae during daytime may help to raise the pH in the boundary layer where the vacuoles are formed (Erez, 2003). It is therewith not

clarified whether the presence of symbiotic algae has an effect on the incorporation of Mg into calcite, but it is proven that symbiont-bearing foraminifera have a metabolism different from that in symbiont-barren species. However, many further studies on cultured and field samples are required to comprehensively understand the link between seawater carbonate chemistry, metabolism and foraminiferal Mg/Ca.

6.5 Conclusions

Laboratory culture experiments on the benthic foraminifer species *H. depressa* and *A. tepida* revealed that the response of Mg/Ca to changes in the calcite saturation state is species-specific. Whereas Mg/Ca in *H. depressa* increased with increasing Ω at a gradient of 1.67 mmol/mol per unit Ω , Mg/Ca in *A. tepida* decreased at a gradient of -0.21 mmol/mol/ Ω . The different behavior suggests that these species use different biomineralization mechanisms that are, in turn, influenced by the carbonate chemistry of seawater. We propose that *H. depressa* calcified the shell via a transient amorphous CaCO_3 precursor. The amorphous CaCO_3 was stabilized by Mg as an inhibitor of spontaneous precipitation at higher Ω values. In contrast, *A. tepida* removed Mg from the calcification site through Mg^{2+} buffering by ATP in order to favor calcite precipitation. Maybe the Mg^{2+} buffer capacity was reduced at higher Ω values, which resulted in lower Mg/Ca ratios. Our results demonstrate that the effect of the carbonate chemistry of seawater on the Mg incorporation into foraminiferal shells must be quantified separately for each species.

Acknowledgments

We greatly thank Gijs Nobbe, Helen de Waard, and Paul Mason for laboratory assistance. Many thanks go also to Jordahna Haig, Jos Wit, and Shauna Ní Fhlaithearta for their support and helping us with the maintenance of the culture experiments. Jeroen Groeneveld is acknowledged for critical comments on this manuscript. This study profited from the international graduate college EUROPROX, funded by the Deutsche Forschungsgemeinschaft (DFG).

7. Carbonate system proxies B/Ca and U/Ca

B/Ca and U/Ca in benthic foraminifers:

New proxies for the seawater carbonate system

Markus Raitzsch, Ed C. Hathorne, Henning Kuhnert, Jeroen Groeneveld, Torsten Bickert
MARUM – Center for Marine Environmental Sciences, University of Bremen, Leobener Straße,
28359 Bremen, Germany

Under review in *Geology* since July 24, 2008

We analyzed B/Ca and U/Ca in benthic foraminifers from South Atlantic core top samples to further develop new proxies for the reconstruction of deep ocean carbonate chemistry. The Laser Ablation ICP-MS we used is a micro-analytical method that provides information on intra-test trace element heterogeneity and does not suffer from B blank problems like traditional solution techniques. B/Ca and U/Ca are related to the calcite saturation state of seawater with the highest correlations between $\Delta[\text{CO}_3^{2-}]$ and B/Ca in *Planulina wuellerstorfi* (positive linear relationship), and between $\Delta[\text{CO}_3^{2-}]$ and U/Ca in *Cibicides mundulus* (negative exponential relationship). These carbonate system proxy relationships were used to correct foraminiferal Mg/Ca for the influence of seawater carbonate ion variations. The corrected Mg/Ca-based seawater temperature estimates are more accurate, improving on average from more than $\pm 1.6^\circ\text{C}$ inaccurate to less than $\pm 0.9^\circ\text{C}$ inaccurate.

7.1 Introduction

It has been recently shown that, secondary to seawater temperature, the calcite saturation state $\Delta[\text{CO}_3^{2-}]$ influences Mg incorporation into benthic foraminiferal calcite, potentially biasing estimates of past deep-water temperatures (Elderfield et al., 2006; Raitzsch et al., 2008; Rosenthal et al., 2006). The positive linear gradients are presumably species-specific and range from 0.009 to 0.017 mmol/mol Mg/Ca per 1 $\mu\text{mol/kg}$ $\Delta[\text{CO}_3^{2-}]$. $\Delta[\text{CO}_3^{2-}]$ varies with water depth and the carbonate ion concentration $[\text{CO}_3^{2-}]$ of seawater, which is intrinsically linked to the other carbonate system parameters of DIC, alkalinity and pH (Zeebe and Wolf-Gladrow, 2001). Consequently, a change in pH can affect the

benthic foraminiferal Mg/Ca ratio. Such a change in the Mg/Ca signal caused by glacial-interglacial variations in deep-water carbonate chemistry may be misinterpreted as a temperature change.

To correctly reconstruct the deep ocean temperatures using Mg/Ca, an independent proxy for the carbonate ion concentration has to be applied. As has been shown recently, B/Ca in benthic foraminifers seems to be a highly promising proxy for deep-water calcite saturation state (Yu and Elderfield, 2007; Yu et al., 2008). Boron speciation in seawater is pH-dependant with $\text{B}(\text{OH})_4^-$ more abundant at high pH, and $\text{B}(\text{OH})_3$ at low pH. As only $\text{B}(\text{OH})_4^-$ is

thought to be incorporated into calcium carbonate, the B content of calcium carbonate is a function of solution pH (Hemming and Hanson, 1992). Accordingly, the boron concentration of foraminiferal calcite (expressed as the B/Ca ratio) increases with increasing seawater pH (Sanyal et al., 1995; Spivack et al., 1993), but studies of planktonic foraminifera have demonstrated that calcification temperature, growth rate, and post-depositional dissolution exert additional controls on B/Ca (Ni et al., 2007; Wara et al., 2003; Yu et al., 2007b). In contrast, B/Ca in benthic foraminifera seems to faithfully record $\Delta[\text{CO}_3^{2-}]$ with minimal secondary effects, making this proxy a valuable tool for the reconstruction of deep-water calcite saturation state (Yu and Elderfield, 2007; Yu et al., 2007a).

Here we aim to progress in the development for deep ocean carbonate ion proxies by introducing U/Ca ratios in benthic foraminifers as a new proxy. Uranium exists in seawater in the form of different uranyl carbonate complexes and the relative abundance of each species is related to pH (Krestou et al., 2003) and thus $[\text{CO}_3^{2-}]$. Russell et al. (2004) suggest $\text{UO}_2(\text{CO}_3)_2^{2-}$ and UO_2CO_3 are the species that are preferentially incorporated into calcite because they are more abundant at lower pH and $[\text{CO}_3^{2-}]$, but structural investigations of inorganic calcite could not distinguish the U coordination (Reeder et al., 2000). U/Ca in planktonic foraminifera is negatively related to pH and thus to $[\text{CO}_3^{2-}]$ (Russell et al., 2004), but the relationship between U/Ca and seawater carbonate chemistry has not yet been shown for benthic foraminifera.

We compare B/Ca and U/Ca data for the benthic foraminifer species *Planulina wuellerstorfi* and *Cibicides mundulus* from core tops in the South Atlantic with calcite saturation state data for these sites (Appendix 1). We then demonstrate how empirical relationships between benthic foraminiferal B or U/Ca and calcite saturation can be used to revise the Mg/Ca paleothermometer by correcting for the carbonate ion effect on Mg/Ca.

7.2 Material and methods

Foraminifer tests (size $>250 \mu\text{m}$, 3-5 tests per sample and species) of the benthic species *P. wuellerstorfi* and *C. mundulus* were picked from a total of 23 South Atlantic core top samples distributed in different basins over a depth range of 1805 to 4675 m (Appendix 1). Rose Bengal stained individuals show that samples reported here were recently living. We used Laser Ablation (LA)-ICP-MS to measure the element distribution in the foraminifer tests by modifying the protocols of Rathmann et al. (2004) and Raitzsch et al. (2008). LA-ICP-MS is a technique that provides information for the intra-shell heterogeneity of trace element/Ca ratios, and it does not suffer from high-B background from the introduction system like conventional solution methods (Yu et al., 2007b). Shells were not chemically or physically treated before analysis. Instead, ablation sites were pre-ablated for ~ 1 s in order to remove surface contaminations. Only the umbilical sides of the shells, where pores are sparsely distributed, were analyzed to avoid the ablation of pore fillings.

Trace element composition was measured using a NewWave UP193 Solid State Laser

Ablation System ($\lambda=193$ nm) connected to a Thermo-Finnigan Element 2 sector field ICP-MS, using a pulse rate of 5 Hz, spot sizes between 50 and 75 μm , and irradiances between 0.16 and 0.24 GW/cm^2 . Each measurement was preceded by a 40 s gas blank, and the transient signals of ^{11}B , ^{25}Mg , ^{27}Al , ^{43}Ca , ^{55}Mn , ^{64}Zn , and ^{238}U were monitored. Al and Mn acted as indicators of sedimentary clay and ferro-manganese coatings, respectively. Zn was monitored in order to detect ablation of the sample holder consisting of a double-sided adhesive tape. Signals were calibrated using the NIST612 and 610 glasses (Pearce et al., 1997) that was measured before and after five measurements of each shell. Calibration of B/Ca and U/Ca ratios in carbonate samples using the NIST612 glass has been demonstrated to be accurate (Hathorne et al., 2008a), but repeat analysis of a powder pellet of the Jct-1 carbonate standard (Inoue et al., 2004) was performed to ensure accuracy and estimate analytical precision (Appendix 2). Time resolved data were evaluated with the *GeoPro*[™] software (CETAC) using ^{43}Ca as internal standard.

CTD (conductivity-temperature-depth) data provided local bottom-water temperatures. For stations, where CTD data were not available ($n=8$), temperatures were derived from the World Ocean Atlas (WOA 2001) (Stephens et al., 2002). Carbonate ion saturation state was determined by subtracting the carbonate ion saturation (Jansen et al., 2002) from the in-situ carbonate ion concentration. Carbonate ion concentrations were taken from the nearest (at max. distance of 250 km in the abyssal zone, max. of 50 km in the bathyal zone) GEOSECS stations (Bainbridge, 1981) or

calculated from SAVE data (Takahashi et al., 1995) with the *CO2SYS* program (Pierrot et al., 2006). The difference between both data sets is sufficiently small (5-10 $\mu\text{mol}/\text{kg}$) for the purposes of this study.

7.3 Suitability of LA-ICP-MS for determination of B/Ca, Mg/Ca, and U/Ca

Laser ablation depth profiling provides an insight into trace element/Ca variability within single tests and between different tests from one sample (Figure 7-1 and Appendix 2). The intra-individual trace element variations are similar to those between individuals which is in accordance with previous work (Reichert et al., 2003). Based on five measurements across each shell from each sample, the average trace element/Ca variability shows a clear ranking from B/Ca ($\sim 14\%$) to Mg/Ca ($\sim 18\%$) to U/Ca ($\sim 36\%$). This indicates that boron is more homogeneously distributed within shell calcite than magnesium, in spite of its much lower concentration. Generally, we did not observe a difference in variability between *P. wuellerstorfi* and *C. mundulus* tests. Intra-test B/Ca and Mg/Ca variability is greater than analytical noise determined with the Jct-1 (Appendix 2), and a standard example is shown in Figure 7-1. *Planulina wuellerstorfi* Mg/Ca decreases from chamber f-3 or f-2 toward the final chamber where the lowest ratios are found in f-1 and f (Figure 7-1). The opposite trend is seen in B/Ca that increases within the last chambers with the highest values in the last two ones. The intra-test variation shown in Figure 7-1 (and Appendix 3) is likely the result of a strong biological control on the metal

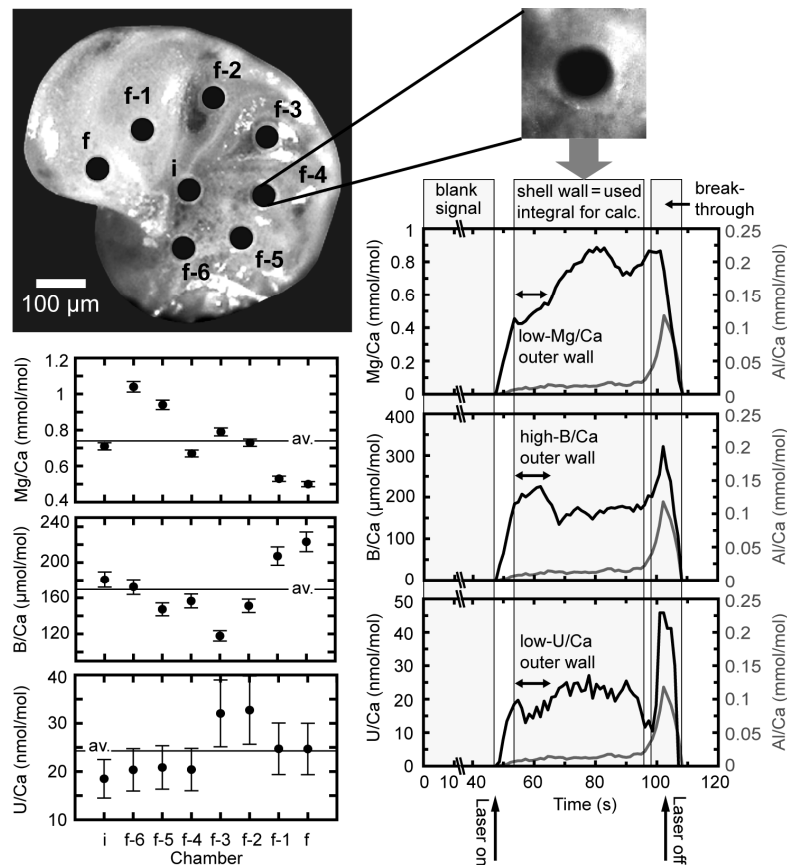


Figure 7-1. Upper panel: photograph of *P. wuellerstorfi* (from sample GeoB 1118) showing laser pits. Right panel: Chromatograms illustrate variations in element/Ca ratios over the thickness of the test wall. High Al/Ca towards the end of the ablation indicates clay minerals adhering to the inner shell surface. Although the analytical noise is ~30% for depth profile data (Appendix 2), an increasing trend in Mg/Ca toward the inner shell is evident. The left panel shows an example for the inter-chamber element/Ca variability indicating a trend of decreasing Mg/Ca and increasing B/Ca from chamber f-3 toward the final chamber (f) (more in Appendix 3).

incorporation since *P. wuellerstorfi* is epibenthic. A similar trend is apparent for *C. mundulus* (Appendix 3).

The U content of foraminiferal shells as well as of Jct-1 is very low compared to B/Ca accounting for comparatively high variability and analytical noise. However, due to the extremely low analytical background of uranium, the low concentrations in foraminifer samples are detectable. Furthermore, the time-resolved data of laser ablation measurements allows the distinction

between shell calcite and potential secondary manganese-rich carbonate overgrowths that may strongly affect bulk U/Ca (Russell et al., 2004). Following Boyle (1983), we excluded all phases with Mn/Ca ratios higher than 0.01 mmol/mol from the data evaluation. Such phases can not be easily removed from primary shell calcite by chemical or physical cleaning. Hence laser ablation may produce more credible U/Ca ratios than the conventional solution methods where foraminifer tests are contaminated by secondary carbonates.

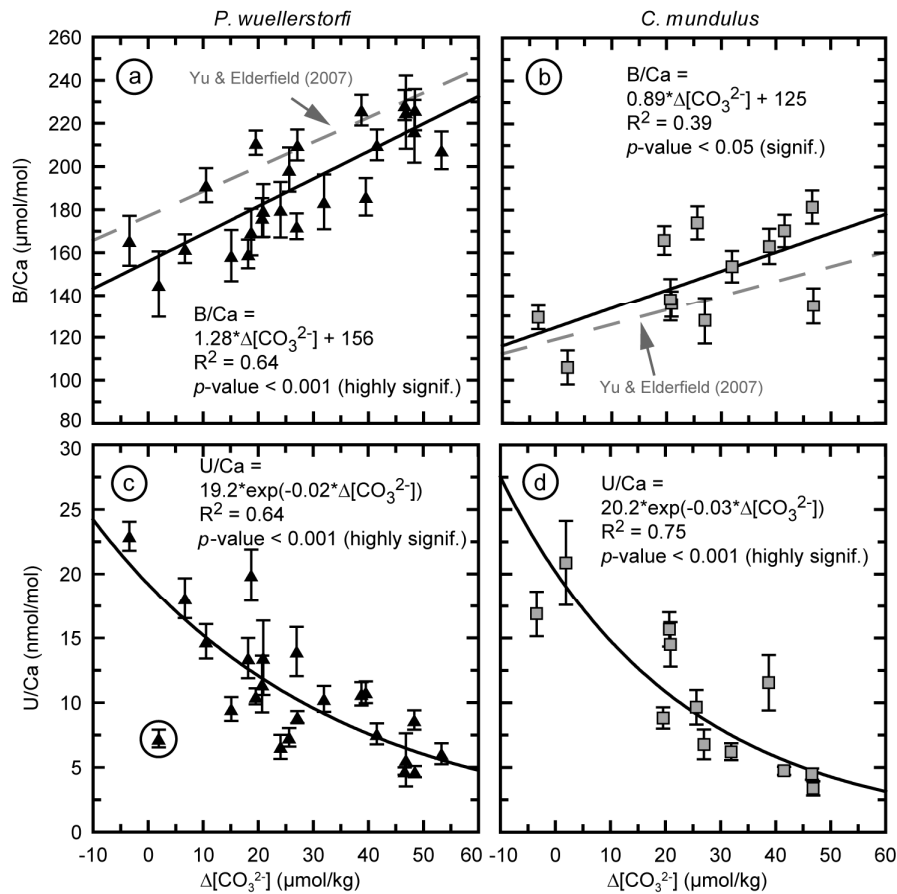


Figure 7-2. Empirical relationships between calcite saturation state and (a) B/Ca in *P. wuellerstorfi*, (b) B/Ca in *C. mundulus*, (c) U/Ca in *P. wuellerstorfi*, and (d) U/Ca in *C. mundulus* are statistically significant (p value from F test statistics < 0.05). Vertical error bars represent standard errors of the mean based on up to 25 spot measurements. Dashed lines are the relationships for B/Ca determined by Yu and Elderfield (2007). The correlations between U/Ca and $\Delta[\text{CO}_3^{2-}]$ are high for both species. The framed data point in (c) has been considered an outlier and was not used for line fitting.

7.4 B/Ca and U/Ca related to calcite saturation state

A significant positive linear relationship between average B/Ca in *P. wuellerstorfi* and the calcite saturation state can be ascertained (Figure 7-2a). The gradient is about $1.3 \mu\text{mol/mol}$ B/Ca per $1 \mu\text{mol/kg}$ $\Delta[\text{CO}_3^{2-}]$, which is similar to the empirical relationship found by Yu and Elderfield (2007). Intuitively, shell B/Ca should vary with seawater pH because of the pH-dependence of $[\text{B}(\text{OH})_4^-]$, the boron species incorporated into calcite, but a straight link between benthic foraminiferal B/Ca and deep-water pH could not be established by

Yu and Elderfield (2007). The reason for this inconsistency may be that the boron incorporation into foraminiferal calcite is modified by physiological processes, since benthic foraminifera calcify from an internal pool that might have a chemical composition different from that of ambient seawater (Bentov and Erez, 2005, 2006; Elderfield et al., 1996; Erez, 2003). Yu and Elderfield (2007) proposed that the enrichment of total boron in the internal calcification fluid is proportional to deep-water $\Delta[\text{CO}_3^{2-}]$, and the variability of $[\text{B}(\text{OH})_4^-]/[\text{HCO}_3^-]$ is controlled by changes in the internal total boron concentration. If correct, foraminiferal B/Ca would indirectly

reflect deep-water $\Delta[\text{CO}_3^{2-}]$, which is also in accordance with our observations.

Interestingly, the correlation of *C. mundulus* B/Ca with $\Delta[\text{CO}_3^{2-}]$ in our samples is much less significant than for *P. wuellerstorfi* (Figure 7-2b), although the generally lower ratios and the flatter regression slope compare well with a previous study (Yu and Elderfield, 2007). Since *C. mundulus* lives partly within the uppermost millimeters of sediment, the boron incorporation may vary with changing pore-water pH during vertical migration through the sediment. In the South Atlantic the pH typically decreases from 8 at the sediment surface to 7.8 at 5 mm sediment depth (Hensen and Zabel, 2003). Consequently, we would also expect a higher B/Ca intra-shell variability compared to *P. wuellerstorfi*. However, we did neither observe this (Appendix 3) nor a size effect on B/Ca as shown for planktonic foraminifera (Ni et al., 2007).

U/Ca in *C. mundulus* and *P. wuellerstorfi* is significantly correlated with $\Delta[\text{CO}_3^{2-}]$ (Figures 7-2c, d). U/Ca decreases exponentially with increasing $\Delta[\text{CO}_3^{2-}]$, which is analogous to the relationship between shell U/Ca in cultured planktonic species and $[\text{CO}_3^{2-}]$ found by Russell et al. (2004). These authors explain the inverse relationship between U/Ca and $[\text{CO}_3^{2-}]$ in two ways: (1) with increasing $[\text{CO}_3^{2-}]$ the abundance of uranium species preferentially incorporated into calcite decreases; (2) with increasing $[\text{CO}_3^{2-}]$ the calcification rate increases impeding the uranyl carbonate species to adjust sterically to fit into the calcite lattice. As a consequence of either process U/Ca in foraminiferal calcite decreases when $\Delta[\text{CO}_3^{2-}]$ increases. The second possibility is

questionable since the calcification rate of benthic foraminifers is considered to be much slower than that for planktics (Erez, 2003). U/Ca in benthic foraminifers is more likely related to the availability of the adaptable uranium species $\text{UO}_2(\text{CO}_3)_2^{2-}$ and UO_2CO_3 which vary with solution pH. A considerable difference in the total U concentration between pore water and bottom water is not expected within the uppermost millimeters of sediment as pore waters are oxic and where uranium remains mobile. Reduction and removal of U from seawater via fixation in solid phases takes place in greater sediment depths under suboxic and anoxic conditions (Barnes and Cochran, 1990). If U/Ca in *C. mundulus* was influenced by pore water pH, we would expect higher U/Ca ratios (due to lower pH of pore water), a higher scatter, and a flatter regression slope against $\Delta[\text{CO}_3^{2-}]$ compared to *P. wuellerstorfi*. This is not identifiable from our data, indicating that U/Ca is predominantly a function of bottom water $\Delta[\text{CO}_3^{2-}]$. Whether a pressure effect plays a prevalent role in the trace metal incorporation into deep benthic foraminifera is an important question since $\Delta[\text{CO}_3^{2-}]$ is largely governed by water depth. However, culturing studies conducted at atmospheric pressure have not found significant differences in shell Mg/Ca (Hintz et al., 2006a). The detailed mechanisms behind metal incorporation into foraminiferal calcite are still largely unknown and make further investigations necessary.

Overall, our data show that U/Ca in benthic foraminifers seems to be a valuable proxy for the calcite saturation state of deep water. The advantages of foraminiferal U/Ca as a proxy for $\Delta[\text{CO}_3^{2-}]$ are: (1) it

seems to be independent from temperature (Russell et al., 1996; Russell et al., 2004), (2) and it does not suffer from changing U/Ca of seawater on timescales $< \sim 0.5$ Ma because of the long residence times of uranium (~ 0.5 Ma) (Dunk et al., 2002) and calcium.

7.5 Correction for the carbonate ion effect on Mg/Ca

As shown above, the carbonate saturation state correlates best with B/Ca in *P. wuellerstorfi* and U/Ca in *C. mundulus*, providing promising tools for reconstructions of past deep-water $\Delta[\text{CO}_3^{2-}]$. Moreover, these relationships have the potential to be

used for improving the Mg/Ca-thermometer, particularly at low temperatures, where a large carbonate ion effect on benthic foraminiferal Mg/Ca has been reported recently (Elderfield et al., 2006; Raitzsch et al., 2008; Rosenthal et al., 2006). Here we have calculated corrected Mg/Ca temperature estimates by substituting corrected Mg/Ca for measured Mg/Ca ratios (see Appendix 4 for full derivation):

$$T_{corr} = 6.90 \pm 0.61 * \ln (\text{Mg/Ca} - 0.0082 \pm 0.0217 * \text{B/Ca} + 1.30 \pm 0.29) + 1.29 \pm 0.16 \text{ for } P. \text{ wuellerstorfi} \quad (7-1)$$

$$T_{corr} = 6.99 \pm 0.54 * \ln (\text{Mg/Ca} + 0.542 \pm 0.255 * \ln \text{U/Ca} - 1.49 \pm 0.98) + 3.26 \pm 0.03 \text{ for } C. \text{ mundulus} \quad (7-2)$$

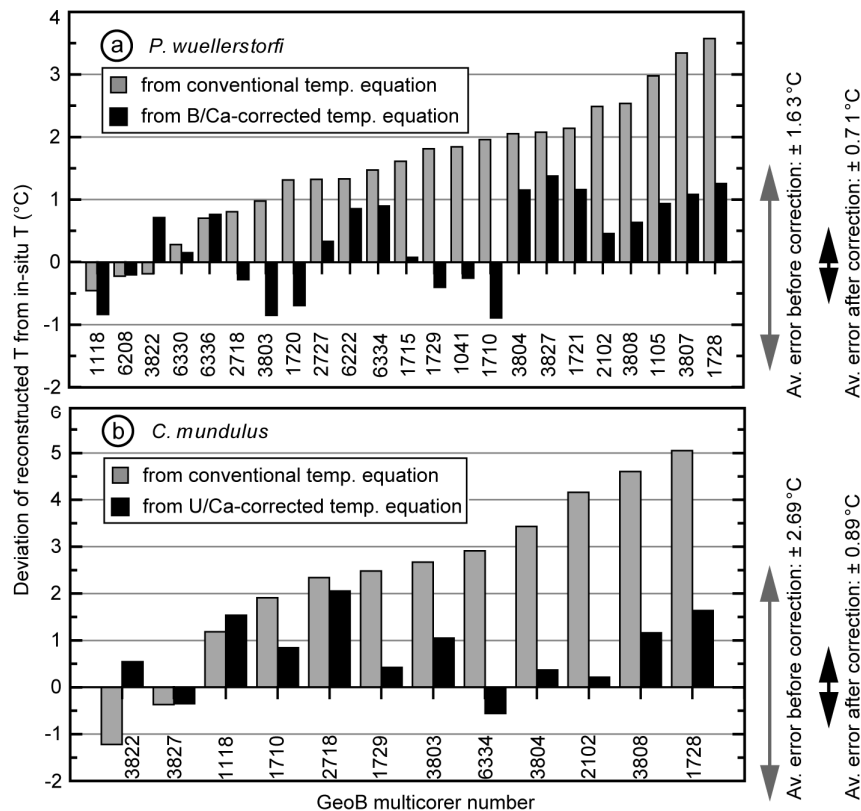


Figure 7-3. Differences between reconstructed and actual bottom water temperatures. Reconstructed temperatures were calculated directly from Mg/Ca (gray bars) and were corrected for the carbonate ion effect (black bars) using (a) B/Ca (eq. 7-1) for *P. wuellerstorfi* and (b) U/Ca (eq. 7-2) for *C. mundulus*. In most cases, reconstructed temperatures were corrected toward the “real” values using the new equations. The average absolute error improved from more than $\pm 1.6^\circ\text{C}$ to better than $\pm 0.9^\circ\text{C}$.

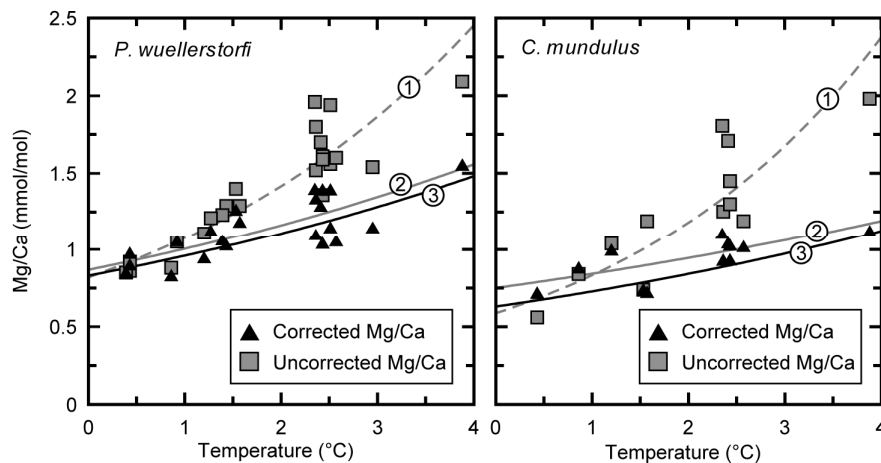


Figure 7-4. Correlation of uncorrected and corrected Mg/Ca, respectively, with bottom water temperature. Numbered lines refer to exponential regression curves based on (1) uncorrected Mg/Ca, (2) all samples corrected with B/Ca or U/Ca, and (3) calibration ignoring samples bathed in NADW (Raitzsch et al., 2008). Uncorrected Mg/Ca fall along a steeper line than predicted by the calibration curves (3). After correction for the carbonate ion effect, the majority of Mg/Ca ratios falls closer to the calibration line.

The deviations of Mg/Ca reconstructed temperatures from actual measured temperatures are shown in Figure 7-3. In most cases (74%), corrected Mg/Ca-temperatures are closer to the zero line (actual temperature), and 17% of cases showed little improvement, although the sign of the deviation occasionally changed. In only 9%, the deviation from the zero line of the corrected temperatures is considerably greater than for the uncorrected values (Figure 7-3).

When plotted against bottom water temperature (Figure 7-4), uncorrected Mg/Ca ratios for both species show a steeper trend than predicted by the calibration curves of Raitzsch et al. (2008) (Figure 7-4). This is evidence for the influence of the calcite saturation state on shell Mg/Ca which is strong particularly at low temperatures ($<4^{\circ}\text{C}$) where the slope of the exponential Mg/Ca change is also low. After correction for the carbonate ion effect, most of the Mg/Ca ratios are more consistent with the Mg/Ca-temperature

calibration line (Figure 7-4). Interestingly, the samples from about 2.5°C display a larger correction. This temperature is not associated with any water mass boundary in the South Atlantic but lies within the North Atlantic Deep Water (NADW), which has a higher $[\text{CO}_3^{2-}]$. As such, temporal variations in NADW and its carbonate chemistry potentially have influenced downcore Mg/Ca.

The majority of Mg/Ca-based temperatures are improved by correcting for the carbonate ion effect, suggesting that the simultaneous measurement of Mg/Ca, B/Ca and U/Ca offers a valuable tool in two aspects. Besides providing important information about the past seawater chemistry, benthic foraminiferal B/Ca and U/Ca form the basis of novel temperature equations that reduce the uncertainty of Mg/Ca temperatures from the carbonate ion effect. The average accuracy of reconstructed temperatures has been reduced from more than $\pm 1.6^{\circ}\text{C}$ to less than $\pm 0.9^{\circ}\text{C}$ (Figure 7-3), which is a significant improvement of reconstructed

deep-sea temperatures given their generally narrow range and low variability.

Acknowledgments

Jeroen Groeneveld and Ed C. Hathorne are funded by MARUM Fellowships. This study was carried out within the international graduate college EUROPROX, funded by the Deutsche Forschungsgemeinschaft (DFG).

7.6 Appendix 1. Sampling locations

| SAMPLING LOCATIONS AND FORAMINIFERAL SHELL COMPOSITIONS | | | | | | | | | | | |
|---|----------|--------|--------------|---------------|---|-------------------------|------------------------------------|------------------------|-------------------------|------------------------------------|------------------------|
| GeoB Sample | Location | | Depth (m) | Temp. (°C) | $\Delta[\text{CO}_3^{2-}]^*$ ($\mu\text{mol}/\text{kg}$) | <i>P. wuellerstorfi</i> | | | <i>C. mundulus</i> | | |
| | Lat. | Long. | | | | Mg/Ca (mmol/ mol) | B/Ca ($\mu\text{mol}/$ mol) | U/Ca (nmol/ mol) | Mg/Ca (mmol/ mol) | B/Ca ($\mu\text{mol}/$ mol) | U/Ca (nmol/ mol) |
| 1041 | -3.48 | -7.59 | 4035 | 2.51 | 27.11 | 1.56 | 209.96 | 8.88 | N.D. | N.D. | N.D. |
| 1105 | -1.67 | -12.43 | 3231 | 2.36 | 48.33 | 1.80 | 216.35 | 8.66 | N.D. | N.D. | N.D. |
| 1118 | -3.34 | -16.26 | 4675 | 0.86 | -3.43 | 0.88 | 165.55 | 22.93 | 0.84 | 129.37 | 16.89 |
| 1710 | -23.43 | 11.7 | 2987 | 2.57 | 38.74 | 1.60 | 226.17 | 10.68 | 1.19 | 163.09 | 11.55 |
| 1715 | -26.47 | 11.64 | 4095 | 1.43 | 10.5 | 1.29 | 191.33 | 14.75 | N.D. | N.D. | N.D. |
| 1720 | -29.00 | 13.83 | 2011 | 2.95 | 53.29 | 1.54 | 207.51 | 6.05 | N.D. | N.D. | N.D. |
| 1721 | -29.17 | 13.09 | 3045 | 2.43 | 39.55 | 1.61 | 185.94 | 10.80 | N.D. | N.D. | N.D. |
| 1728 | -29.84 | 2.41 | 2887 | 2.35 | 46.6 | 1.96 | 228.50 | 4.71 | 1.81 | 181.36 | 4.48 |
| 1729 | -28.89 | 1.00 | 4401 | 2.36 | 19.55 | 1.52 | 211.03 | 10.48 | 1.25 | 165.85 | 8.82 |
| 2102 | -23.98 | -41.20 | 1805 | 3.88 | 46.81 | 2.09 | 225.18 | 5.58 | 1.98 | 134.98 | 3.38 |
| 2718 | -47.31 | -58.17 | 2991 | 1.2 | 20.89 | 1.11 | 179.58 | 13.48 | 1.04 | 135.81 | 14.51 |
| 2727 | -48.01 | -56.54 | 2819 | 1.39 | 24.04 | 1.23 | 179.97 | 6.59 | N.D. | N.D. | N.D. |
| 3803 | -30.35 | -8.57 | 4173 | 2.43 | 25.6 | 1.36 | 198.57 | 7.32 | 1.30 | 174.01 | 9.65 |
| 3804 | -30.74 | -8.77 | 3882 | 2.43 | 31.93 | 1.59 | 183.57 | 10.29 | 1.45 | 153.57 | 6.21 |
| 3807 | -30.75 | -13.20 | 2515 | 2.51 | 48.45 | 1.94 | 226.35 | 4.66 | N.D. | N.D. | N.D. |
| 3808 | -30.81 | -14.71 | 3213 | 2.41 | 41.52 | 1.70 | 210.01 | 7.59 | 1.71 | 170.30 | 4.74 |
| 3822 | -27.63 | -37.95 | 4273 | 0.43 | 1.91 | 0.86 | 145.10 | 7.23 | 0.56 | 105.85 | 20.86 |
| 3827 | -25.03 | -38.55 | 3842 | 1.53 | 20.7 | 1.40 | 176.26 | 11.43 | 0.74 | 137.85 | 15.68 |
| 6208 | -31.81 | -45.67 | 3693 | 0.39 | 18.17 | 0.85 | 159.40 | 13.44 | N.D. | N.D. | N.D. |
| 6222 | -34.08 | -48.62 | 3450 | 1.27 | 18.7 | 1.21 | 169.62 | 19.92 | N.D. | N.D. | N.D. |
| 6330 | -46.15 | -57.56 | 3874 | 0.43 | 6.69 | 0.92 | 161.84 | 18.11 | N.D. | N.D. | N.D. |
| 6334 | -46.09 | -58.52 | 2597 | 1.57 | 26.98 | 1.29 | 172.32 | 13.96 | 1.19 | 127.93 | 6.78 |
| 6336 | -46.14 | -57.84 | 3398 | 0.92 | 15.08 | 1.05 | 158.61 | 9.50 | N.D. | N.D. | N.D. |

* Calculated from GEOSECS and SAVE data using the equation of Jansen et al. (2002).

N.D. = no data.

GeoB stations with accordant bottom water temperature at sample depth and calcite saturation state derived from GEOSECS and SAVE data. Also shown are measured Mg/Ca, B/Ca and U/Ca in the benthic foraminifer species *Planulina wuellerstorfi* and *Cibicidoides mundulus*.

7.7 Appendix 2. Carbonate standard JCT-1

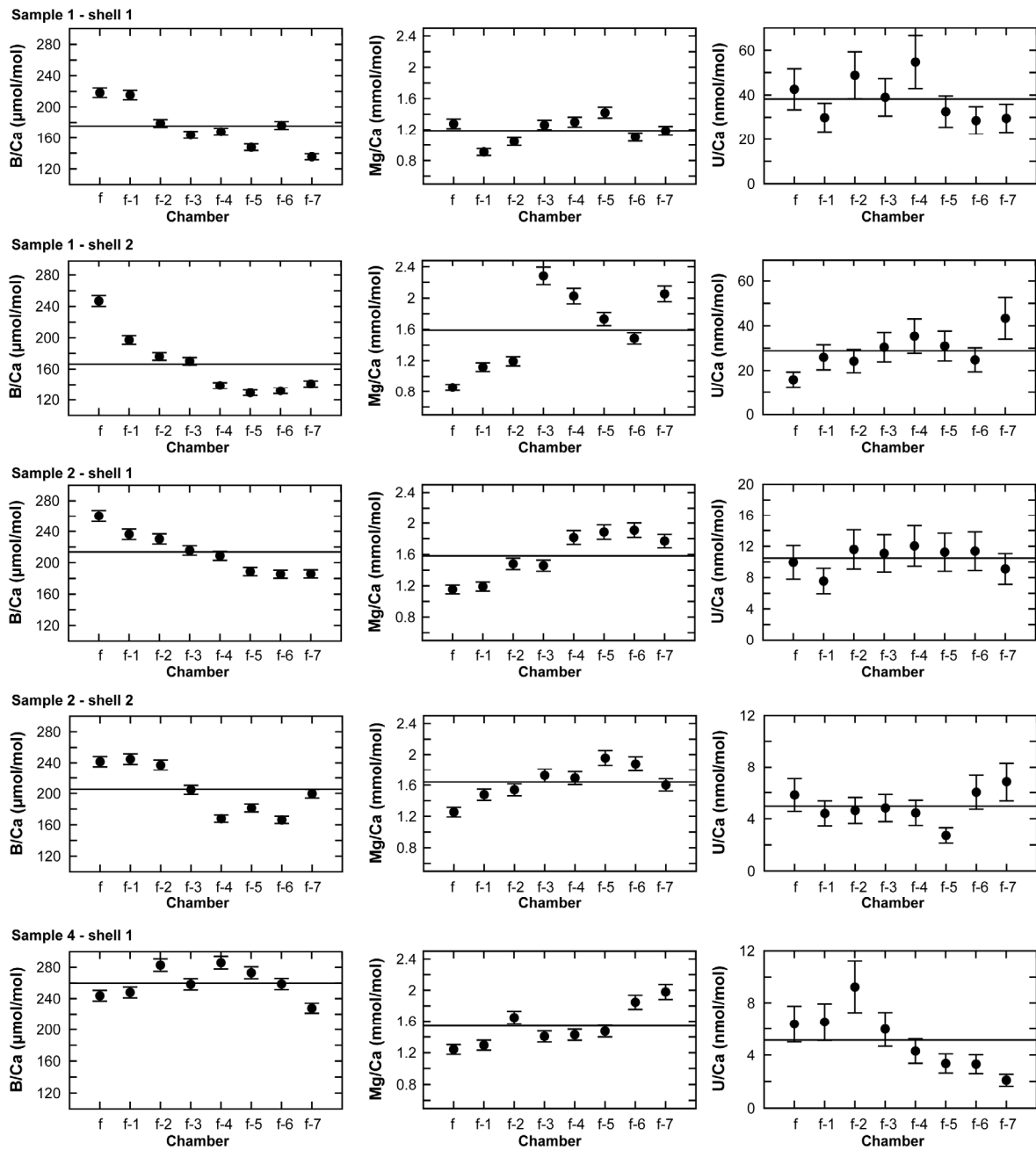
| CARBONATE STANDARD JCT-1 FOR LASER ABLATION ANALYSES OF SHELL CALCITE | | | | |
|---|--|---------------------|--------------------------|--------------------|
| | | Mg/Ca (mmol/mol) | B/Ca (μ mol/mol) | U/Ca (nmol/mol) |
| Shell calcite | Representative value | 0.93 | 194 | 29.4 |
| | Spot to spot reproducibility* | 18.2 | 13.9 | 36.2 |
| | Within spot reproducibility [†] | 26.8 | 36.2 | 117.8 |
| JCT-1 carbonate standard | Literature value (Inoue et al., 2004) | 1.24 | 184 | 21.1 |
| | Measured value (NIST612 – calibrated) | 1.58 | 172 | 21.5 |
| | Measured value (NIST610 – calibrated) | 1.27 | 197 | 21.8 |
| | Spot to spot reproducibility* | 2.8 | 4.9 | 21.6 |
| | Within spot reproducibility [†] | 27.2 | 33.3 | 42.0 |

* Relative standard deviation (%) calculated from average concentrations between five different ablation holes.

[†] Temporal relative standard deviation (%) reflects the time resolved reproducibility within an ablation pit, calculated according to the method of González et al. (2005) where the transient signals are separated into segments of four seconds each. Therefore the TRSD represents the concentration variation every four seconds during a measurement (González et al., 2006).

7.8 Appendix 3. Intra-test variability

Intra-test variability of *Planulina wuellerstorfi*

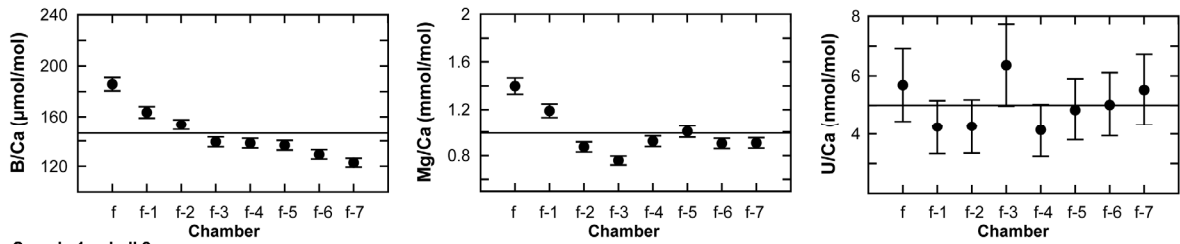


Note: Lines represent average values.

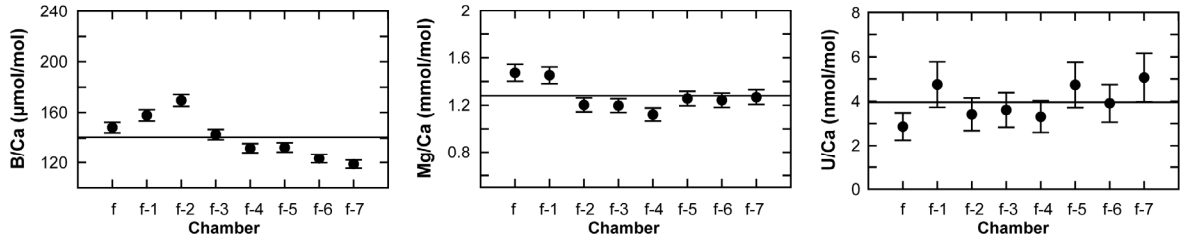
Appendix 3. Intra-test variability – continued

Intra-test variability of *Cibicidoides mundulus*

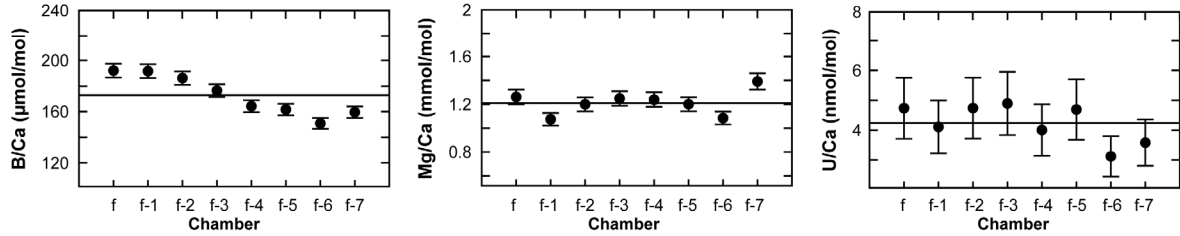
Sample 1 - shell 1



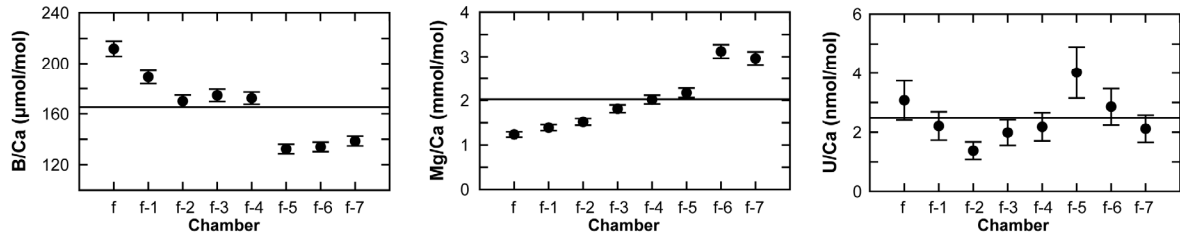
Sample 1 - shell 2



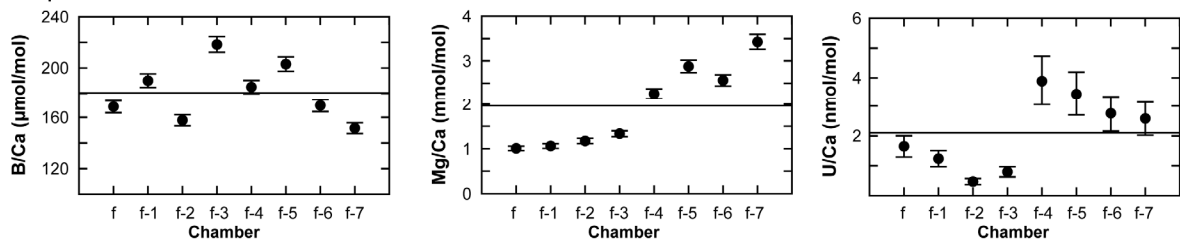
Sample 2 - shell 1



Sample 3 - shell 1



Sample 3 - shell 2



Note: Lines represent average values.

7.9 Appendix 4. Correction of Mg/Ca-thermometer

We have calculated corrected Mg/Ca temperature estimates by substituting corrected Mg/Ca for measured Mg/Ca ratios in the equations of Raitzsch et al. (2008), where Mg/Ca_{corr} is the difference between measured Mg/Ca and the portion of Mg/Ca influenced by $\Delta[CO_3^{2-}]$ ($\Delta Mg/Ca$). $\Delta Mg/Ca$ was calculated making use of the equations from Raitzsch et al. (2008). By substituting the relationships between $\Delta[CO_3^{2-}]$ and B/Ca of *P. wuellerstorfi* and U/Ca of *C. mundulus* (Figure 7-2) for $\Delta Mg/Ca$, a corrected Mg/Ca-temperature relationship is established for each species:

For *P. wuellerstorfi*:

Temperature calibration (Raitzsch et al., 2008):

$$(1) \quad Mg/Ca = 0.83 \pm 0.03 * \exp(0.145 \pm 0.013 * BWT)$$

Calibration of B/Ca versus $\Delta[CO_3^{2-}]$, this study:

$$(2) \quad B/Ca = 1.28 \pm 0.21 * \Delta[CO_3^{2-}] + 156.0 \pm 6.5$$

Temperature calibration corrected for carbonate ion effect (from B/Ca):

$$(3) \quad T_{corr} = (\ln (Mg/Ca - (0.010 \pm 0.025 * (B/Ca - 156.0 \pm 6.5) / 1.28 \pm 0.21 - 0.03 \pm 0.08)) - \ln 0.83 \pm 0.03) / 0.145 \pm 0.013$$

This is simplified to:

$$(4) \quad T_{corr} = 6.90 \pm 0.61 * \ln (Mg/Ca - 0.0082 \pm 0.0217 * B/Ca + 1.30 \pm 0.29) + 1.29 \pm 0.16$$

For *C. mundulus*:

Temperature calibration (Raitzsch et al., 2008):

$$(5) \quad Mg/Ca = 0.63 \pm 0.07 * \exp(0.143 \pm 0.011 * BWT)$$

Calibration of U/Ca versus $\Delta[CO_3^{2-}]$, this study:

$$(6) \quad U/Ca = 20.18 \pm 0.18 * \exp(-0.031 \pm 0.006 * \Delta[CO_3^{2-}])$$

Temperature calibration corrected for carbonate ion effect (from U/Ca):

$$(7) \quad T_{corr} = (\ln (Mg/Ca - (0.017 \pm 0.005 * (\ln U/Ca - \ln 20.18 \pm 0.18) / -0.031 \pm 0.006) + 0.14 \pm 0.17) - \ln 0.63 \pm 0.07) / 0.143 \pm 0.011$$

This is simplified to:

$$(8) \quad T_{corr} = 6.99 \pm 0.54 * \ln (Mg/Ca + 0.542 \pm 0.255 * \ln U/Ca - 1.49 \pm 0.98) + 3.26 \pm 0.03$$

IV. SUMMARY AND OUTLOOK

This thesis demonstrates that Mg/Ca in benthic foraminiferal shells as a proxy for bottom water temperatures is far from being well established. Compared to planktonic taxa, the Mg content of benthic foraminifera also depends strongly on the carbonate chemistry of seawater, in particular on the calcite saturation state. This so-called “carbonate ion effect” was verified by our study of core top samples from the South Atlantic (Chapter 5), which accords with other recent studies on this phenomenon by Elderfield et al. (2006), Rosenthal et al. (2006) and Healey et al. (2008). Close positive relationships were found between benthic foraminiferal Mg/Ca and the calcite saturation state with sensitivities of 0.010 and 0.017 mmol/mol per $\mu\text{mol/kg } \Delta[\text{CO}_3^{2-}]$ in *P. wuellerstorfi* and *C. mundulus*, respectively. The sensitivity of Mg/Ca to temperature is very low at the cold end, which may enable the influence of seawater carbonate chemistry to exceed that of temperature. For instance, a drop in deep-water $[\text{CO}_3^{2-}]$ by 25 $\mu\text{mol/kg}$ in the North Atlantic during the LGM, as estimated by Broecker and Clark (2001) and Yu and Elderfield (2007), would cause a decrease in Mg/Ca by roughly 0.4 mmol/mol. This in turn would lead to an underestimation by approximately 3.5°C at an actual temperature of 3°C. This magnitude is enormous when considering the generally low temperatures of roughly 5°C in the deep sea. Consequently, any $\delta^{18}\text{O}$ record corrected for such erroneous temperatures may be afflicted with sizeable errors.

To better constrain the positive link between $\Delta[\text{CO}_3^{2-}]$ and Mg/Ca in benthic foraminifera, culturing studies on the shallow-water benthic species *H. depressa* and *A. tepida* were carried out at the University of Utrecht (Chapter 6). In these experiments, the calcite saturation state (here defined as Ω) was varied by changing $[\text{Ca}^{2+}]$, which had the same effect as changing $[\text{CO}_3^{2-}]$. Surprisingly, we found that Mg/Ca in *A. tepida* decreased with increasing Ω , similarly to planktonic foraminifera, whereas Mg/Ca in *H. depressa* increased in a linear manner. These results suggest that these differences were caused by different biomineralization mechanisms, which in turn are influenced by ambient environmental conditions. This observation is generally in good agreement with the study of Bentov and Erez (2006).

However, further studies on core top and culture samples are required to decipher the different effects of temperature and carbonate ions on Mg/Ca in foraminiferal shells. An ongoing collaboration with the culture working group at the University of Utrecht follows up on the question whether variations in $[\text{CO}_3^{2-}]$ lead to the same change in Mg/Ca as observed in the $[\text{Ca}^{2+}]$ experiments. These experiments are much more complex since those have to be insulated from the atmosphere in order to prevent equilibration of the seawater with atmospheric CO_2 . This approach is afflicted with difficulties due to the long-term run of two months required for the growth of benthic foraminifera. However, despite the great advantage of culture experiments over core top studies of exactly knowing the environmental conditions, these conditions are not necessarily the same as in natural systems. The most principle question is whether pressure plays an important role in the trace metal uptake into shells, a question not answered so far. Elderfield et al. (1996) supposed that water depth

plays a role in the calcification process and thus in the trace metal incorporation. But for all that, it would be highly interesting to confirm this hypothesis by culture experiments under high pressure conditions. Despite the technical challenge, this task is an important issue that must be accomplished in future studies.

In order to progress in the development of the benthic Mg/Ca-temperature proxy, it is essential to establish carbonate system proxies that are largely independent from other parameters. These proxies would then allow to correct Mg/Ca for the carbonate ion effect to improve the inaccuracy of temperature reconstructions. In Chapter 7, B/Ca and U/Ca are presented as such highly promising tools for estimating calcite saturation state in seawater. Yu and Elderfield (2007) showed that B/Ca is relatively insensitive to factors others than $\Delta[\text{CO}_3^{2-}]$. We found that also U/Ca in benthic foraminifer shells is closely related to $\Delta[\text{CO}_3^{2-}]$ without significant correlations with temperature or salinity. The basic principle of these proxies is that both boron and uranium exist in seawater as different species, the relative amounts of which are determined by the pH. Only definite species are preferentially incorporated into foraminiferal shells while others are excluded from calcification. Consequently, the amount of boron and uranium incorporated into shell calcite is a function of pH, which in turn is intrinsically linked to $[\text{CO}_3^{2-}]$. Since both shell B/Ca and U/Ca correlate well with $\Delta[\text{CO}_3^{2-}]$ that is largely determined by water depth, there is potentially a pressure effect on the incorporation of these elements. However, using the B/Ca- and U/Ca- $\Delta[\text{CO}_3^{2-}]$ relationships for correcting Mg/Ca, the inaccuracy of estimated temperatures improved on average from more than $\pm 1.6^\circ\text{C}$ to less than $\pm 0.9^\circ\text{C}$.

An important issue of future work will be the application of these new proxies, particularly U/Ca, to downcore records to reconstruct changes in the past seawater carbonate chemistry. It was shown on the basis of dissolution indicators (sand content) that during glacial periods North Atlantic Deep Water (NADW), which is supersaturated with respect to calcite, was reduced and substituted by the corrosive Lower Circumpolar Deep Water (LCDW) (Bickert and Wefer, 1996). This glacial-interglacial vertical shift of the lysocline would be an excellent opportunity to test the carbonate ion proxies B/Ca and U/Ca in a future study. So far our knowledge on the interaction between climate changes, ocean circulation, and the carbonate system is based only on calcite dissolution indices and reconstructions of past CCD (for example Broecker and Clark, 2001; Anderson and Archer, 2002). The application of carbonate system proxies would for example help to answer one of the main open questions whether variations in the deep-water carbonate system played an important role in the global cooling during the middle Miocene. There are still uncertainties in the role of the ocean due to insufficient data on the past carbonate system parameters. Such data are important since alkalinity, $[\text{CO}_3^{2-}]$ and $\Delta[\text{CO}_3^{2-}]$ determine the ocean's capability to take up atmospheric CO_2 .

V. REFERENCES

- Addadi, L., Raz, S. and Weiner, S. (2003). Taking advantage of disorder: Amorphous calcium carbonate and its roles in biomineralization. *Adv. Mater.*, 15: 959-970.
- Allison, N. and Austin, W.E.N. (2008). Serial Mg/Ca and Sr/Ca chronologies across single benthic foraminifera tests. *Chem. Geol.*, 253: 83-88.
- Anand, P. and Elderfield, H. (2005). Variability of Mg/Ca and Sr/Ca between and within the planktonic foraminifers *Globigerina bulloides* and *Globorotalia truncatulinoides*. *Geochem. Geophys. Geosyst.*, 6: Q11D15, doi:10.1029/2004GC000811.
- Anand, P., Elderfield, H. and Conte, M.H. (2003). Calibration of Mg/Ca thermometry in planktonic foraminifera from a sediment trap time series. *Paleoceanography*, 18: 1050, doi:10.1029/2002PA000846.
- Anderson, D.M. and Archer, D. (2002). Glacial-interglacial stability of ocean pH inferred from foraminifer dissolution rates. *Nature*, 416: 70-73.
- Bainbridge, A.E. (1981). GEOSECS Atlantic expedition, Hydrographic data, 1972-1973, 1. National Science Foundation, U.S. Govt. Print. Off., Washington, D.C., 121 pp.
- Barnes, C.E. and Cochran, J.K. (1990). Uranium removal in oceanic sediments and the oceanic U balance. *Earth Planet. Sci. Lett.*, 97: 94-101.
- Bender, M.L., Lorens, R.B. and Williams, F.D. (1975). Sodium, magnesium, and strontium in the tests of planktonic foraminifera. *Micropaleontology*, 21: 448-459.
- Beniash, E., Aizenberg, J., Addadi, L. and Weiner, S. (1997). Amorphous calcium carbonate transforms into calcite during sea urchin larval spicule growth. *Proc. R. Soc. London, Ser. B*, 264: 461-465.
- Bentov, S. and Erez, J. (2005). Novel observations on biomineralization processes in foraminifera and implications for Mg/Ca ratio in the shells. *Geology*, 33: 841-844.
- Bentov, S. and Erez, J. (2006). Impact of biomineralization processes on the Mg content of foraminiferal shells: A biological perspective. *Geochem. Geophys. Geosyst.*, 7: Q01P08, doi:10.1029/2005GC001015.
- Berger, W.H. (1970). Planktonic foraminifera: Selective dissolution and the lysocline. *Mar. Geol.*, 8: 111-118.
- Berges, J.A., Franklin, D.J. and Harrison, P.J. (2001). Evolution Of An Artificial Seawater Medium: Improvements In Enriched Seawater, Artificial Water Over The Last Two Decades. *J. Phycol.*, 37: 1138-1145.
- Bernhard, J.M., Blanks, J.K., Hintz, C.J. and Chandler, G.T. (2004). Use of fluorescent calcite marker calcein to label foraminiferal tests. *J. Foraminifer. Res.*, 34: 96-101.
- Bickert, T. and Wefer, G. (1996). Late Quaternary Deep Water Circulation in the South Atlantic: Reconstruction from Carbonate Dissolution and Benthic Stable Isotopes. In: G. Wefer, W.H. Berger, G. Siedler and D.J. Webb (Eds.), *The South Atlantic: Present and Past Circulation*. Springer-Verlag, Berlin Heidelberg: 599-620.

- Bijma, J., Spero, H.J. and Lea, D.W. (1999). Reassessing foraminiferal stable isotope geochemistry: Impact of the oceanic carbonate system (experimental results). In: G. Fischer and G. Wefer (Eds.), *Uses of Proxies in Paleoceanography: Examples from the South Atlantic*. Springer Verlag, Berlin Heidelberg: 489-512.
- Billups, K. and Schrag, D.P. (2002). Paleotemperatures and ice-volume of the past 27 myr revisited with paired Mg/Ca and stable isotope measurements on benthic foraminifera. *Paleoceanography*, 17: doi:10.1029/2000PA000567.
- Billups, K. and Schrag, D.P. (2003). Application of benthic foraminiferal Mg/Ca ratios to questions of Cenozoic climate change. *Earth Planet. Sci. Lett.*, 209: 181-195.
- Blackmon, P.D. and Todd, R. (1959). Mineralogy of some foraminifera as related to their classification and ecology. *J. Paleontol.*, 33: 1-15.
- Boyle, E.A. (1983). Manganese carbonate overgrowths on foraminifera tests. *Geochim. Cosmochim. Acta*, 47: 1815-1819.
- Broecker, W.S. and Clark, E. (2001). Glacial-to-Holocene Redistribution of Carbonate Ion in the Deep Sea. *Science*, 294: 2152-2155.
- Broecker, W.S. and Peng, T.H. (1982). *Tracers in the Sea*. Lamont Doherty Geol. Obs. Publication, Columbia University, New York, 689 pp.
- Broecker, W.S. and Peng, T.H. (1989). The cause of the glacial to interglacial atmospheric CO₂ change. *Global Biogeochem. Cy.*, 3: 215-239.
- Brown, S.J. and Elderfield, H. (1996). Variations in Mg/Ca and Sr/Ca ratios of planktonic foraminifera caused by postdepositional dissolution: Evidence of shallow Mg-dependent dissolution. *Paleoceanography*, 11: 543-551.
- Chave, K.E. (1954). Aspects of biochemistry of magnesium: 1. Calcareous marine organisms. *J. Geol.*, 62: 266-283.
- Chilingar, G.V. (1962). Dependence on temperature of Ca/Mg ratio of skeletal structures of organisms and direct chemical precipitates out of seawater. *Bull. South. Calif. Acad. Sci.*, 61: 45-61.
- Clarke, F.W. and Wheeler, W.C. (1922). *The inorganic constituents of marine invertebrates*. USGS Prof. Pap., 124: 55.
- Curry, W.B. and Marchitto, T.M. (2008). A secondary ionization mass spectrometry calibration of *Cibicides pachyderma* Mg/Ca with temperature. *Geochem. Geophys. Geosyst.*, 9: Q04009, doi:10.1029/2007GC001620.
- de Nooijer, L.J., Reichart, G.-J., Dueñas-Bohórquez, A., Wolthers, M., Ernst, S.R., Mason, P.R.D. and van der Zwaan, G.J. (2007). Copper incorporation in foraminiferal calcite: results from culturing experiments. *Biogeosciences*, 4: 493-504.
- Dekens, P.S., Lea, D.W., Pak, D.K. and Spero, H.J. (2002). Core top calibration of Mg/Ca in tropical foraminifera: Refining paleotemperature estimation. *Geochem. Geophys. Geosyst.*, 3: 10.1029, doi: 2001GC000200.
- Delaney, M.L., Bé, A.W.H. and Boyle, E.A. (1985). Li, Sr, Mg, and Na in foraminiferal calcite shells from laboratory culture, sediment traps, and sediment cores. *Geochim. Cosmochim. Acta*, 49: 1327-1341.

- Demicco, R.V., Lowenstein, T.K. and Hardie, L.A. (2003). Atmospheric pCO₂ since 60 Ma from records of seawater pH, calcium, and primary carbonate mineralogy. *Geology*, 31: 793-796.
- Diepenbroek, M., Grobe, H. and Sieger, R. (Eds.) (2000). PanMap. Available from <http://www.pangaea.de/Software/PanMap>.
- Dittert, N. and Henrich, R. (2000). Carbonate dissolution in the South Atlantic Ocean: evidence from ultrastructure breakdown in *Globigerina bulloides*. *Deep-Sea Res.*, I: 603-620.
- Djogic, R., Sipos, L. and Branica, M. (1986). Characterization of uranium(VI) in seawater. *Limnol. Oceanogr.*, 31: 1122-1131.
- Dunk, R.M., Mills, R.A. and Jenkins, W.J. (2002). A reevaluation of the oceanic uranium budget for the Holocene. *Chem. Geol.*, 190: 45-67.
- Eggins, S., De Deckker, P. and Marshall, J. (2003). Mg/Ca variation in planktonic foraminifera tests: implications for reconstructing paleo-seawater temperature and habitat migration. *Earth Planet. Sci. Lett.*, 212: 291-306.
- Eggins, S., Sadekov, A. and De Deckker, P. (2004). Modulation and daily banding of Mg/Ca in *Orbulina universa* tests by symbiont photosynthesis and respiration: a complication for seawater thermometry? *Earth Planet. Sci. Lett.*, 225: 411-419.
- Elderfield, H., Bertram, C.J. and Erez, J. (1996). A biomineralization model for the incorporation of trace elements into foraminiferal calcium carbonate. *Earth Planet. Sci. Lett.*, 142: 409-423.
- Elderfield, H. and Ganssen, G. (2000). Past temperature and $\delta^{18}\text{O}$ of surface ocean waters inferred from foraminiferal Mg/Ca ratios. *Nature*, 405: 442-445.
- Elderfield, H., Yu, J., Anand, P., Kiefer, T. and Nyland, B. (2006). Calibrations for benthic foraminiferal Mg/Ca paleothermometry and the carbonate ion hypothesis. *Earth Planet. Sci. Lett.*, 250: 633-649.
- Erez, J. (1978). Vital effect on stable-isotope composition seen in foraminifera and coral skeletons. *Nature*, 273: 199-202.
- Erez, J. (2003). The source of ions for biomineralization in foraminifera and their implications for paleoceanographic proxies. *Rev. Mineral. Geochem.*, 54: 115-149.
- Ferguson, J.E., Henderson, G.M., Kucera, M. and Rickaby, R.E.M. (2008). Systematic change of foraminiferal Mg/Ca ratios across a strong salinity gradient. *Earth Planet. Sci. Lett.*, 265: 153-166.
- Foster, G.L. (2008). Seawater pH, pCO₂ and [CO₃²⁻] variations in the Caribbean Sea over the last 130 kyr; a boron isotope and B/Ca study of planktic foraminifera. *Earth Planet. Sci. Lett.*: doi: 10.1016/j.epsl.2008.04.015.
- Gao, K., Aruga, Y., Asada, K., Ishihara, T., Akano, T. and Kiyohara, M. (1993). Calcification in the coralline alga *Corallina pilulifera*, with special reference to the effect of elevated CO₂ concentration. *Mar. Biol.*, 117: 129-132.
- Gattuso, J.-P., Frankignoulle, M., Bourge, I., Romaine, S. and Buddemeier, R.W. (1998). Effect of calcium carbonate saturation of seawater on coral calcification. *Global Planet. Change*, 18: 37-46.

- Gehlen, M., Bassinot, F., Beck, L. and Khodja, H. (2004). Trace element cartography of *Globigerinoides ruber* shells using particle-induced X-ray emission. *Geochem. Geophys. Geosyst.*, 5: Q12D12, doi:10.1029/2004GC000822.
- Gerhardt, S. and Henrich, R. (2001). Shell preservation of *Limacina inflata* (Pteropoda) in surface sediments from the Central and South Atlantic Ocean: A new proxy to determine the aragonite saturation state of water masses. *Deep-Sea Res. I*, 48: 2051-2071.
- González, J., Dundas, S.H., Liu, C.Y., Mao, X. and Russo, R.E. (2006). UV-femtosecond and nanosecond laser ablation-ICP-MS: internal and external repeatability. *J. Anal. At. Spectrom.*, 21: 778-784.
- González, J., Liu, C., Yoo, J., Mao, X. and Russo, R.E. (2005). Double-pulse laser ablation inductively coupled plasma mass spectrometry. *Spectrochim. Acta, Part B*, 60: 27-31.
- Groeneveld, J., Nürnberg, D., Tiedemann, R., Reichart, G.-J., Steph, S., Reuning, L., Crudeli, D. and Mason, P. (2008). Foraminiferal Mg/Ca increase in the Caribbean during the Pliocene: Western Atlantic Warm Pool formation, salinity influence, or diagenetic overprint? *Geochem. Geophys. Geosyst.*, 9: Q01P23, doi:10.1029/2006GC001564.
- Groeneveld, J., Raitzsch, M., Siccha, M., Trommer, G., Hemleben, C. and Kučera, M. (2007). Salinity influence on planktonic foraminiferal Mg/Ca: A case study from the Red Sea. 9th International Conference on Paleoceanography (Shanghai), Program and Abstracts: 54.
- Groeneveld, J., Steph, S., Tiedemann, R., Garbe-Schönberg, D., Nürnberg, D. and Sturm, A. (2006). Pliocene mixed-layer oceanography for Site 1241, using combined Mg/Ca and $\delta^{18}\text{O}$ analyses of *Globigerinoides sacculifer*. In: R. Tiedemann, A.C. Mix, C. Richter and W.F. Ruddiman (Eds.), *Proc. ODP, Sci. Results*, 202, College Station, TX (Ocean Drilling Program): 1-27.
- Hastings, D.W., Russell, A.D. and Emerson, S.R. (1998). Foraminiferal magnesium in *Globigerinoides* as a paleotemperature proxy. *Paleoceanography*, 13: 161-169.
- Hathorne, E.C., Alard, O., James, R.H. and Rogers, N.W. (2003). Determination of trace elements in foraminifera by laser ablation inductively coupled plasma-mass spectrometry. *Geochem. Geophys. Geosyst.*, 4: 8408, doi:10.1029/2003GC000539.
- Hathorne, E.C., James, R.H., Savage, P. and Alard, O. (2008a). Physical and chemical characteristics of particles produced by laser ablation of biogenic calcium carbonate. *J. Anal. At. Spectrom.*, 23: 240-243.
- Hathorne, E.C., Raitzsch, M. and Kuhnert, H. (2008b). Non matrix-matched calibration of 193nm laser ablation ICP-MS analysis of calcium carbonate samples using NIST 612 and 610 glasses: Inaccurate Mg calibration and variable laser parameters. 9th European Workshop on Laser Ablation in Elemental and Isotopic Analysis (Prague), Workshop programme and abstracts: 54.
- Healey, S.L., Thunell, R.C. and Corliss, B.H. (2008). The Mg/Ca-Temperature Relationship of Benthic Foraminiferal Calcite: New Core-top Calibrations in the 4°C Temperature Range. *Earth Planet. Sci. Lett.*: doi: 10.1016/j.epsl.2008.05.023.
- Hecht, A.D., Eslinger, E.V. and Garmon, L.B. (1975). Experimental studies on the dissolution of planktonic foraminifera. In: W.V. Sitter, A.W.H. Bé and W.H. Berger (Eds.), *Dissolution of Deep-sea Carbonates*. Cushman Foundation for Foraminiferal Research: 59-69.

- Hemming, N.G. and Hanson, G.N. (1992). Boron isotopic composition and concentration in modern marine carbonates. *Geochim. Cosmochim. Acta*, 56: 537-543.
- Hemming, N.G., Reeder, R.J. and Hanson, G.N. (1995). Mineral-fluid partitioning and isotopic fractionation of boron in synthetic calcium carbonate. *Geochim. Cosmochim. Acta*, 59: 371-379.
- Hensen, C. and Zabel, M. (2003). Geochemistry of porewater in sediment core GeoB1715-3. PANGAEA: doi:10.1594/PANGAEA.105409.
- Hintz, C.J., Shaw, T.J., Chandler, G.T., Bernhard, J.M., McCorkle, D.C. and Blanks, J.K. (2006a). Trace/minor element:calcium ratios in cultured benthic foraminifera. Part I: Interspecies and inter-individual variability. *Geochim. Cosmochim. Acta*, 70: 1952-1963.
- Hintz, C.J., Shaw, T.J., Chandler, G.T., Bernhard, J.M., McCorkle, D.C. and Blanks, J.K. (2006b). Trace/minor element:calcium ratios in cultured benthic foraminifera. Part II: Ontogenetic variation. *Geochim. Cosmochim. Acta*, 70: 1964-1976.
- Holbourn, A.E. and Henderson, A.S. (2002). Re-illustration and revised taxonomy for selected deep-sea benthic foraminifers, *Palaeontologia Electronica*, 34 pp.
- Hönisch, B., Bickert, T. and Hemming, N.G. (2008). Modern and Pleistocene boron isotope composition of the benthic foraminifer *Cibicides wuellerstorfi*. *Earth Planet. Sci. Lett.*, 272: 309-318.
- Horita, J., Zimmermann, H. and Holland, H.D. (2002). Chemical evolution of seawater during the Phanerozoic: Implications from the record of marine evaporites. *Geochim. Cosmochim. Acta*, 66: 3733-3756.
- Hover, V.C., Walter, L.M. and Peacor, D.R. (2001). Early marine diagenesis of biogenic aragonite and Mg-calcite: New constraints from high-resolution STEM and AEM analyses of modern platform carbonates. *Chem. Geol.*, 175: 221-248.
- Inoue, M., Nohara, M., Okai, T., Suzuki, A. and Kawahata, H. (2004). Concentrations of Trace Elements in Carbonate Reference Materials Coral JCp-1 and Giant Clam Jct-1 by Inductively Plasma-Mass Spectrometry. *Geostand. Geoanalyt. Res.*, 28: 411-416.
- Izuka, S.K. (1988). Relationship of magnesium and other minor elements in tests of *Cassidulina subglobosa* and *C. oriangukata* to physical oceanic properties. *J. Foram. Res.*, 18: 151-157.
- Jansen, H., Zeebe, R.E. and Wolf-Gladrow, D.A. (2002). Modeling the dissolution of settling CaCO₃ in the ocean. *Global Biogeochem. Cy.*, 16: 1027, doi:10.1029/2000GB001279.
- Katz, A. (1973). The interaction of magnesium with calcite during crystal growth at 25-90°C and one atmosphere. *Geochim. Cosmochim. Acta*, 37: 1563-1586.
- Katz, M.E., Miller, K.G., Wright, J.D., Wade, B.S., Browning, J.V., Cramer, B.S. and Rosenthal, Y. (2008). Stepwise transition from the Eocene greenhouse to the Oligocene icehouse. *Nature*, 1: 329-334.
- Kester, D.R., Duedall, I.W., Connors, D.N. and Pytkowicz, R.M. (1967). Preparation of Artificial Seawater. *Limnol. Oceanogr.*, 12: 176-179.
- Krestou, A., Xenidis, A. and Panias, D. (2003). Mechanism of aqueous uranium (VI) uptake by natural zeolitic tuff. *Miner. Eng.*, 16: 1363-1370.

- Krinsley, D. (1960). Trace elements in the tests of planktic foraminifera. *Micropaleontology*, 63: 297-300.
- Kristjánsson, G.B., Lea, D.W., Jennings, A.E., Pak, D.K. and Belanger, C. (2007). New spatial Mg/Ca-temperature calibrations for three Arctic, benthic foraminifera and reconstruction of north Iceland shelf temperature for the past 4000 years. *Geochem. Geophys. Geosyst.*, 8: Q03P21, doi:10.1029/2006GC001425.
- Kısakürek, B., Eisenhauer, A., Böhm, F., Garbe-Schönberg, D. and Erez, J. (2008). Controls on shell Mg/Ca and Sr/Ca in cultured planktonic foraminifera, *Globigerinoides ruber* (white). *Earth Planet. Sci. Lett.*: doi: 10.1016/j.epsl.2008.06.026.
- Langdon, C., Takahashi, T., Sweeney, C., Chipman, D., Goddard, J., Marubini, F., Aceves, H., Barnett, H. and Atkinson, M.J. (2000). Effect of calcium carbonate saturation state on the calcification rate of an experimental coral reef. *Global Biogeochem. Cy.*, 14: 639-654.
- Lea, D. (2003). Elemental and Isotopic Proxies of Past Ocean Temperatures. In: H. Elderfield (Ed.), *Treatise on Geochemistry*. Elsevier: 625.
- Lea, D.W., Mashiotta, T.A. and Spero, H.J. (1999). Controls on magnesium and strontium uptake in planktonic foraminifera determined by live culturing. *Geochim. Cosmochim. Acta*, 63: 2369-2380.
- Lea, D.W., Pak, D.K. and Spero, H.J. (2000). Climate impact of Late Quaternary equatorial Pacific sea surface temperatures. *Science*, 289: 1719-1723.
- Lear, C.H., Elderfield, H. and Wilson, P.A. (2000). Cenozoic deep-sea temperatures and global ice volumes from Mg/Ca in benthic foraminiferal calcite. *Science*, 287: 269-272.
- Lear, C.H., Rosenthal, Y. and Slowey, N. (2002). Benthic foraminiferal Mg/Ca-paleothermometry: A revised core-top calibration. *Geochim. Cosmochim. Acta*, 66: 3375-3387.
- Lear, C.H., Rosenthal, Y. and Wright, J.D. (2003). The closing of a seaway: ocean water masses and global climate change. *Earth Planet. Sci. Lett.*, 210: 425-436.
- Lewis, E. and Wallace, D.W.R. (Eds.) (1998). Program Developed for CO₂ System Calculation. ORNL/CDIAC-105. Carbon Dioxide Information Analysis Center, Oak Ridge National Laboratory, U.S. Department of Energy, Oak Ridge, Tennessee.
- Lorens, R.B., Williams, D.F. and Bender, M.L. (1977). The early nonstructural chemical diagenesis of foraminiferal calcite. *J. Sed. Petrol.*, 47: 1602-1609.
- Lutze, G.F. and Thiel, H. (1989). Epibenthic foraminifera from elevated microhabitats: *Cibicides wuellerstorfi* and *Planulina ariminensis*. *J. Foram. Res.*, 19: 153-158.
- Macintyre, I.G. and Reid, R.P. (1995). Crystal alteration in a living calcareous alga (*Halimeda*); implications for studies in skeletal diagenesis. *J. Sed. Res.*, 65: 143-153.
- Macintyre, I.G. and Reid, R.P. (1998). Recrystallization in living porcelaneous Foraminifera (*Archaias angulatis*): textural changes without mineralogic alteration. *J. Sed. Res.*, 68: 11-19.

- Marchitto, T.M., Bryan, S.P., Curry, W.B. and McCorkle, D.C. (2007). Mg/Ca temperature calibration for the benthic foraminifer *Cibicidoides pachyderma*. *Paleoceanography*, 22: PA1203, doi:10.1029/2006PA0011287.
- Marchitto, T.M. and deMenocal, P.B. (2003). Late Holocene variability of upper North Atlantic Deep Water temperature and salinity. *Geochem. Geophys. Geosyst.*, 4: 1100, doi:10.1029/2003GC000598.
- Martin, P.A., Lea, D.W., Rosenthal, Y., Shackleton, N.J., Sarnthein, M. and Papenfuss, T. (2002). Quaternary deep sea temperature histories derived from benthic foraminiferal Mg/Ca. *Earth Planet. Sci. Lett.*, 198: 193-209.
- Martin, R.E. (1995). Cyclic and Secular Variation in Microfossil Biomineralization - Clues to the Biogeochemical Evolution of Phanerozoic Oceans. *Global Planet Change*, 11: 1-23.
- Martin, W.R. and Sayles, F.L. (1996). CaCO₃ dissolution in sediments of the Ceara Rise, western equatorial Atlantic. *Geochim. Cosmochim. Acta*, 60: 243-263.
- Martin, W.R. and Sayles, F.L. (2006). Organic matter oxidation in deep-sea sediments: distribution in the sediment column and implications for calcite dissolution. *Deep-Sea Res. II*, 53: 771-792.
- Mashiotta, T.A., Lea, D.W. and Spero, H.J. (1999). Glacial-interglacial changes in subantarctic sea surface temperature and the $\delta^{18}\text{O}$ of seawater using foraminiferal Mg. *Earth Planet. Sci. Lett.*, 170: 417-432.
- McConnell, M.C. and Thunell, R.C. (2005). Calibration of the planktonic foraminiferal Mg/Ca paleothermometer: Sediment trap results from the Guaymas Basin, Gulf of California. *Paleoceanography*, 20: PA2016, doi:10.1029/2004PA001077.
- McCorkle, D.C., Martin, P.A., Lea, D.W. and Klinkhammer, G.P. (1995). Evidence of a dissolution effect on benthic foraminiferal shell chemistry $\delta^{13}\text{C}$, Cd/Ca, Ba/Ca, and Sr/Ca results from the Ontong Java Plateau. *Paleoceanography*, 10: 699-714.
- McKenna, V.S. and Prell, W.L. (2004). Calibration of the Mg/Ca of *Globorotalia truncatulinoides* (R) for the reconstruction of marine temperature gradients. *Paleoceanography*, 19: PA2006, doi:10.1029/2000PA000604.
- Mehrbach, C., Culberso, C.H., Hawley, J.E. and Pytkowic, R.M. (1973). Measurement of apparent dissociation-constants of carbonic-acid in seawater at atmospheric-pressure. *Limnol. Oceanogr.*, 18: 897-907.
- Mercier, H., Speer, K.G. and Honnorez, J. (1994). Tracing the Antarctic Bottom Water through the Romanche and Chain Fracture Zones. *Deep-Sea Res.*, 41: 1457-1477.
- Morse, J.W. and Bender, M.L. (1990). Partition coefficients in calcite: Examination of factors influencing the validity of experimental results and their application to natural systems. *Chem. Geol.*, 82: 265-277.
- Mucci, A. (1987). Influence of temperature on the composition of magnesian calcite overgrowths precipitated from seawater. *Geochim. Cosmochim. Acta*, 51: 1977-1984.
- Mucci, A. and Morse, J.W. (1983). The incorporation of Mg²⁺ and Sr²⁺ into calcite overgrowths: influences of growth rate and solution composition. *Geochim. Cosmochim. Acta*, 47: 217-233.

- Mulquiney, P.J. and Kuchel, P.W. (1997). Model of the pH dependence of the concentrations of complexes involving metabolites, haemoglobin and magnesium ions in the human erythrocyte. *Eur. J. Biochem.*, 245: 71-83.
- Ni, Y., Foster, G.L., Bailey, T., Elliott, T., Schmidt, D.N., Pearson, P., Haley, B. and Coath, C. (2007). A core top assessment of proxies for the ocean carbonate system in surface-dwelling foraminifers. *Paleoceanography*, 22: PA3212, doi:10.1029/2006PA001337.
- Nürnberg, D., Bijma, J. and Hemleben, C. (1996). Assessing the reliability of magnesium in foraminiferal calcite as a proxy for water mass temperatures. *Geochim. Cosmochim. Acta*, 60: 803-814.
- Nürnberg, D. and Groeneveld, J. (2006). Pleistocene variability of the Subtropical Convergence at East Tasman Plateau: Evidence from planktonic foraminiferal Mg/Ca (ODP Site 1172A). *Geochem. Geophys. Geosyst.*, 7: Q04P11, doi:10.1029/2005GC000984.
- Oomori, T., Kameshima, H., Maezato, Y. and Kitano, Y. (1987). Distribution coefficient of Mg²⁺ ions between calcite and solution at 10-50°C. *Mar. Chem.*, 20: 327-336.
- Pearce, N.J.G., Perkins, W.T., Westgate, J.A., Gorton, M.P., Jackson, S.E., Neal, C.L. and Chenery, S.P. (1997). A compilation of new and published major and trace element data for NIST SRM 610 and NIST SRM 612 glass reference materials. *Geostand. Newsl.*, 21: 115-144.
- Pierrot, D., Lewis, E. and Wallace, D.W.R. (Eds.) (2006). MS Excel Program Developed for CO₂ System Calculations. ORNL/CDIAC-105. Carbon Dioxide Information Analysis Center, Oak Ridge National Laboratory, U.S. Department of Energy, Oak Ridge, Tennessee.
- Puigdomenech, I. (Ed.), (2004). Hydra/Medusa Chemical Equilibrium Database and Plotting Software. KTH Royal Institute of Technology, Stockholm. Available from <http://www.kemi.kth.se/medusa/>.
- Raitzsch, M., Kuhnert, H., Groeneveld, J. and Bickert, T. (2008). Benthic foraminifer Mg/Ca anomalies in South Atlantic core top sediments and their implications for paleothermometry. *Geochem. Geophys. Geosyst.*, 9: Q05010, doi:10.1029/2007GC001788.
- Rathburn, A.E. and Corliss, B.H. (1994). The ecology of living (stained) deep-sea benthic foraminifera from the Sulu Sea. *Paleoceanography*, 9: 87-150.
- Rathburn, A.E. and De Deckker, P. (1997). Magnesium and strontium composition of Recent benthic foraminifera from the Coral Sea, Australia and Prydz Bay, Antarctica. *Mar. Micropaleontol.*, 32: 231-248.
- Rathmann, S., Hess, S., Kuhnert, H. and Mulitza, S. (2004). Mg/Ca ratios of the benthic foraminifera *Oridorsalis umbonatus* obtained by laser ablation from core top sediments: Relationship to bottom water temperature. *Geochem. Geophys. Geosyst.*, 5: Q12013, doi:10.1029/2004GC000808.
- Rathmann, S. and Kuhnert, H. (2008). Carbonate ion effect on Mg/Ca, Sr/Ca and stable isotopes on the benthic foraminifera *Oridorsalis umbonatus* off Namibia. *Mar. Micropaleontol.*, 66: 120-133.
- Raz, S., Weiner, S. and Addadi, L. (2000). Formation of high-magnesian calcites via an amorphous precursor phase: Possible biological implications. *Adv. Mater.*, 12: 38-42.

- Reeder, R.J., Nugent, M., Lamble, G.M., Tait, C.D. and Morris, D.E. (2000). Uranyl incorporation into calcite and aragonite: XAFS and luminescence studies. *Environ. Sci. Technol.*, 34: 638-644.
- Regenberg, M., Nürnberg, D., Steph, S., Groeneveld, J., Garbe-Schönberg, D., Tiedemann, R. and Dullo, W.-C. (2006). Assessing the effect of dissolution on planktonic foraminiferal Mg/Ca ratios: Evidence from Caribbean core tops. *Geochem. Geophys. Geosyst.*, 7: doi:10.1029/2005GC001019.
- Reichert, G.-J., Jorissen, F., Anschutz, P. and Mason, P.R.D. (2003). Single foraminiferal test chemistry records the marine environment. *Geology*, 31: 355-358.
- Rickaby, R. and Halloran, P. (2005). Cool La Niña during the warmth of the Pliocene? *Science*, 307: 1948-1952.
- Ries, J.B. (2004). Effect of ambient Mg/Ca on Mg fractionation in calcareous marine invertebrates: A record of the oceanic Mg/Ca ratio over the Phanerozoic. *Geology*, 32: 981-984.
- Rosenthal, Y. and Boyle, E.A. (1993). Factors controlling the fluoride content of planktonic foraminifera: An evaluation of its paleoceanographic applicability. *Geochim. Cosmochim. Acta*, 57: 335-346.
- Rosenthal, Y., Boyle, E.A. and Slowey, N. (1997). Temperature control on the incorporation of magnesium, strontium, fluorine, and cadmium into benthic foraminiferal shells from Little Bahama Bank: Prospects for thermocline paleoceanography. *Geochim. Cosmochim. Acta*, 61: 3633-3643.
- Rosenthal, Y., Lear, C.H., Oppo, D.W. and Linsley, B.K. (2006). Temperature and carbonate ion effects on Mg/Ca and Sr/Ca ratios in benthic foraminifera: Aragonitic species *Hoeglundina elegans*. *Paleoceanography*, 21: PA1007, doi:10.1029/2005PA001158.
- Rosenthal, Y. and Lohmann, G.P. (2002). Accurate estimation of sea surface temperatures using dissolution-corrected calibrations for Mg/Ca paleothermometry. *Paleoceanography*, 17: 1044, doi:10.1029/2001PA000749.
- Rosenthal, Y., Lohmann, G.P., Lohmann, K.C. and Sherrell, R.M. (2000). Incorporation and preservation of Mg in *Globigerinoides sacculifer*: Implications for reconstructing the temperature and $^{18}\text{O}/^{16}\text{O}$ of seawater. *Paleoceanography*, 15: 135-145.
- Rosenthal, Y., Oppo, D. and Linsley, B.K. (2003). The amplitude and phasing of climate change during the last deglaciation in the Sulu Sea, western equatorial Pacific. *Geophys. Res. Lett.*, 30: 1428, doi:10.1029/2002GL016612.
- Russell, A.D., Emerson, S., Mix, A.C. and Peterson, L.C. (1996). The use of foraminiferal uranium/calcium ratios as an indicator of changes in seawater uranium content. *Paleoceanography*, 11: 649-663.
- Russell, A.D., Emerson, S., Nelson, B.K., Erez, J. and Lea, D.W. (1994). Uranium in foraminiferal calcite as a recorder of seawater uranium concentrations. *Geochim. Cosmochim. Acta*, 58: 671-681.
- Russell, A.D., Hönisch, B., Spero, H.J. and Lea, D.W. (2004). Effects of seawater carbonate ion concentration and temperature on shell U, Mg, and Sr in cultured planktonic foraminifera. *Geochim. Cosmochim. Acta*, 68: 4347-4361.

- Sadekov, A.Y., Eggins, S.M. and De Deckker, P. (2005). Characterization of Mg/Ca distributions in planktonic foraminifera species by electron microprobe mapping. *Geochem. Geophys. Geosyst.*, 6: Q12P06, doi:10.1029/2005GC000973.
- Sanyal, A., Hemming, N.G., Broecker, W.S. and Hanson, G.N. (1997). Changes in pH in the eastern equatorial Pacific across stage 5-6 boundary based on boron isotopes in foraminifera. *Global Biogeochem. Cy.*, 11: 125-133.
- Sanyal, A., Hemming, N.G., Hanson, N. and Broecker, W.S. (1995). Evidence for a higher pH in the glacial ocean from boron isotopes in foraminifera. *Nature*, 373: 234-236.
- Sanyal, A., Nugent, M., Reeder, R.J. and Bijma, J. (2000). Seawater pH control on the boron isotopic composition of calcite: Evidence from inorganic calcite precipitation experiments. *Geochim. Cosmochim. Acta*, 64: 1551-1555.
- Saraswat, R., Nigam, R., Weldeab, S., Mackensen, A. and Naidu, P.D. (2005). A first look at past sea surface temperatures in the equatorial Indian Ocean from Mg/Ca in foraminifera. *Geophys. Res. Lett.*, 32: L24605, doi:10.1029/2005GL024093.
- Savin, S.M. and Douglas, R.G. (1973). Stable isotope and magnesium geochemistry of Recent planktonic foraminifera from the South Pacific. *Geol. Soc. Amer. Bull.*, 84: 2327-2342.
- Schlitzer, R. (2000). Electronic Atlas of WOCE Hydrographic and Tracer Data Now Available. *EOS Trans. AGU*, 81: 45.
- Schlitzer, R. (Ed.), (2005). *Ocean Data View*. Alfred Wegener Inst., Bremerhaven, Germany. Available from <http://www.awi-bremerhaven.de/GEO/ODV>.
- Schmidt, G.A., Hoffmann, G. and Thresher, D. (2001). Isotopic tracers in coupled models: a new paleo-tool. *PAGES News*, 9: 10-11.
- Schrag, D.P., Hampt, G. and Murray, D.W. (1996). Pore fluid constraints on the temperature and oxygen isotopic composition of the glacial ocean. *Science*, 272: 1930-1932.
- Segev, E. and Erez, J. (2006). Effect of Mg/Ca ratio in seawater on shell composition in shallow benthic foraminifera. *Geochem. Geophys. Geosyst.*, 7: Q02P09, doi:10.1029/2005GC000969.
- Shannon, L.V. and Chapman, P. (1991). Evidence of Antarctic Bottom Water in the Angola Basin at 32°S. *Deep-Sea Res.*, 38: 1299-1304.
- Shevenell, A.E., Kennett, J.P. and Lea, D.W. (2008). Middle Miocene ice sheet dynamics, deep-sea temperatures, and carbon cycling: A Southern Ocean perspective. *Geochem. Geophys. Geosyst.*, 9: Q02006, doi:10.1029/2007GC001736.
- Siedler, G., Müller, T.J., Onken, R., Arhan, M., Mercier, H., King, B.A. and Saunders, P.M. (1996). The Zonal WOCE Sections in the South Atlantic. In: G. Wefer, W.H. Berger, G. Siedler and D.J. Webb (Eds.), *The South Atlantic: Present and Past Circulation*. Springer, Berlin Heidelberg: 83-104.

- Skinner, L.C., Shackleton, N.J. and Elderfield, H. (2003). Millennial-scale variability of deep-water temperature and $\delta^{18}\text{O}_{\text{dw}}$ indicating deep-water source variations in the Northeast Atlantic, 0-34 cal. ka BP. *Geochem. Geophys. Geosyst.*, 4: 1098, doi:10.1029/2003GC000585.
- Spero, H.J., Bijma, J., Lea, D.W. and Davis, B.E. (1997). Effect of seawater carbonate concentration on foraminiferal carbon and oxygen isotopes. *Nature*, 390: 497-500.
- Spivack, A.J., You, C.F. and Smith, H.J. (1993). Foraminifera boron isotope ratios as a proxy for surface ocean pH over the past 21 Myr. *Nature*, 363: 149-151.
- Stanley, S.M. and Hardie, L.A. (1999). Hypercalcification: Paleontology links plate tectonics and geochemistry to sedimentology. *GSA Today*, 9: 2-7.
- Stephens, C., Antonov, J.I., Boyer, T.P., Conkright, M.E., Locarnini, R.A., O'Brien, T.D. and Garcia, H.E. (2002). *World Ocean Atlas 2001, vol. 1, Temperature*, NOAA Atlas NESDIS 49. U.S. Govt. Print. Off., Washington, D. C., 167 pp.
- Striegl, R.G., Kortelainen, P., Chanton, J.P., Wickland, K.P., Bugna, G.C. and Rantakari, M. (2001). Carbon Dioxide Partial Pressure and ^{13}C Content of North Temperate and Boreal Lakes at Spring Ice Melt. *Limnol. Oceanogr.*, 46: 941-945.
- Takahashi, T., Peng, T.-H. and Sutherland, S. (1995). Carbon Data Obtained During the South Atlantic Ventilation Experiment (SAVE) Expeditions (1987-1989). Carbon Dioxide Information Analysis Center, Oak Ridge National Laboratory, US Department of Energy, Oak Ridge, Tennessee.
- ter Kuile, B. and Erez, J. (1987). Uptake of inorganic carbon and internal carbon cycling in symbiont-bearing benthonic foraminifera. *Mar. Biol.*, 94: 499-510.
- ter Kuile, B. and Erez, J. (1988). The size and function of the internal carbon pool of the foraminifer, *Amphistegina lobifera*. *Mar. Biol.*, 99: 481-487.
- ter Kuile, B., Erez, J. and Padan, E. (1989a). Competition for inorganic carbon between photosynthesis and calcification in the symbiont-bearing foraminifer *Amphistegina lobifera*. *Mar. Biol.*, 103: 253-259.
- ter Kuile, B., Erez, J. and Padan, E. (1989b). Mechanisms for the uptake of inorganic carbon by two species of symbiontbearing foraminifera. *Mar. Biol.*, 103: 241-251.
- Toyofuku, T. and Kitazato, H. (2005). Micromapping of Mg/Ca values in cultured specimens of the high-magnesium benthic foraminifera. *Geochem. Geophys. Geosyst.*, 6: Q11P05, doi:10.1029/2005GC000961.
- Toyofuku, T., Kitazato, H., Kawahata, H., Tsuchiya, M. and Nohara, M. (2000). Evaluation of Mg/Ca thermometry in foraminifera: Comparison of experimental results and measurements in nature. *Paleoceanography*, 15: 456-464.
- Wara, M.W., Delaney, M.L., Bullen, T.D. and Ravelo, A.C. (2003). Possible roles of pH, temperature, and partial dissolution in determining boron concentration and isotopic composition in planktonic foraminifera. *Paleoceanography*, 18: 1100, doi:10.1029/2002PA000797.
- Whitko, A.N., Hastings, D.W. and Flower, B.P. (2002). Past sea surface temperatures in the tropical South China Sea based on a new foraminiferal Mg calibration. *MARSci*: doi:MARSci.2002.01.020101.

- Wolf-Gladrow, D.A., Bijma, J. and Zeebe, R.E. (1999). Model simulation of the carbonate chemistry in the microenvironment of symbiont bearing foraminifera. *Mar. Chem.*, 64: 181-198.
- Yu, J. and Elderfield, H. (2007). Benthic foraminiferal B/Ca ratios reflect deep water carbonate saturation state. *Earth Planet. Sci. Lett.*, 258: 73-86.
- Yu, J., Elderfield, H., Greaves, M. and Day, J. (2007a). Preferential dissolution of benthic foraminiferal calcite during laboratory reductive cleaning. *Geochem. Geophys. Geosyst.*, 8: Q06016, doi:10.1029/2006GC001571.
- Yu, J., Elderfield, H. and Hönisch, B. (2007b). B/Ca in planktonic foraminifera as a proxy for surface seawater pH. *Paleoceanography*, 22: PA2202, doi:10.1029/2006PA001347.
- Yu, J., Elderfield, H. and Piotrowski, A.M. (2008). Seawater carbonate ion – $\delta^{13}\text{C}$ systematics and application to glacial-interglacial North Atlantic ocean circulation. *Earth Planet. Sci. Lett.*: doi:10.1016/j.epsl.2008.04.010.
- Zachos, J.C., Wara, M.W., Bohaty, S., Delaney, M.L., Petrizzo, M.R., Brill, A., Bralower, T.J. and Premoli-Silva, I. (2003). A Transient Rise in Tropical Sea Surface Temperature During the Paleocene-Eocene Thermal Maximum. *Science*, 302: 1551-1554.
- Zeebe, R.E. and Wolf-Gladrow, D.A. (2001). *CO₂ in Seawater: Equilibrium, Kinetics, Isotopes*, 65. Elsevier Oceanography Series, Amsterdam, 346 pp.